An Initial Moving-Boundary Value Problem

Associated with the Spinning Wave Equation

by

Stephanie K. Olafson

B. Sc., University of Manitoba, 1999

A thesis submitted to the

Faculty of the Graduate Studies of the

University of Manitoba in partial fulfillment

of the requirements for the degree of

Master of Science

Department of Mathematics

2001

THE UNIVERSITY OF MANITOBA

FACULTY OF GRADUATE STUDIES

*****

COPYRIGHT PERMISSION

AN INITIAL MOVING-BOUNDARY VALUE PROBLEM ASSOCIATED WITH THE SPINNING WAVE EQUATION

BY

STEPHANIE K. OLAFSON

A Thesis/Practicum submitted to the Faculty of Graduate Studies of The University of Manitoba in partial fulfillment of the requirement of the degree

of

MASTER OF SCIENCE

Abstract

In this thesis we consider a mathematical model for a spinning string with specified initial-conditions and general Dirichlet-type boundary-conditions specified at the ends of a string, which are allowed to move in a prescribed manner. The resulting problem is known as an initial moving-boundary value problem and represents a model for the dynamics of a tether connecting two separating rocket payload components, which have been spin-stabilized prior to separation.

Two distinct versions of this problem are considered:

1. The "homogenous" problem occurs when the endpoints of the string are allowed to move only along the system's longitudinal axis (i.e. no transverse displacements are allowed).
2. The "non-homogeneous" problem allows the endpoints to experience transverse displacements from the longitudinal axis during the deployment of the tether.

The solution of each of these problems involves a number of transformations of variables, which reduce the system of coupled partial differential equations to the standard hypergeometric ordinary differential equation. In the homogeneous case, the resulting solution is obtained through the use of a (complex) Fourier exponential series expansion. Two illustrative examples are constructed. In the non-homogeneous case, the introduction of the Laplace transform gives rise to a "theoretical" solution whose practicality is questionable. An example illustrating this situation is completed using the method of d'Alembert.

Although much of this discussion allows for a general separation scheme of the two payloads, all of the examples assume that the end points separate at a constant velocity.

To my Parents…

my wings.

Acknowledgements

I would like to express my sincere appreciation for my advisor, Dr. Thomas G. Berry. His enthusiasm, determination and perseverance through the last two years of this research have been unfaltering. I thank him for all he has taught me in and outside of the classroom, and throughout the course of this research.

I also thank the Department of Mathematics for their financial support and for providing me with the opportunity to teach during my graduate studies.

And to Steven Theriault who has shown me, by way of example, the importance of loving what you do.

Finally, I am indebted to my parents for all of their love and support. Their belief in me has allowed me to believe all is possible. They have given me a truly blessed life.

Contents

Chapter

Figures

Figure

Tables

Table

Chapter 1

Mathematical Model for a Spinning String with a General Moving Boundary

1.1 Introduction

Tethered spacecraft have received considerable worldwide attention in recent years. The second edition of the NASA publication "Tethers in Space Handbook" [Tet] proposed numerous applications for tethers in space. Although many of these applications have not yet been developed, several missions involving tethered spacecraft have been flown with varying degrees of success. The most notable are the tethered satellite system (TSS1 and TSS1R), jointly sponsored by NASA and the Italian Space Agency, and Project Oedipus, jointly sponsored by NASA and the Canadian Space Agency. Of particular and unique interest in the Canadian program is the spin-stabilization of the sounding rocket payload prior to tether deployment.

In the Canadian Space Agency's Oedipus Project, a rocket was deployed and separated into two spin-stabilized sub-payloads (referred to as the forward and aft payloads). Each payload consisted of scientific instrumentation and telemetry systems, and was

connected to the other by a flexible, electrical-conducting tether. Flight data was obtained and post-flight analysis was used as a basis for the development of the mathematical model to be presented and expanded in this thesis.

The purpose of this thesis is to contribute to the understanding of the dynamics of tethers for space applications, through the use of analytical techniques. In particular, wave dynamics models involving partial differential equations, as extensions of the one-dimensional wave equation, with appropriate initial- and boundary-conditions, will be investigated. The boundary conditions will be specified on moving boundaries, corresponding to the end conditions at the moving ends of a deploying tether subjected to forces resulting from the gross payload dynamics.

1.2 Mathematical Formulation of Model

For the purpose of the following discussion, we consider the right-handed coordinate system (x, u_1, u_2) as shown in Diagram 1.2.1.

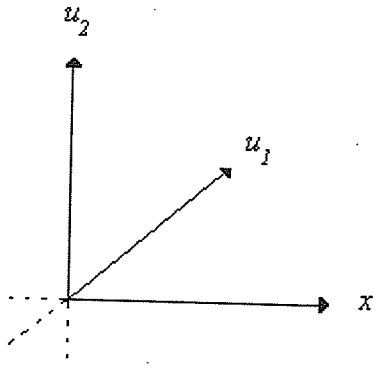

Diagram 1.2.1

In this coordinate system we shall regard the x-axis as representing the equilibrium position of the tether, and hence x labels the position of a point along the tether, and we shall interpret the two-dimensional vector $\vec{u} = \vec{u}(x,t) = u_1(x,t)\hat{j} + u_2(x,t)\hat{k}$ as representing the vectorial transverse displacement of a point on the tether from its equilibrium position at position x at time t.

The initial attempts [Ber 1], [Qin] to model the "forced" transverse vibrations of the Oedipus tether involved the use of the two-dimensional wave equation

$$\frac{\partial^2 \vec{u}}{\partial t^2} = c^2 \frac{\partial^2 \vec{u}}{\partial x^2} + \vec{f}\left(x, t, \vec{u}, \frac{\partial \vec{u}}{\partial x}, \frac{\partial \vec{u}}{\partial t}\right),$$

in which the two-dimensional vector field

$$\vec{f}\left(x, t, \vec{u}, \frac{\partial \vec{u}}{\partial x}, \frac{\partial \vec{u}}{\partial t}\right) = f_y \hat{j} + f_z \hat{k}$$

is to be interpreted as the transverse force per unit mass acting on the tether, and the positive constant c represents the transmission velocity for the waves propagating along the tether. As usual, the value of c may be calculated as

$$c = \sqrt{T/\rho}$$

in which T denotes the longitudinal tension in the tether and ρ is the linear mass density of the tether [Zau p.193].

For completeness and for future reference, we note that the above model and its subsequent generalization are based on a variety of essential assumptions, as have been summarized previously by J. Qin [Qin], namely:

1) Each point on the tether is allowed to move only within a transverse plane, i.e., in a plane perpendicular to the equilibrium position. Only transverse motion is allowed. This may be interpreted to mean that

the longitudinal component of the tension is constant along the tether so that no compression or stretching occurs.

2) Deflections are small in comparison with the total length of the tether, so that their squares or higher powers may be neglected.

3) The slope at any point of the deflected tether is small compared with the length of the tether.

In view of the above assumptions Qin [Qin] states that the following mathematical interpretations can be deduced:

a) The difference between the length of the tether and the distance between its end-points is negligible,

b) The tension is constant along the tether as well as constant in time.

The Oedipus-A flight data exhibited that the aft payload experienced a "coning" motion which was likely caused by the interaction of the dynamics of the tether with that of the sub-payloads, all of which were spinning about the longitudinal axis of the system at a rate of approximately 1 cycle per second [Ber 2 p.25]. Thus, to account for the spin of the system during tether deployment, we introduce the "rotational-time-derivative" of a general 3-dimensional vector $\vec{v} = \vec{v}(x,t)$, which is defined as

$$D_t \vec{v} \equiv \frac{D\vec{v}}{Dt} = \frac{\partial \vec{v}}{\partial t} + \vec{\omega} \times \vec{v}, \tag{1.2.1}$$

where $\frac{\partial \vec{v}}{\partial t}$ denotes the time-derivative of $\vec{v}$, $\times$ denotes the vector cross-product operator, and $\vec{\omega} \times \vec{v}$ is the rotational velocity at position x at time t induced by the local spin vector $\vec{\omega} = \vec{\omega}(x,t) = \omega_x \hat{i} + \omega_y \hat{j} + \omega_z \hat{k}$.

Following Qin [Qin], the basic two-dimensional wave dynamics model is thus modified to the form

$$\frac{D^2\vec{u}}{Dt^2} = c^2 \frac{\partial^2 \vec{u}}{\partial x^2} + \vec{f}\left(x, t, \vec{u}, \frac{\partial \vec{u}}{\partial x}, \frac{\partial \vec{u}}{\partial t}\right),$$

or equivalently, by virtue of (1.2.1),

$$\frac{\partial^2 \vec{u}}{\partial t^2} + \frac{\partial \vec{\omega}}{\partial t} \times \vec{u} + 2\left(\vec{\omega} \times \frac{\partial \vec{u}}{\partial t}\right) - \omega^2 \vec{u} + (\vec{\omega} \cdot \vec{u})\vec{\omega}$$

$$= c^2 \frac{\partial^2 \vec{u}}{\partial x^2} + \vec{f}\left(x, t, \vec{u}, \frac{\partial \vec{u}}{\partial x}, \frac{\partial \vec{u}}{\partial t}\right). \qquad (1.2.2)$$

To simplify this model we now employ a number of physical assumptions, introduced previously by Qin [Qin]:

a) Since only transverse displacements of the tether are allowed, the generalized displacement vector $\vec{u} = \vec{u}(x,t) = u_x \hat{i} + u_y \hat{j} + u_z \hat{k}$ satisfies the conditions

$$u_x = 0\,,\ u_y = u_1\,,\ u_z = u_2\,.$$

b) We also assume the angular velocity $\vec{\omega}(x,t)$ is constant, so that the angular acceleration is zero, i.e.,

$$\frac{\partial \vec{\omega}}{\partial t} = \vec{0}\,.$$

c) Due to fact that system spins about its longitudinal axis, and since all displacements of the tether are assumed to be small, the local spin vector $\vec{\omega} = \vec{\omega}(x,t)$ may be approximated as

$$\vec{\omega} = \omega \hat{i}\,,$$

where the "spin scalar" ω is constant in both position and time. In addition, since $\vec{u}$ and $\vec{\omega}$ are perpendicular to each other at each point along the tether,

$$\vec{\omega} \cdot \vec{u} = 0 .$$

d) Lastly, since the longitudinal tension in the tether is assumed to be constant, there are no longitudinal external forces acting along the tether, and therefore

$$f_x = 0 .$$

With the above assumptions, Qin shows that the system (1.2.2) reduces to

$$\frac{\partial^2 \vec{u}}{\partial t^2} + 2\vec{\omega} \times \frac{\partial \vec{u}}{\partial t} - \omega^2 \vec{u} = c^2 \frac{\partial^2 \vec{u}}{\partial x^2} + \vec{f}\left(x, t, \vec{u}, \frac{\partial \vec{u}}{\partial x}, \frac{\partial \vec{u}}{\partial t} \right). \qquad (1.2.3)$$

So that we have consistency in our notation, we now write in addition to $\vec{u} = u_y \hat{j} + u_z \hat{k} = u_1 \hat{j} + u_2 \hat{k}$ that $\vec{f} = F_1 \hat{j} + F_2 \hat{k}$, so that (1.2.3) can be written in component form to yield the pair of scalar partial differential equations

$$\frac{\partial^2 u_1}{\partial t^2} - 2\omega \frac{\partial u_2}{\partial t} - \omega^2 u_1 = c^2 \frac{\partial^2 u_1}{\partial x^2} + F_1\left(x, t, u_1, u_2, \frac{\partial u_1}{\partial x}, \frac{\partial u_2}{\partial x}, \frac{\partial u_1}{\partial t}, \frac{\partial u_2}{\partial t} \right),$$

$$\frac{\partial^2 u_2}{\partial t^2} + 2\omega \frac{\partial u_1}{\partial t} - \omega^2 u_2 = c^2 \frac{\partial^2 u_2}{\partial x^2} + F_2\left(x, t, u_1, u_2, \frac{\partial u_1}{\partial x}, \frac{\partial u_2}{\partial x}, \frac{\partial u_1}{\partial t}, \frac{\partial u_2}{\partial t} \right).$$

Moreover, we shall assume throughout the remainder of this thesis that there are no external forces acting on the tether, since throughout the deployment phase of the mission the system is in a state of free-fall in a vacuum, negating the presence of forces due to gravity and aerodynamic drag. The result is the following coupled, linear, homogeneous system of second-order partial differential equations, namely

$$\left.\begin{aligned} \frac{\partial^2 u_1}{\partial t^2} - 2\omega \frac{\partial u_2}{\partial t} - \omega^2 u_1 &= c^2 \frac{\partial^2 u_1}{\partial x^2}, \\ \frac{\partial^2 u_2}{\partial t^2} + 2\omega \frac{\partial u_1}{\partial t} - \omega^2 u_2 &= c^2 \frac{\partial^2 u_2}{\partial x^2}, \end{aligned}\right\} \tag{1.2.4}$$

where $u_1 = u_1(x,t)$ and $u_2 = u_2(x,t)$ denote the two components of the transverse displacement of the tether at position x at time t in the orthogonal coordinate system (x, u_1, u_2) and ω is a constant representing the rotation rate of the system about its longitudinal axis.

System (1.2.4) will be studied in an effort to investigate the dynamics of the tether as a result of the state of the system at some initial time (for convenience, assumed to be $t = 0$) and the ensuing dynamics of the payload components at its ends. The initial state of the system is described through the initial conditions

$$\left.\begin{aligned} \vec{u}(x,0) &= f_1(x)\hat{j} + f_2(x)\hat{k}, \\ \left.\frac{\partial \vec{u}}{\partial t}\right|_{(x,0)} &= g_1(x)\hat{j} + g_2(x)\hat{k}, \end{aligned}\right\} \tag{1.2.5}$$

(which represent, respectively, the transverse displacement of the tether from its equilibrium position at time t, and the initial velocity distribution for the tether). Moreover, it is assumed that the sub-payloads may be regarded as point-masses and their positions may be identified with the points $x = 0$ and $x = S(t)$, with their motions described by the Dirichlet boundary conditions

$$\left.\begin{aligned} \vec{u}(0,t) &= p_1(t)\hat{j} + p_2(t)\hat{k}, \\ \vec{u}(S(t),t) &= q_1(t)\hat{j} + q_2(t)\hat{k}, \end{aligned}\right\} \tag{1.2.6}$$

which identify the transverse displacements of the ends of the tether (and hence at the sub-payloads) as functions of time at positions $x = 0$ and $x = S(t)$, respectively.

Remarks: 1) In view of the fact that the boundary-conditions are assumed to be prescribed, it is tacitly assumed in the above that the dynamics of the sub-payloads have a non-trivial impact on the dynamics of the tether, but that the dynamics of the tether have a negligible impact on the dynamics of the payloads (whose motions are assumed to be known).

2) Since tether deployment is our prime concern, we shall assume that the function $S(t)$, which describes the instantaneous position of the moving tether endpoint, satisfies the condition that

$$0 \leq S'(t) < c,$$

the first inequality being introduced to guarantee a non-negative separation velocity of the sub-payload components, and the latter imposed to avoid the presence of "shock waves" which could result when the separation velocity of the endpoints of the tether exceeds the wave transmission velocity c along the tether [Car]. More precisely, we will take the motion of the forward payload relative to the aft payload. Thus, the aft payload remains at $x = 0$ while the forward has the position $x = S(t)$.

Comment: The case of a fixed length tether is a special case corresponding to the condition $S'(t) = 0$.

1.3 Summary of Mathematical Model

For future reference, it is our purpose in this thesis to investigate analytical solutions of the coupled system of second order, linear, partial differential equations (1.2.4), namely

$$\left.\begin{aligned} \frac{\partial^2 u_1}{\partial t^2} - 2\omega\frac{\partial u_2}{\partial t} - \omega^2 u_1 &= c^2\frac{\partial^2 u_1}{\partial x^2}, \\ \frac{\partial^2 u_2}{\partial t^2} + 2\omega\frac{\partial u_1}{\partial t} - \omega^2 u_2 &= c^2\frac{\partial^2 u_2}{\partial x^2}, \end{aligned}\right\} \quad \text{for } t \geq 0,\ \ 0 \leq x \leq S(t) \tag{1.3.1a}$$

subject to appropriate initial-conditions (1.2.5), or equivalently

$$\left.\begin{aligned} u_1(x,0) &= f_1(x), \qquad \frac{\partial u_1}{\partial t}(x,0) = g_1(x), \\ u_2(x,0) &= f_2(x), \qquad \frac{\partial u_2}{\partial t}(x,0) = g_2(x), \end{aligned}\right\} \tag{1.3.1b}$$

in which $0 \leq x \leq S(t)$, and subject to "moving" boundary-conditions (1.2.6), namely

$$u_1(0,t) = p_1(t), \qquad u_2(0,t) = p_2(t), \tag{1.3.1c}$$

$$u_1(S(t),t) = q_1(t), \qquad u_2(S(t),t) = q_2(t), \tag{1.3.1d}$$

for $t \geq 0$.

The system (1.3.1a) – (1.3.1d), referred to collectively as (1.3.1), is hence known as an initial-moving-boundary-value problem (IMBVP).

1.4 Outline of Thesis

Throughout this thesis, a number of techniques are applied to the IMBVP (1.3.1) in order that a solution to this problem may be found. In both the homogeneous problem studied in Chapter 3, and in the non-homogeneous problem, as investigated in Chapter 4, the

techniques applied are extensions and/or generalizations of work previously done by T. G. Berry, C. F. Carrier, N. Corbett, H. P Greenspan, J. Qin and J. J. Williams. These extensions and generalizations are as follows:

1. In section 3 of Chapter 2, a boundary transformation previously introduced by Berry and Williams [Ber 4], and Qin [Qin] is generalized to allow for the analysis of the dynamics of a deploying tether with an increasing distance between the forward and aft payloads. Of course the case of a tether of fixed length, as discussed by Qin [Qin], is simply a special case. To study this phenomenon of the moving-boundary, the function $S(t)$ that represents the general moving-boundary is included in this transformation.
2. In section 4 of Chapter 2, a transformation originally presented by Carrier [Car] and Greenspan [Gre], which considers only a linearly moving-boundary $S(t) = kt + L$, is generalized to include the case of the general moving-boundary $S(t)$.
3. In section 2 of Chapter 4, the moving-boundary is chosen to be a linearly moving-boundary $S(t) = kt + L$ as was done in [Cor]. However, rather than beginning with homogeneous boundary-conditions at both ends, we consider the case of two general (non-zero) boundary conditions. By inclusion of the modified boundary transformation from §2.3, we are able to extend the analysis in [Gre] which allows only for a non-homogeneous boundary-condition at one end.

Chapter 2

Transformations

2.1 Introduction

In this chapter we will introduce a succession of transformations of variables to the system (1.3.1) in an effort to reduce the system to a form to which standard techniques may be applied to obtain analytical solutions. In addition, the results of the application of these transformations allow us to draw some conclusions concerning the order of differentiability of solutions of the system based on the assumed form of the initial- and boundary-data appearing in (1.3.1b) – (1.3.1d).

2.2 Complex Transformations

The effect of the first transformation is to reduce the coupled system (1.3.1) into a single second-order partial differential equation in a complex function. To do so, we consider the complex transformation

$$V(x,t) = u_1(x,t) + iu_2(x,t). \tag{2.2.1}$$

By differentiation of this function $V(x,t)$ and substitution into the system (1.3.1), we obtain

$$\frac{\partial^2 V}{\partial t^2} + 2i\omega \frac{\partial V}{\partial t} - \omega^2 V = c^2 \frac{\partial^2 V}{\partial x^2}, \tag{2.2.2a}$$

$$V(x,0) = f_1(x) + if_2(x), \qquad \frac{\partial V}{\partial t}(x,0) = g_1(x) + ig_2(x), \tag{2.2.2b}$$

$$V(0,t) = p_1(t) + ip_2(t), \qquad V(S(t),t) = q_1(t) + iq_2(t), \tag{2.2.2c,d}$$

in which $t \geq 0$, and $0 \leq x \leq S(t)$.

The differential equation (2.2.2a) is more compact than (1.3.1a), and may be written in an alternate form in which we eliminate the first derivative term. In particular, we let

$$W(x,t) = e^{i\omega t} V(x,t), \tag{2.2.3}$$

which implies that

$$\frac{\partial V}{\partial x} = e^{-i\omega t} \frac{\partial W}{\partial x},$$

$$\frac{\partial^2 V}{\partial x^2} = e^{-i\omega t} \frac{\partial^2 W}{\partial x^2},$$

$$\frac{\partial V}{\partial t} = e^{-i\omega t} \left(\frac{\partial W}{\partial t} - i\omega W \right),$$

$$\frac{\partial^2 V}{\partial t^2} = e^{-i\omega t} \left(\frac{\partial^2 W}{\partial t^2} - 2i\omega \frac{\partial W}{\partial t} - \omega^2 W \right).$$

Substitution of the above derivatives into (2.2.2) yields

$$\frac{\partial^2 W}{\partial t^2} = c^2 \frac{\partial^2 W}{\partial x^2}, \tag{2.2.4a}$$

which is the standard one-dimensional wave equation. In addition, the corresponding transformed initial- and boundary-conditions may be rewritten as

$$W(x,0) = F(x), \qquad \frac{\partial W}{\partial t}(x,0) = G(x), \quad \text{for} \quad 0 \leq x \leq S(t), \tag{2.2.4b}$$

and

$$W(0,t) = P(t), \qquad W(S(t),t) = Q(t), \quad \text{for } t \geq 0, \tag{2.2.4c,d}$$

where for simplicity we have adopted the notation

$$\left.\begin{aligned} F(x) &= f_1(x) + if_2(x), \\ G(x) &= g_1(x) - \omega f_2(x) + i[g_2(x) + \omega f_1(x)], \\ P(t) &= p_1(t)\cos(\omega t) - p_2(t)\sin(\omega t) + i[p_1(t)\sin(\omega t) + p_2(t)\cos(\omega t)], \\ Q(t) &= q_1(t)\cos(\omega t) - q_2(t)\sin(\omega t) + i[q_1(t)\sin(\omega t) + q_2(t)\cos(\omega t)]. \end{aligned}\right\} \tag{2.2.5}$$

The system (2.2.4) is in the form of the standard wave equation with standard initial- and boundary-conditions, and hence solutions may be sought using known techniques. One such method uses the d'Alembert solution, where the assumed solution is of the form

$$W(x,t) = \varphi(x+ct) + \psi(x-ct)$$

in which $\varphi(x+ct)$ and $\psi(x-ct)$ denote differentiable functions whose forms depend on the initial- and boundary-conditions (2.2.4b) – (2.2.4d) [Myi p.55], [Cor p.8].

This observation leads us to draw some conclusions concerning the differentiability of solutions of (2.2.4) and compatibility conditions that must be imposed on our initial- and boundary-conditions so that our solution $W(x,t)$ is of the appropriate differentiability class.

As in section 2.3 of [Cor], the order of differentiability of solutions of (2.2.4) is determined through the following conditions:

1. If $F(x)$, $P(t)$, $Q(t)$, $S(t) \in C^0$, $G(x)$ is integrable, $F(0) = P(0)$ and $F(S(0)) = Q(0)$, then $W(x,t) \in C^0$.

2. If $F(x),\ P(t),\ Q(t),\ S(t) \in C^1$, $G(x) \in C^0$, $F(0) = P(0)$,

   $F(S(0)) = Q(0)$, $G(0) = P'(0)$ and $S'(0)F'(S(0)) + G(S(0)) = Q'(0)$,

   then $W(x,t) \in C^1$.

3. If $F(x),\ P(t),\ Q(t),\ S(t) \in C^2$, $G(x) \in C^1$, $F(0) = P(0)$,

   $F(S(0)) = Q(0)$, $G(0) = P'(0)$, $S'(0)F'(S(0)) + G(S(0)) = Q'(0)$,

   $F''(0) = P''(0)$ and

   $([S'(0)]^2 + 1)F''(S(0)) + 2S'(0)G'(S(0)) + S''(0)F'(S(0)) = Q''(0)$,

   then $W(x,t) \in C^2$.

In the above, C^0, C^1, and C^2 respectively represent the class of continuous functions, the class of functions whose first derivatives are continuous, and the class of functions whose second derivatives are continuous.

2.3 Boundary Transformation

With the introduction of two complex transformations, the system (1.3.1) was reduced to a one-dimensional complex wave equation with general complex initial- and boundary-conditions. Our next goal is to force this system to have zero boundary-conditions which is accomplished by use of the transformation

$$Z(x,t) = W(x,t) + \frac{x}{S(t)}[P(t) - Q(t)] - P(t), \tag{2.3.1}$$

in which it is necessary to assume that $S(t) \neq 0$. We observe that this transformation was introduced in [Ber 4], [Qin p.83] in the special case when $S(t) = L$ (constant).

It is noted that the differentiability class of $Z(x,t)$ is the same as that of $W(x,t)$, $P(t)$, $Q(t)$ and $S(t)$, so that the above observations concerning the differentiability and compatibility conditions apply equally well to $Z(x,t)$ as they do to $W(x,t)$.

We continue our analysis by considering the partial derivatives of (2.3.1):

$$\frac{\partial W}{\partial x} = \frac{\partial Z}{\partial x} - \frac{1}{S(t)}[P(t) - Q(t)],$$

$$\frac{\partial^2 W}{\partial x^2} = \frac{\partial^2 Z}{\partial x^2},$$

$$\frac{\partial W}{\partial t} = \frac{\partial Z}{\partial t} - \frac{x}{S(t)}[P'(t) - Q'(t)] + \frac{xS'(t)}{[S(t)]^2}[P(t) - Q(t)] + P'(t),$$

$$\frac{\partial^2 W}{\partial t^2} = \frac{\partial^2 Z}{\partial t^2} + \frac{x}{S(t)}\left\{\frac{S''(t)}{S(t)} - 2\left[\frac{S'(t)}{S(t)}\right]^2\right\}[P(t) - Q(t)] + \frac{2xS'(t)}{[S(t)]^2}[P'(t) - Q'(t)]$$

$$- \frac{x}{S(t)}[P''(t) - Q''(t)] + P''(t).$$

Therefore, the partial differential equation (2.2.4) becomes

$$\frac{\partial^2 Z}{\partial t^2}(x,t) = c^2 \frac{\partial^2 Z}{\partial x^2}(x,t) + A(x,t), \tag{2.3.2a}$$

in which $A(x,t)$ denotes the function

$$A(x,t) = \frac{x}{S(t)}[P''(t) - Q''(t)] - \frac{x}{[S(t)]^2}\left\{S''(t) - 2\frac{[S'(t)]^2}{S(t)}\right\}[P(t) - Q(t)]$$

$$- \frac{2xS'(t)}{[S(t)]^2}[P'(t) - Q'(t)] - P''(t). \tag{2.3.3}$$

For this new system, the initial- and boundary-conditions are given by

$$Z(x,0) = \alpha(x), \qquad \frac{\partial Z}{\partial t}(x,0) = \beta(x), \quad \text{for } 0 \le x \le S(t), \tag{2.3.2b}$$

$$Z(0,t) = Z(S(t),t) = 0, \quad \text{for } t \ge 0, \tag{2.3.2c,d}$$

with $\alpha(x)$ and $\beta(x)$ given by

$$\left.\begin{aligned} \alpha(x) &= F(x) + \frac{x}{S(0)}[P(0) - Q(0)] - P(0), \\ \beta(x) &= G(x) + \frac{x}{S(0)}[P'(0) - Q'(0)] - \frac{xS'(0)}{[S(0)]^2}[P(0) - Q(0)] - P'(0). \end{aligned}\right\} \tag{2.3.4}$$

Observations: 1) Although we now have zero boundary-conditions, which may lead one to consider the possibility for the solution to be found using a Fourier sine series expansion [Ber 4], this has come at the expense of now having a non-homogeneous partial differential equation. In [Qin], a Fourier sine series solution of the form

$$Z(x,t) = \sum_{n=1}^{\infty} Z_n(t) \sin \frac{n\pi x}{L}$$

was successfully found for the case when $S'(t) = 0$; however, when $S'(t) \neq 0$, this method fails. The problem lies in the fact that for a general $S(t)$, the analogous solution would be of the form

$$Z(x,t) = \sum_{n=1}^{\infty} Z_n(t) \sin \frac{n\pi x}{S(t)}.$$

The appearance of $S(t)$ in the sine function, prevents the separation of the two variables x and t, which is the whole purpose of Fourier series analysis.

2) $A(x,t)$ has a very simple dependence on x, namely, $A(x,t)$ is a linear function in x, with coefficients being functions of t. We will emphasize this simple dependence by rewriting (2.3.3) as

$$A(x,t) = xR(t) - P''(t), \tag{2.3.5}$$

where

$$R(t) = \frac{1}{S(t)}[P''(t) - Q''(t)] - \frac{1}{[S(t)]^2}\left\{S''(t) - 2\frac{[S'(t)]^2}{S(t)}\right\}[P(t) - Q(t)]$$

$$- \frac{2S'(t)}{[S(t)]^2}[P'(t) - Q'(t)], \tag{2.3.6}$$

and thus (2.3.2a) may be written in the alternate form

$$\frac{\partial^2 Z}{\partial t^2}(x,t) = c^2 \frac{\partial^2 Z}{\partial x^2}(x,t) + xR(t) - P''(t).$$

3) If the original problem (1.3.1) or (2.2.4) has zero boundary-conditions, so that $P(t) = Q(t) = 0$ are prescribed, the boundary transformation (2.3.1) is trivial, and moreover $A(x,t) = 0$, a fact which will be exploited in Chapter 3.

2.4 Generalized Carrier-Greenspan Transformation

In this section we introduce an additional transformation, which is a generalization of one first introduced by Carrier [Car] and later by Greenspan [Gre] and has the effect of turning the general moving-boundary "domain" into a vertical strip as shown in Diagrams 2.4.1 and 2.4.2.

Consider the dimensionless variables (ξ, τ), defined by

$$\xi = \frac{S'(0)}{cS(t)}x, \qquad \tau = \ln\left[\frac{S(t)}{S(0)}\right], \tag{2.4.1}$$

in which the function $S(t)$ represents as usual the position of the moving end of the tether, and is required to satisfy the restriction that $0 \le S'(t) < c$. As mentioned in section 1.2, $S'(t) < 0$ corresponds to tether retrieval (rather than tether deployment) and hence will be ignored. In addition, the case of a fixed length tether corresponds to the case when $S'(t) = 0$, and has been discussed in [Qin].

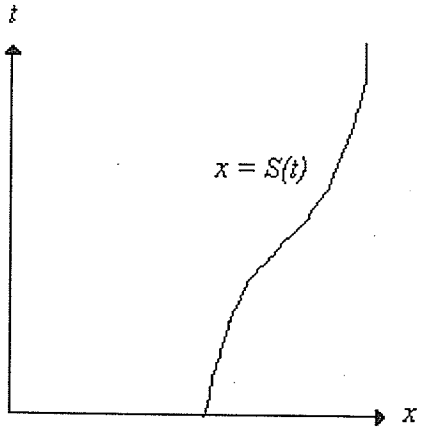

Diagram 2.4.1

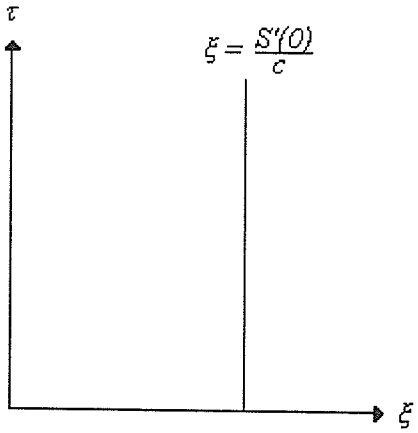

Diagram 2.4.2

From (2.4.1) we have

$$\frac{\partial(\xi,\tau)}{\partial(x,t)} = \begin{vmatrix} \xi_x & \xi_t \\ \tau_x & \tau_t \end{vmatrix}$$

$$= \begin{vmatrix} \dfrac{S'(0)}{cS(t)} & -\dfrac{S'(0)S'(t)x}{c[S(t)]^2} \\ 0 & \dfrac{S'(t)}{S(t)} \end{vmatrix}$$

$$= \frac{1}{c}\frac{S'(0)S'(t)}{[S(t)]^2}$$

which is clearly positive provided $S(t) \neq 0$ and $S'(t) > 0$, and hence (2.4.1) is invertible [Zau p.50]. In particular, if $S'(t) > 0$, $S(t)$ is a monotonic (increasing) function, and the function $v = S(t)$ has an inverse of the form $t = \vartheta(v) = S^{-1}(v)$ [Ste p.351]. In addition, it may be readily shown that the transformation (2.4.1) has as its inverse the transformation

$$\left.\begin{aligned} x &= \frac{cS(0)\xi e^{\tau}}{S'(0)} \equiv \Psi(\xi,\tau), \\ t &= \vartheta(S(0)e^{\tau}) \equiv \Gamma(\tau). \end{aligned}\right\} \tag{2.4.2}$$

Moreover, if we let

$$\widetilde{Z}(\xi,\tau) \equiv Z(\Psi(\xi,\tau),\Gamma(\tau))$$

$$\Leftrightarrow Z(x,t) \equiv \widetilde{Z}\left(\frac{S'(0)x}{cS(t)}, \ln\left[\frac{S(t)}{S(0)}\right]\right),$$

we may immediately write (2.3.2a) in the form

$$\left[\left(\frac{\partial\xi}{\partial t}\right)^2 - c^2\left(\frac{\partial\xi}{\partial x}\right)^2\right]\frac{\partial^2\widetilde{Z}}{\partial\xi^2} + 2\left(\frac{\partial\xi}{\partial t}\right)\left(\frac{\partial\tau}{\partial t}\right)\frac{\partial^2\widetilde{Z}}{\partial\xi\partial\tau} + \left(\frac{\partial\tau}{\partial t}\right)^2\frac{\partial^2\widetilde{Z}}{\partial\tau^2}$$

$$+\left(\frac{\partial^2\xi}{\partial t^2}\right)\frac{\partial\widetilde{Z}}{\partial\xi} + \left(\frac{\partial^2\tau}{\partial t^2}\right)\frac{\partial\widetilde{Z}}{\partial\tau} = \widetilde{A}(\xi,\tau), \tag{2.4.3a}$$

where

$$\widetilde{A}(\xi,\tau) \equiv A\big(\Psi(\xi,\tau),\Gamma(\tau)\big)$$

and

$$\frac{\partial\xi}{\partial x} = \frac{S'(0)}{cS(t)},$$

$$\frac{\partial \xi}{\partial t} = -\frac{x}{c}\frac{S'(0)S'(t)}{[S(t)]^2},$$

$$\frac{\partial^2 \xi}{\partial t^2} = -\frac{xS'(0)}{c}\left\{\frac{S(t)S''(t) - 2[S'(t)]^2}{[S(t)]^3}\right\},$$

$$\frac{\partial \tau}{\partial t} = \frac{S'(t)}{S(t)},$$

$$\frac{\partial^2 \tau}{\partial t^2} = \frac{1}{S(t)}\left\{S''(t) - \frac{[S'(t)]^2}{S(t)}\right\},$$

in which it is now advisable to eliminate x and t through the use of (2.4.2). In addition, the initial- and boundary-conditions become

$$\widetilde{Z}(\xi,0) = \widetilde{\alpha}(\xi), \qquad \frac{\partial \widetilde{Z}}{\partial \tau}(\xi,0) = \widetilde{\beta}^*(\xi), \qquad \text{for } 0 \le \xi \le \frac{S'(0)}{c}, \tag{2.4.3b}$$

$$\widetilde{Z}(0,\tau) = \widetilde{Z}\left(\frac{S'(0)}{c},\tau\right) = 0, \qquad \text{for } \tau \ge 0. \tag{2.4.3c,d}$$

where

$$\widetilde{\beta}^*(\xi) = \frac{S(0)}{S'(0)}\widetilde{\beta}(\xi) - \xi\widetilde{\alpha}'(\xi)\left[\frac{S(0)S''(0) - [S'(0)]^2}{[S'(0)]^2}\right], \tag{2.4.4a}$$

and

$$\widetilde{\alpha}(\xi) \equiv \alpha(\Psi(\xi,0)) = \alpha\big(\Psi(\xi,\tau)\big)\Big|_{\tau=0}, \tag{2.4.4b}$$

$$\widetilde{\beta}(\xi) \equiv \beta(\Psi(\xi,0)) = \beta\big(\Psi(\xi,\tau)\big)\Big|_{\tau=0}. \tag{2.4.4c}$$

Note: Since ξ is restricted to lie between the two constant values 0 and $\frac{S'(0)}{c}$, the tether is now effectively of "fixed length" (relative to this system of coordinates).

Chapter 3

The Homogeneous Problem

3.1 Introduction

In this chapter, we consider homogeneous forms of the various problems (2.2.2), (2.3.2) and (2.4.3) appearing in the previous chapter, in an effort to find special solutions of the system (1.3.1). The homogeneities that we consider may appear either in the boundary-conditions or in the governing partial differential equation itself, and are selected to appear at various stages in the transformation process discussed in Chapter 2.

3.2 The Imposition of Homogeneity Conditions

As noted earlier, when $P(t) = Q(t) = 0$, the "boundary transformation" (2.3.1) of section 2.3 has no effect and our IMBVP (2.2.2) or (2.3.2) involves both a homogeneous partial differential equation and homogeneous boundary-conditions, and may be solved readily, under appropriate conditions, using either of the following two methods:

i) d'Alembert's method, as in sections 6.2 and 6.3 of [Qin], in which there is assumed to be a linearly-moving boundary given by $S(t) = kt + L$ for k, L positive real constants with $k < c$,

ii) Fourier sine series representation of $W(x,t)$ (or equivalently $Z(x,t)$), as in sections 5.3 and 5.4 of [Qin], in the case of a fixed length string (i.e., when $S(t) = L$).

In either of the above, the Carrier-Greenspan transformation (2.4.1) of section 2.4 is not used. As an alternative to these two procedures, we shall investigate in section 3.3 the effect of the inclusion of the Carrier-Greenspan transformation in the case when $P(t) = Q(t) = 0$. This analysis involves a separation of variables technique, based on the use of complex exponential functions, and culminates in two illustrative examples which display respectively planar and non-planar waves on a spinning string with a linearly-moving endpoint, and represents a generalization of the procedure outlined in section 3.2 of [Cor].

On the other hand, it is noted that when $P(t) \neq 0$ and/or $Q(t) \neq 0$, (2.3.2) involves (in general) a non-homogeneous differential equation subject to homogeneous boundary-conditions (2.3.2c,d), and the question naturally arises as to whether it is possible to make both the differential equation and its boundary-conditions homogeneous? To this end, we demand that

$$A(x,t) \equiv 0 \tag{3.2.1}$$

in which $A(x,t)$ is given by (2.3.3). It should be noted that when (3.2.1) is satisfied, $\tilde{A}(\xi,\tau)$ is also identically zero, so that both (2.3.2) and (2.4.3) involve homogeneous partial differential equations with homogeneous boundary-conditions.

By virtue of (2.3.5), we may conclude that (3.2.1) is certainly satisfied if $R(t) \equiv 0$ and $P''(t) \equiv 0$. The latter condition, of course, implies that $P(t)$ is a linear function in t, i.e.,

$$P(t) = at + b \tag{3.2.2}$$

for some real or complex constants a and b. In addition, (2.3.6) implies that $R(t) \equiv 0$ is clearly satisfied if $Q(t) = P(t) = at + b$, in which case the two ends of the tether are "driven" in exactly the same manner, although one endpoint is "moving" while the other is "stationary." Although such a situation is conceivable, the fact that the amplitudes of the driving displacements at the two ends become unbounded makes this case physically uninteresting. Thus, this case will not be pursued here.

More generally, if $P''(t) \equiv 0$ (and as noted above $P(t)$ must then be of the form $P(t) = at + b$), then $R(t) \equiv 0$ implies, by virtue of (2.3.6), that

$$-\frac{1}{S(t)}[Q''(t)] - \frac{1}{[S(t)]^2}\left\{S''(t) - 2\frac{[S'(t)]^2}{S(t)}\right\}[at + b - Q(t)]$$

$$-\frac{2S'(t)}{[S(t)]^2}[a - Q'(t)] = 0\,. \tag{3.2.3}$$

In particular, if we consider the case of a linearly-moving endpoint, given by

$$S(t) = kt + L$$

in which k and L are fixed positive real constants and $k < c$, $Q(t)$ is determined as a solution of the second-order non-homogeneous differential equation

$$(kt + L)^2 Q''(t) - 2k(kt + L)Q'(t) + 2k^2 Q(t) = 2k(bk - aL)\,. \tag{3.2.4}$$

Let us introduce a change of variables such that

$$\zeta = kt + L\,,$$

with its corresponding inverse

$$t = \frac{\zeta - L}{k},$$

so that

$$\overline{Q}(\zeta) = Q\left(\frac{\zeta - L}{k}\right) = Q(t)\Big|_{t=\frac{\zeta-L}{k}},$$

$$Q(t) = \overline{Q}(kt + L) = \overline{Q}(\zeta)\Big|_{\zeta=kt+L},$$

$$Q'(t) = \frac{dQ}{dt} = \frac{d\overline{Q}}{d\zeta}\frac{d\zeta}{dt} = k\dot{\overline{Q}}(\zeta),$$

and similarly

$$Q''(t) = k^2\ddot{\overline{Q}}(\zeta)$$

where $\cdot$ denotes $\frac{d}{d\zeta}$.

Substitution of the above derivatives into (3.2.4) yields

$$\zeta^2\ddot{\overline{Q}}(\zeta) - 2\zeta\dot{\overline{Q}}(\zeta) + 2\overline{Q}(\zeta) = 2k(bk - aL) \tag{3.2.5}$$

which is a second-order Cauchy-Euler differential equation and its solution is easily obtained.

Firstly, the homogeneous form of the differential equation (3.2.5) is considered, namely

$$\zeta^2\ddot{\overline{Q}}_h(\zeta) - 2\zeta\dot{\overline{Q}}_h(\zeta) + 2\overline{Q}_h(\zeta) = 0, \tag{3.2.6}$$

and its solution $\overline{Q}_h(\zeta)$ is assumed to be of the form

$$\overline{Q}_h(\zeta) = \zeta^m, \tag{3.2.7}$$

where m is some arbitrary constant [Zil p.259]. Through substitution of (3.2.7) into (3.2.6) we determine that $m = 1,\ 2$ and therefore the general solution of (3.2.6) is

$$\overline{Q}_h(\zeta) = a_1\zeta + a_2\zeta^2$$

with a_1, a_2 unknown constants [Zil p.260].

Secondly, we return to the non-homogenous differential equation (3.2.5), and by using the fact that the right-hand side of (3.2.5) is a constant, we assume the particular solution $\overline{Q}_p(\zeta)$ is a constant such that

$$\overline{Q}_p(\zeta) = K.$$

Substitution of this constant function into (3.2.5) determines that

$$K = k(bk + aL).$$

Because $\overline{Q}(\zeta) = \overline{Q}_h(\zeta) + \overline{Q}_p(\zeta)$ is the formal solution of (3.2.5), we have

$$\overline{Q}(\zeta) = a_1\zeta + a_2\zeta^2 + k(bk + aL),$$

and thus by reversing the change of variables $\zeta = kt + L$, the general solution of (3.2.4) is found to be

$$Q(t) = a_1(kt + L) + a_2(kt + L)^2 + k(bk + aL) \qquad (3.2.8)$$

where a_1, a_2 are constants yet to be determined.

Theoretically, once again these forms (3.2.2) and (3.2.8) for the boundary-conditions would yield a homogenous version of (2.3.2). However, the physical significance of these boundary-conditions is questionable and will not be pursued further.

Although the above discussion is by no means complete, it does suggest that attempts to force the differential equation (2.3.2) to be homogeneous with non-homogeneous boundary-conditions are not physically realizable, and hence will be abandoned. This poses no difficulty, because as we have seen the "boundary transformation" (2.3.1) allows us to rewrite the homogeneous differential equation (2.2.4a) with non-homogeneous boundary-conditions (2.2.4c,d) in the form of a non-homogeneous differential equation (2.3.2a) with homogeneous boundary-conditions (2.3.2c,d).

Throughout the remainder of this chapter we will consider the case when the given "boundary" functions $p_1(t)$, $p_2(t)$, $q_1(t)$, $q_2(t)$ in (1.3.1) are all identically zero, so that

$$P(t) = Q(t) \equiv 0 .$$

As indicated above, these conditions not only guarantee homogeneous boundary-conditions but also force the differential equation to be homogeneous. This case is known as the homogeneous IMBVP. Discussion of the non-homogeneous IMBVP will be postponed until Chapter 4.

Throughout the remainder of this thesis, we will consider only the case of a linearly moving endpoint at $x = S(t)$, with $S(t)$ given by

$$S(t) = kt + L$$

in which k and L are positive real constants and $k < c$. It is noted that the special case $k = 0$ corresponds simply to a tether of fixed length, which has been discussed in detail in [Qin].

3.3 The Homogeneous IMBVP

Since our attempt at forcing $A(x,t)$ to be zero, based on certain specifications of the boundary functions $P(t)$ and $Q(t)$, did not produce a physical meaningful model of a spinning string, we now turn our attention to the case of homogeneous boundary-conditions i.e., $P(t) = Q(t) = 0$. As indicated above, these conditions force $A(x,t) = xR(t) - P''(t)$ to be zero and thus make (2.3.2a) homogenous. Let us seek a general solution for this situation, in the case of the linearly-moving endpoint, given by $S(t) = kt + L$. Thus, we wish to solve the system of coupled partial differential equations

$$\left.\begin{aligned} \frac{\partial^2 u_1}{\partial t^2} - 2\omega\frac{\partial u_2}{\partial t} - \omega^2 u_1 &= c^2\frac{\partial^2 u_1}{\partial x^2}, \\ \frac{\partial^2 u_2}{\partial t^2} + 2\omega\frac{\partial u_1}{\partial t} - \omega^2 u_2 &= c^2\frac{\partial^2 u_2}{\partial x^2}, \end{aligned}\right\} \quad t \geq 0, \quad 0 \leq x \leq kt + L \qquad (3.3.1a)$$

subject to the initial-conditions

$$\left.\begin{aligned} u_1(x,0) &= f_1(x), \quad \frac{\partial u_1}{\partial t}(x,0) = g_1(x), \\ u_2(x,0) &= f_2(x), \quad \frac{\partial u_2}{\partial t}(x,0) = g_2(x), \end{aligned}\right\} \quad 0 \leq x \leq kt + L \qquad (3.3.1b)$$

and the homogeneous boundary-conditions

$$u_1(0,t) = u_2(0,t) = u_1(kt + L, t) = u_2(kt + L, t) = 0, \quad t \geq 0. \qquad (3.3.1c)$$

As noted earlier, because we already have zero boundary-conditions, the boundary transformation (2.3.1) does not need to be performed and thus, no non-homogeneities are introduced into the differential equation. Therefore, based on the analysis of the previous chapter, we continue our investigation starting with the differential equation (2.4.3a) which, with $S(t) = kt + L$, becomes

$$(1-\xi^2)\frac{\partial^2 \tilde{Z}}{\partial \xi^2} + 2\xi\frac{\partial^2 \tilde{Z}}{\partial \xi \partial \tau} - \frac{\partial^2 \tilde{Z}}{\partial \tau^2} - 2\xi\frac{\partial \tilde{Z}}{\partial \xi} + \frac{\partial \tilde{Z}}{\partial \tau} = 0 \qquad (3.3.2)$$

where, in agreement with (2.4.1), we have

$$\xi = \frac{kx}{c(kt+L)}, \qquad \tau = \ln\left(\frac{kt+L}{L}\right), \qquad (3.3.3)$$

with the corresponding inverse given by

$$x = \frac{cL}{k}\xi e^{\tau}, \qquad t = \frac{L(e^{\tau}-1)}{k}. \qquad (3.3.4)$$

In seeking a solution, we assume an exponential Fourier series expansion of the form

$$\tilde{Z}(\xi,\tau)=\sum_{n=-\infty}^{\infty} e^{i\lambda_n\tau}P_n(\xi) \tag{3.3.5}$$

where, for each value of n, λ_n is some constant yet to be determined, and $P_n(\xi)$ is a function of ξ only. This is equivalent to the standard separation of variables technique. Substitution of (3.3.5) into (3.3.2) yields

$$\sum_{n=-\infty}^{\infty} e^{i\lambda_n\tau}\left[(1-\xi^2)P_n''(\xi)+2(i\lambda_n-1)\xi P_n'(\xi)+\lambda_n(i+\lambda_n)P_n(\xi)\right]=0\,. \tag{3.3.6}$$

Essentially, what needs to be solved is the system of ordinary differential equations

$$(1-\xi^2)P_n''(\xi)+2(i\lambda_n-1)\xi P_n'(\xi)+\lambda_n(i+\lambda_n)P_n(\xi)=0\,,\quad \text{for } n=0,\pm1,\pm2,\ldots \tag{3.3.7}$$

To this end, consider the hypergeometric equation

$$t(1-t)y''(t)+[\gamma-(\eta+\varsigma+1)t]y'(t)-\eta\varsigma y(t)=0\,, \tag{3.3.8}$$

where η,ς,γ are constants and appropriate restrictions on γ are derived below . Through the introduction of a change of variables, $t=\frac{1}{2}(1-z)$, with $y(t)=y\left(\frac{1}{2}(1-z)\right)\equiv Y(z)$, (3.3.8) becomes

$$(1-z^2)Y''(z)+[\eta+\varsigma+1-2\gamma-(\eta+\varsigma+1)z]Y'(z)-\eta\varsigma Y(z)=0\,, \tag{3.3.9}$$

whose form is strikingly similar to that of (3.3.7), under the identification

$$\left.\begin{aligned}&\eta+\varsigma+1-2\gamma=0\\&\eta+\varsigma+1=-2(i\lambda_n-1)=-2\sigma_n\\&\eta\varsigma=-\lambda_n(i+\lambda_n)=\sigma_n(\sigma_n+1)\end{aligned}\right\} \tag{3.3.10}$$

in which

$$\sigma_n = i\lambda_n - 1. \tag{3.3.11}$$

The general solution of (3.3.8) (and hence (3.3.9) and finally (3.3.7)) may be obtained by the method of Frobenius, in which we assume a solution of the form

$$y(t) = t^s \sum_{k=0}^{\infty} C_k t^k = \sum_{k=0}^{\infty} C_k t^{k+s} = a y_1(t) + b y_2(t),$$

with a, b arbitrary constants, $C_0 \neq 0$, and s is to be suitably chosen, and $y_1(t)$ and $y_2(t)$ are particular solutions whose forms are determined below.

Substitution into (3.3.8) gives rise to

$$s(s-1+\gamma)C_0 t^{s-1} + \sum_{k=0}^{\infty} \{(k+s+1)(k+s+\gamma)C_{k+1} - [(k+s)(k+s+\eta+\varsigma)+\eta\varsigma]C_k\} t^{k+s} = 0, \tag{3.3.12}$$

from which we conclude that either $s = 0$ or $s = 1-\gamma$.

In the first case (i.e., $s = 0$), (3.3.12) reduces to

$$\sum_{k=0}^{\infty} \{(k+1)(k+\gamma)C_{k+1} - [k(k+\eta+\varsigma)+\eta\varsigma]C_k\} t^k = 0$$

and thus

$$C_{k+1} = \frac{(k+\eta)(k+\varsigma)}{(k+1)(k+\gamma)} C_k, \qquad k = 0,1,2,\ldots,$$

in which it is necessary to impose the restriction that $\gamma \neq 0,-1,-2,-3,\ldots$. The coefficients may be rewritten as

$$C_k = \frac{(\eta)_k (\varsigma)_k}{k!(\gamma)_k}, \qquad k = 0,1,2,\ldots$$

in which the Pochammer symbol $(\eta)_k$ [Arf p.632] is defined to be

$$(\alpha)_k = \begin{cases} 1, & k = 0 \\ \eta(\eta+1)(\eta+2)...(\eta+k-1), & k = 1,2,... \end{cases}.$$

Therefore the corresponding particular solution of (3.3.8) is simply

$$y_1(t) = \sum_{k=0}^{\infty} \frac{(\eta)_k (\varsigma)_k}{k!(\gamma)_k} t^k \equiv F(\eta, \varsigma; \gamma; t), \qquad |t|<1, \qquad (3.3.13)$$

where $F(\eta, \varsigma; \gamma; t)$ is known as the hypergeometric series (Leb p.163).

Similarly, for $s = 1-\gamma$, (3.3.12) becomes

$$\sum_{k=0}^{\infty} \{(k+2-\gamma)(k+1)C_{k+1}$$

$$-[(k+1-\gamma)(k+1-\gamma+\eta+\varsigma)+\eta\varsigma]C_k\}t^{k+1-\gamma} = 0,$$

and thus we may conclude that

$$C_k = \frac{(1-\gamma+\eta)_k (1-\gamma+\varsigma)_k}{k!(2-\gamma)_k}, \qquad k = 0,1,2,...$$

in which it is necessary to assume that $\gamma \neq 2,3,4,...$. Therefore, the corresponding particular solution of (3.3.8) is given by

$$y_2(t) = \sum_{k=0}^{\infty} \frac{(1-\gamma+\eta)_k (1-\gamma+\varsigma)}{k!(2-\gamma)_k} t^{k+1-\gamma}$$

$$\equiv t^{1-\gamma} F(1-\gamma+\eta, 1-\gamma+\varsigma; 2-\gamma; t), \qquad |t|<1.$$

Observation: In the above analysis, we have restricted γ in such a way that it cannot be an integer, except possibly 1. But if $\gamma = 1$, the method of Frobenius gives rise to an indicial equation whose roots are both $s = 0$. Thus, for the purposes of

our discussion, we must assume that γ is not an integer, and we may therefore conclude in this case that the general solution of (3.3.8), at least for $-1<t<1$, is of the form

$$y(t) = aF(\eta, \varsigma; \gamma; t) + bt^{1-\gamma} F(1-\gamma+\eta, 1-\gamma+\varsigma; 2-\gamma; t).$$

Recall that $t = \frac{1}{2}(1-z)$, and therefore, the solution of (3.3.9) is given by

$$Y(z) = y\left(\frac{1}{2}(1-z)\right) = aF\left(\eta, \varsigma; \gamma; \frac{1}{2}(1-z)\right)$$

$$+ b\left(\frac{1}{2}(1-z)\right)^{1-\gamma} F\left(1-\gamma+\eta, 1-\gamma+\varsigma; 2-\gamma; \frac{1}{2}(1-z)\right)$$

provided that γ is not an integer.

Under the identification (3.3.10) and (3.3.11), we have

$$\eta + \varsigma + 1 - 2\gamma = 0$$

$$\eta + \varsigma + 1 = -2\sigma_n$$

$$\eta\varsigma = \sigma_n(\sigma_n + 1),$$

which is a non-linear system of three equations in three unknowns η, ς, γ. In solving this system, it is found that

$$(\eta, \varsigma, \gamma) \in \{(-\sigma_n, -\sigma_n - 1, -\sigma_n), (-\sigma_n - 1, -\sigma_n, -\sigma_n)\}.$$

In particular, it is noted that $\gamma = -\sigma_n = 1 - i\lambda_n$ which guarantees not only that γ is not an integer, but rather that γ is complex. Therefore, the general solution of (3.3.7) is

$$P_n(\xi) = AF\left(-\sigma_n, -\sigma_n - 1; -\sigma_n; \frac{1-\xi}{2}\right)$$

$$+ B\left(\frac{1-\xi}{2}\right)^{1+\sigma_n} F\left(1,\ 0;\ 2+\sigma_n; \frac{1-\xi}{2}\right) \tag{3.3.14}$$

where $A = \frac{1}{2}a$ and $B = \frac{1}{2}b$ are arbitrary constants. Finally, substitution of the formal definition of the hypergeometric function (3.3.13) into (3.3.14) yields

$$P_n(\xi) = \sum_{k=0}^{\infty} \left\{ A \frac{(-\sigma_n - 1)_k}{k!} \left(\frac{1-\xi}{2}\right)^k \right\} + B\left(\frac{1-\xi}{2}\right)^{1+\sigma_n}, \ |1-\xi| < 2.$$

The general solution of (3.3.7) obtained in the above fashion is valid only for restricted values of ξ and hence is not sufficient for our purposes. However, it is a trivial exercise to verify that

$$P_n(\xi) = v(\xi) \equiv (1-\xi)^{i\lambda_n},$$

appearing in the final term of $P_n(\xi)$, is a solution for (3.3.7) for all real ξ.

By the reduction of order technique [Zil p.154], a second solution is found by assuming that it has the form

$$P_n(\xi) = u(\xi)v(\xi) = u(\xi)(1-\xi)^{i\lambda_n}. \tag{3.3.15}$$

Substitution of (3.3.15) into (3.3.7) produces

$$(1-\xi^2)v(\xi)u''(\xi) + [2(1-\xi^2)v'(\xi) + 2(i\lambda_n - 1)\xi v(\xi)]u'(\xi)$$

$$+ [(1-\xi^2)v''(\xi) + 2(i\lambda_n - 1)\xi v'(\xi) + \lambda_n(\lambda_n + i)v(\xi)]u(\xi) = 0. \tag{3.3.16}$$

But $v(\xi)$ is a solution of (3.3.7), so we need only concern ourselves with

$$(1-\xi^2)v(\xi)u''(\xi) + [2(1-\xi^2)v'(\xi) + 2(i\lambda_n - 1)\xi v(\xi)]u'(\xi) = 0. \tag{3.3.17}$$

By setting $\hat{u}(\xi) = u'(\xi)$ and replacing $v(\xi)$ and $v'(\xi)$ with

$$v(\xi) = (1-\xi)^{i\lambda_n},$$

$$v'(\xi) = -i\lambda_n(1-\xi)^{i\lambda_n - 1},$$

(3.3.17) becomes

$$\hat{u}'(\xi) - 2\left(\frac{i\lambda_n + \xi}{(1-\xi^2)}\right)\hat{u}(\xi) = 0,$$

which is a separable differential equation whose general solution is

$$\hat{u}(\xi) = \frac{D}{1-\xi^2} e^{\left[i\lambda_n \ln\left(\frac{1+\xi}{1-\xi}\right)\right]},$$

where D is an arbitrary constant of integration. However, $\hat{u}(\xi) = u'(\xi)$ and thus

$$u'(\xi) = \frac{D}{1-\xi^2} e^{\left[i\lambda_n \ln\left(\frac{1+\xi}{1-\xi}\right)\right]},$$

which implies that

$$u(\xi) = Ee^{\left[i\lambda_n \ln\left(\frac{1+\xi}{1-\xi}\right)\right]} = Ee^{i\lambda_n[\ln(1+\xi)-\ln(1-\xi)]}$$

$$= E(1+\xi)^{i\lambda_n}(1-\xi)^{-i\lambda_n},$$

where $E = \frac{D}{2i\lambda_n}$. Therefore, upon substitution into (3.3.15), we obtain a second linearly independent solution of (3.3.7) of the form

$$P_n(\xi) = (1+\xi)^{i\lambda_n},$$

so the general solution of (3.3.7) may be written as

$$P_n(\xi) = A(1+\xi)^{i\lambda_n} + B(1-\xi)^{i\lambda_n}$$

$$= Ae^{i\lambda_n \ln(1+\xi)} + Be^{i\lambda_n \ln(1-\xi)} \qquad (3.3.18)$$

where A, B are arbitrary constants yet to be determined.

Now we invoke the boundary-conditions (2.4.3c,d) to determine the constants and the eigenvalues λ_n. In particular, (3.3.5) and (3.3.18) give

$$\widetilde{Z}(0,\tau)=0 \qquad \Rightarrow P_n(0)=0=Ae^{i\lambda_n \ln(1)}+Be^{i\lambda_n \ln(1)}$$

$$\Rightarrow B=-A\,, \tag{3.3.19}$$

and

$$\widetilde{Z}\left(\frac{k}{c},\tau\right)=0 \qquad \Rightarrow P_n\left(\frac{k}{c}\right)=0=Ae^{i\lambda_n \ln\left(1-k/c\right)}\left[e^{i\lambda_n \ln\left(\frac{1+k/c}{1-k/c}\right)}-1\right].$$

The last condition implies that

$$e^{i\lambda_n \ln\left(\frac{1+k/c}{1-k/c}\right)}=1\,,$$

which occurs when

$$\lambda_n=\frac{2n\pi}{\ln\left(\dfrac{1+k/c}{1-k/c}\right)}, \qquad \text{for } n=0,\ \pm1,\ \pm2,\ldots\,. \tag{3.3.20}$$

Now that we have determined the form for $P_n(\xi)$, we have by virtue of (3.3.5), (3.3.18) and (3.3.19), that

$$\widetilde{Z}(\xi,\tau)=\sum_{n=-\infty}^{\infty}A_n\left[e^{i\lambda_n \ln(1+\xi)}-e^{i\lambda_n \ln(1-\xi)}\right]e^{i\lambda_n\tau}\,, \tag{3.3.21}$$

where the complex coefficients are to be determined from the initial conditions (2.4.3b). For simplicity, we will now reverse the Carrier-Greenspan transformation (3.3.3) and return to the original variables x and t before applying the initial conditions:

$$Z(x,t) = \sum_{n=-\infty}^{\infty} A_n \left[e^{i\lambda_n \ln\left(1+\frac{kx}{c(kt+L)}\right)} - e^{i\lambda_n \ln\left(1-\frac{kx}{c(kt+L)}\right)} \right] e^{i\lambda_n \ln\left(\frac{kt+L}{L}\right)}$$

$$= \sum_{n=-\infty}^{\infty} A_n \left[e^{i\lambda_n \ln\left(1+\frac{k(x+ct)}{cL}\right)} - e^{i\lambda_n \ln\left(1-\frac{k(x-ct)}{cL}\right)} \right]. \qquad (3.3.22)$$

By applying the initial conditions (2.3.2b) we obtain

$$Z(x,0) = \sum_{n=-\infty}^{\infty} A_n \left[e^{i\lambda_n \ln\left(1+\frac{kx}{cL}\right)} - e^{i\lambda_n \ln\left(1-\frac{kx}{cL}\right)} \right] = \alpha(x) \qquad (3.3.23)$$

and

$$\frac{\partial Z}{\partial t}(x,0) = \sum_{n=-\infty}^{\infty} A_n i\lambda_n \frac{k}{L} \left[\left(\frac{1}{1+kx/cL} \right) e^{i\lambda_n \ln\left(1+\frac{kx}{cL}\right)} - \left(\frac{1}{1-kx/cL} \right) e^{i\lambda_n \ln\left(1-\frac{kx}{cL}\right)} \right]$$

$$= \beta(x). \qquad (3.3.24)$$

Integrating (3.3.24) gives

$$B(x) = \int_0^x \beta(x)dx = \sum_{n=-\infty}^{\infty} A_n c \left[e^{i\lambda_n \ln\left(1+\frac{kx}{cL}\right)} + e^{i\lambda_n \ln\left(1-\frac{kx}{cL}\right)} \right]. \qquad (3.3.25)$$

Adding and subtracting (3.3.23) and (3.3.25) yields

$$\sum_{n=-\infty}^{\infty} A_n e^{i\lambda_n \ln\left(1+\frac{kx}{cL}\right)} = \frac{1}{2c}\left[B(x) + c\alpha(x)\right], \qquad (3.3.26)$$

$$\sum_{n=-\infty}^{\infty} A_n e^{i\lambda_n \ln\left(1-\frac{kx}{cL}\right)} = \frac{1}{2c}\left[B(x) - c\alpha(x)\right]. \qquad (3.3.27)$$

As is customary in Fourier analysis, we extend $\alpha(x)$ and $\beta(x)$, which are only defined for $0 \le x \le S(0) = L$, to the interval $-L \le x \le L$ as odd functions, i.e.,

$$\alpha(x) = -\alpha(-x),\ \beta(x) = -\beta(-x),\ \text{for } -L \le x \le L,$$

from which we conclude that $B(x) = \int_0^x \beta(x)dx$ is an even function, i.e.,

$$B(x) = B(-x).$$

Thus, (3.3.27) is a consequence of (3.3.26), and may henceforth be ignored.

Note that if $f(\zeta) = \sum_{n=-\infty}^{\infty} \gamma_n e^{i\lambda_n \zeta}$ is the exponential form of the Fourier series expansion for a periodic function with period $2p$, its Fourier coefficients are given by

$$\gamma_n = \frac{1}{2p}\int_{-p}^{p} f(\zeta)e^{-i\lambda_n\zeta}d\zeta, \qquad n = 0,\ \pm 1,\ \pm 2, \ldots .$$

If we let $\zeta = \ln\left(1 + \frac{kx}{cL}\right)$, with inverse $x = \frac{cL}{k}\left(e^{\zeta} - 1\right)$, the interval $-L \le x \le L$ of length $2L$ corresponds to the interval $\ln\left(1 - \frac{k}{c}\right) \le \zeta \le \ln\left(1 + \frac{k}{c}\right)$ of length

$$\ln\left(1 + \frac{k}{c}\right) - \ln\left(1 - \frac{k}{c}\right) = \ln\left(\frac{c+k}{c-k}\right),$$

so that the Fourier coefficients in (3.3.22) may be written in the form

$$A_n = \frac{1}{2c\ln\left(\frac{c+k}{c-k}\right)}\int_{\ln\left(1-\frac{k}{c}\right)}^{\ln\left(1+\frac{k}{c}\right)} \left[B\left(\frac{cL}{k}(e^{\zeta}-1)\right) + c\alpha\left(\frac{cL}{k}(e^{\zeta}-1)\right)\right] e^{-i\lambda_n\zeta}d\zeta \qquad (3.3.28)$$

or equivalently

$$A_n = \frac{1}{2c\ln\left(\frac{c+k}{c-k}\right)} \int_{\ln\left(1-\frac{k}{c}\right)}^{\ln\left(1+\frac{k}{c}\right)} \left[\hat{B}(\zeta) + c\hat{\alpha}(\zeta)\right] e^{-i\lambda_n \zeta}\, d\zeta \tag{3.3.29}$$

where

$$\hat{B}(\zeta) \equiv B\left(\left(e^{\zeta}-1\right)\frac{cL}{k}\right), \quad \hat{\alpha}(\zeta) \equiv \alpha\left(\left(e^{\zeta}-1\right)\frac{cL}{k}\right). \tag{3.3.30}$$

Generally, it is impossible to compute A_n directly from (3.3.28) or (3.3.29), so numerical integration must be used to approximate these coefficients.

Previously, we had our solution $Z(x,t)$ written in terms of an infinite exponential Fourier series. Expanding (3.3.21), by use of Euler's formula and the compound-angle formula from trigonometry, we have an alternate form for the solution

$$\widetilde{Z}(\xi,\tau) = \sum_{n=-\infty}^{\infty} 2iA_n \sin\left(\lambda_n \ln\sqrt{\frac{1+\xi}{1-\xi}}\right) e^{i\lambda_n\left[\ln\left(\sqrt{1-\xi^2}+\tau\right)\right]}, \tag{3.3.31}$$

which is consistent with Greenspan's solution [Gre p.346].

3.4 Examples of the Homogeneous IMBVP

In this section we present two examples illustrating the results of the above analysis. Since a complete discussion is very lengthy, we show only some of the most significant intermediate results, preferring to illustrate the solutions graphically rather than analytically. As indicated above, the Fourier coefficients A_n are approximated numerically.

Example 3.4.1:

Take $c = 2,\ k = 1,\ L = 10$ and $\omega = 1/5$:

$$\left.\begin{aligned} \frac{\partial^2 u_1}{\partial t^2} - \frac{2}{5}\frac{\partial u_2}{\partial t} - \frac{1}{25}u_1 &= 4\frac{\partial^2 u_1}{\partial x^2}, \\ \frac{\partial^2 u_2}{\partial t^2} + \frac{2}{5}\frac{\partial u_1}{\partial t} - \frac{1}{25}u_2 &= 4\frac{\partial^2 u_2}{\partial x^2}, \end{aligned}\right\} \quad t \geq 0, \quad 0 \leq x \leq t + 10 \qquad (3.4.1a)$$

with initial-conditions

$$\left.\begin{aligned} u_1(x,0) &= \sin\left(\frac{\pi x}{10}\right), & \frac{\partial u_1}{\partial t}(x,0) &= 0, \\ u_2(x,0) &= 0, & \frac{\partial u_2}{\partial t}(x,0) &= -\frac{1}{5}\sin\left(\frac{\pi x}{10}\right), \end{aligned}\right\} \quad 0 \leq x \leq t + 10 \qquad (3.4.1b)$$

and boundary-conditions:

$$u_1(0, t) = u_2(0, t) = u_1(t + 10, t) = u_2(t + 10, t) = 0, \quad \text{for } t \geq 0. \qquad (3.4.1c,d)$$

By arranging the initial conditions such that $g_2(x) = -\omega f_1(x)$, no rotational lag occurs, i.e., $\frac{\partial Z}{\partial t} = 0$. In other words, the resulting wave remains planar throughout its entire rotation [Qin p.71].

In seeking a solution to (3.4.1), we begin our analysis by reversing all the previous transformations. In particular, in this case the Carrier-Greenspan transformation becomes

$$\xi = \frac{x}{2(t + 10)}, \qquad \tau = \ln\left(\frac{t + 10}{10}\right),$$

and has inverse

$$x = 20\xi e^{\tau}, \qquad t = 10(e^{\tau} - 1).$$

This transformation leads us to the general solution (3.3.31) of (3.3.2), so that by reversing this transformation we have

$$Z(x,t) = \sum_{n=-\infty}^{\infty} 2iA_n \sin\left(\lambda_n \ln\sqrt{\frac{1+\dfrac{x}{2(t+10)}}{1-\dfrac{x}{2(t+10)}}}\right) e^{i\lambda_n \ln\left[\sqrt{1-\left(\frac{x}{2(t+10)}\right)^2}+\ln\left(\frac{t+10}{10}\right)\right]}$$

$$= \sum_{n=-\infty}^{\infty} 2iA_n \sin\left(\lambda_n \ln\sqrt{\frac{2(t+10)+x}{2(t+10)-x}}\right) e^{i\lambda_n \ln\left[\sqrt{1-\left(\frac{x}{2(t+10)}\right)^2}+\ln\left(\frac{t+10}{10}\right)\right]}, \quad (3.4.2)$$

where, for $n \in Z$:

$$\lambda_n = \frac{2n\pi}{\ln(3)}, \quad (3.4.3)$$

$$A_n = \frac{1}{4\ln(3)} \int_{\ln(1/2)}^{\ln(3/2)} \left[\hat{B}(\zeta) + 2\hat{\alpha}(\zeta)\right] e^{-i\lambda_n \zeta}\, d\zeta, \quad (3.4.4)$$

and

$$\hat{B}(\zeta) = 0, \qquad \hat{\alpha}(\zeta) = \sin\left[2\pi\left(e^{\zeta}-1\right)\right]. \quad (3.4.5)$$

Therefore,

$$A_n = \frac{1}{2\ln(3)} \int_{\ln(1/2)}^{\ln(3/2)} \sin\left[2\pi\left(e^{\zeta}-1\right)\right] e^{-i\lambda_n \zeta}\, d\zeta$$

$$= \frac{1}{2\ln(3)} \left\{ \int_{\ln(1/2)}^{\ln(3/2)} \sin\left[2\pi\left(e^{\zeta}-1\right)\right] \cos\left[\frac{2n\pi\zeta}{\ln(3)}\right] d\zeta \right.$$

$$- \int_{\ln(1/2)}^{\ln(3/2)} i \sin\left[2\pi\left(e^{\zeta} - 1\right)\right] \sin\left[\frac{2n\pi\zeta}{\ln(3)}\right] d\zeta \Bigg\}. \qquad (3.4.6)$$

These integrals cannot be evaluated explicitly, so we approximate the coefficients A_n numerically by use of the mathematical software package Maple V Release 5, which uses Clenshaw-Curtis quadrature for numerical integration. For numerical and graphical results of our analysis, we truncate the infinite series representation of the solution after a finite number of terms, summing only over the values $n \in \{-N, -N+1, \ldots, N-1, N\}$ in which N is a positive integer.

For $N = 15$ (31 term Fourier series expansion):

Table 3.4.1a: Numerical Approximations of A_n, denoted by $\hat{A}_n$:

n	Re $\hat{A}_n$	Im $\hat{A}_n$
-15	3.841096468E-04	9.368068823E-05
-14	-2.212834018E-04	-3.976084915E-04
-13	-1.645728103E-04	5.031943885E-04
-12	5.669243535E-04	-2.603393693E-04
-11	-6.890653040E-04	-2.865594548E-04
-10	3.130658770E-04	8.535576760E-04
-9	5.174810903E-04	-1.007688429E-03
-8	-1.399977936E-03	3.861559538E-04
-7	1.637234068E-03	1.027132062E-03
-6	-4.766864673E-04	-2.665430385E-03
-5	-2.524270468E-03	3.216852755E-03
-4	6.953698103E-03	-2.827354618E-04
-3	-9.135951470E-03	-1.143891178E-02
-2	-2.371310545E-02	3.879504385E-02
-1	6.846731080E-02	2.259885331E-01

0	-8.063593263E-02	0.000000000E+01
1	6.846731080E-02	-2.259885331E-01
2	-2.371310545E-02	-3.879504385E-02
3	-9.135951470E-03	1.143891178E-02
4	6.953698103E-03	2.827354618E-04
5	-2.524270468E-03	-3.216852755E-03
6	-4.766864673E-04	2.665430385E-03
7	1.637234068E-03	-1.027132062E-03
8	-1.399977936E-03	-3.861559538E-04
9	5.174810903E-04	1.007688429E-03
10	3.130658770E-04	-8.535576760E-04
11	-6.890653040E-04	2.865594548E-04
12	5.669243535E-04	2.603393693E-04
13	-1.645728103E-04	-5.031943885E-04
14	-2.212834018E-04	3.976084915E-04
15	3.841096468E-04	-9.368068823E-05

Thus, (3.4.2) and (3.4.3) provide the approximation

$$Z(x,t) \approx \hat{Z}(x,t) \equiv \sum_{n=-15}^{15} 2i\hat{A}_n \sin\left[\frac{2n\pi}{\ln(3)} \ln \sqrt{\frac{2(t+10)-x}{2(t+10)+x}}\right] e^{\frac{2n\pi i}{\ln(3)} \ln\left[\sqrt{1-\left(\frac{x}{(2(t+10)}\right)^2} + \ln\left(\frac{t+10}{10}\right)\right]}.$$

Since the IMBVP (3.4.1) has zero boundary-conditions, the "boundary transformation" was not necessary, and thus we may write $\hat{W}(x,t) = \hat{Z}(x,t)$ as an approximation for $W(x,t)$.

Finally, by reversing the complex transformations (2.2.3) and (2.2.1), we obtain the approximation

$$\hat{V}(x,t) = e^{-it/5} \sum_{n=-15}^{15} 2i\hat{A}_n \sin\left(\frac{2n\pi}{\ln(3)} \ln \sqrt{\frac{2(t+10)+x}{2(t+10)-x}}\right) e^{i\frac{2n\pi}{\ln(3)} \ln\left[\sqrt{1-\left(\frac{x}{2(t+10)}\right)^2} + \ln\left(\frac{t+10}{10}\right)\right]}$$

$$= \sum_{n=-15}^{15} 2i\hat{A}_n \sin\left(\frac{2n\pi}{\ln(3)} \ln \sqrt{\frac{2(t+10)+x}{2(t+10)-x}}\right) e^{i\left\{\frac{2n\pi}{\ln(3)} \ln\left[\sqrt{1-\left(\frac{x}{2(t+10)}\right)^2} + \ln\left(\frac{t+10}{10}\right)\right] - \frac{t}{5}\right\}}$$

to $V(x,t)$, and the additional approximations

$$\hat{u}_1(x,t) = \mathrm{Re}\,\hat{V}(x,t)$$

$$\hat{u}_2(x,t) = \mathrm{Im}\,\hat{V}(x,t)$$

for $u_1(x,t)$ and $u_2(x,t)$ respectively.

Graphical representations for the resulting wave motion at a sequence of times over the interval $\left[0, \frac{53\pi}{4}\right]$ are shown in Figure 3.4.1a.

Figure 3.4.1a Graphical Illustration of Example 3.4.1 (31 Fourier series approximation)

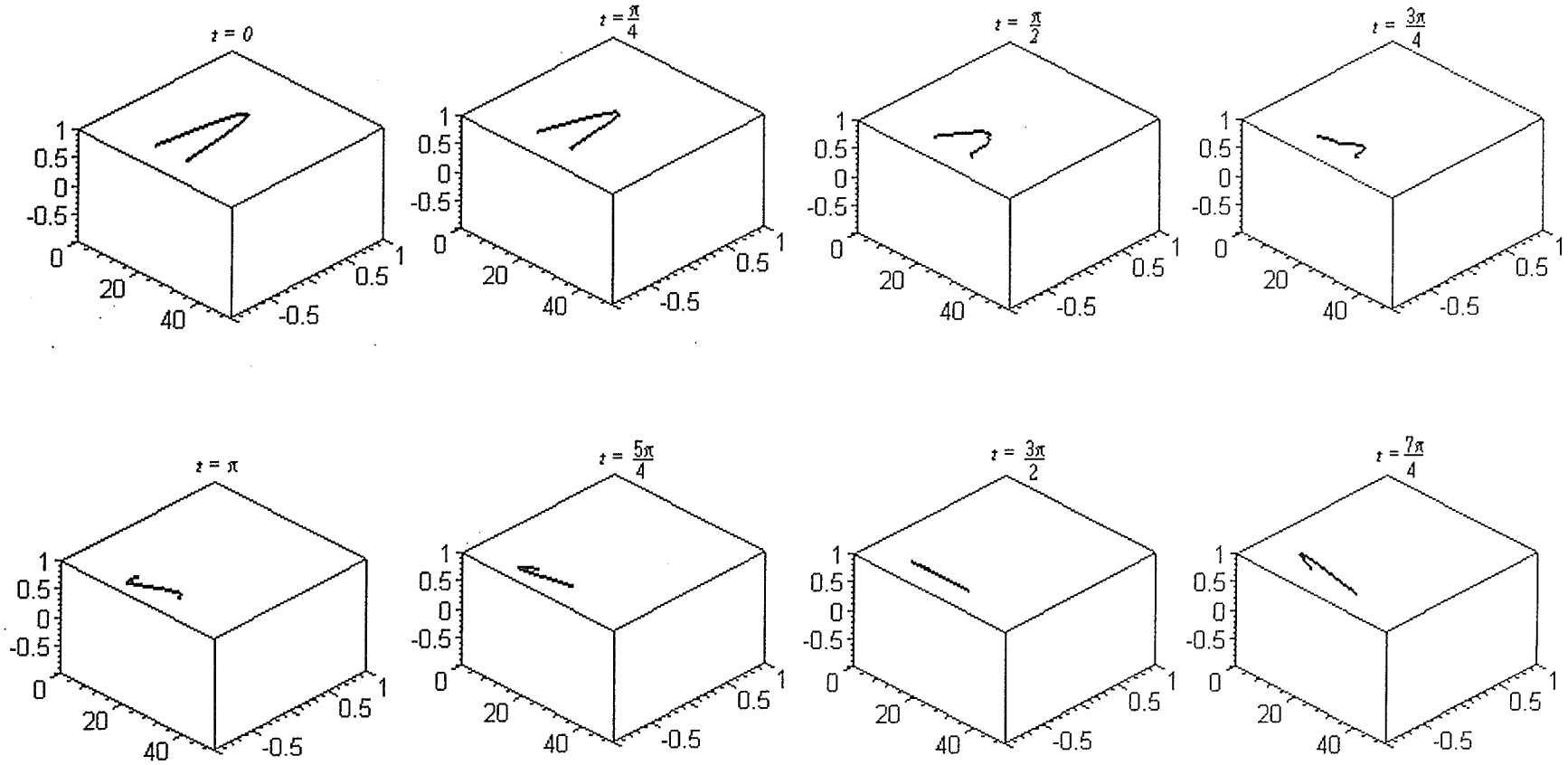

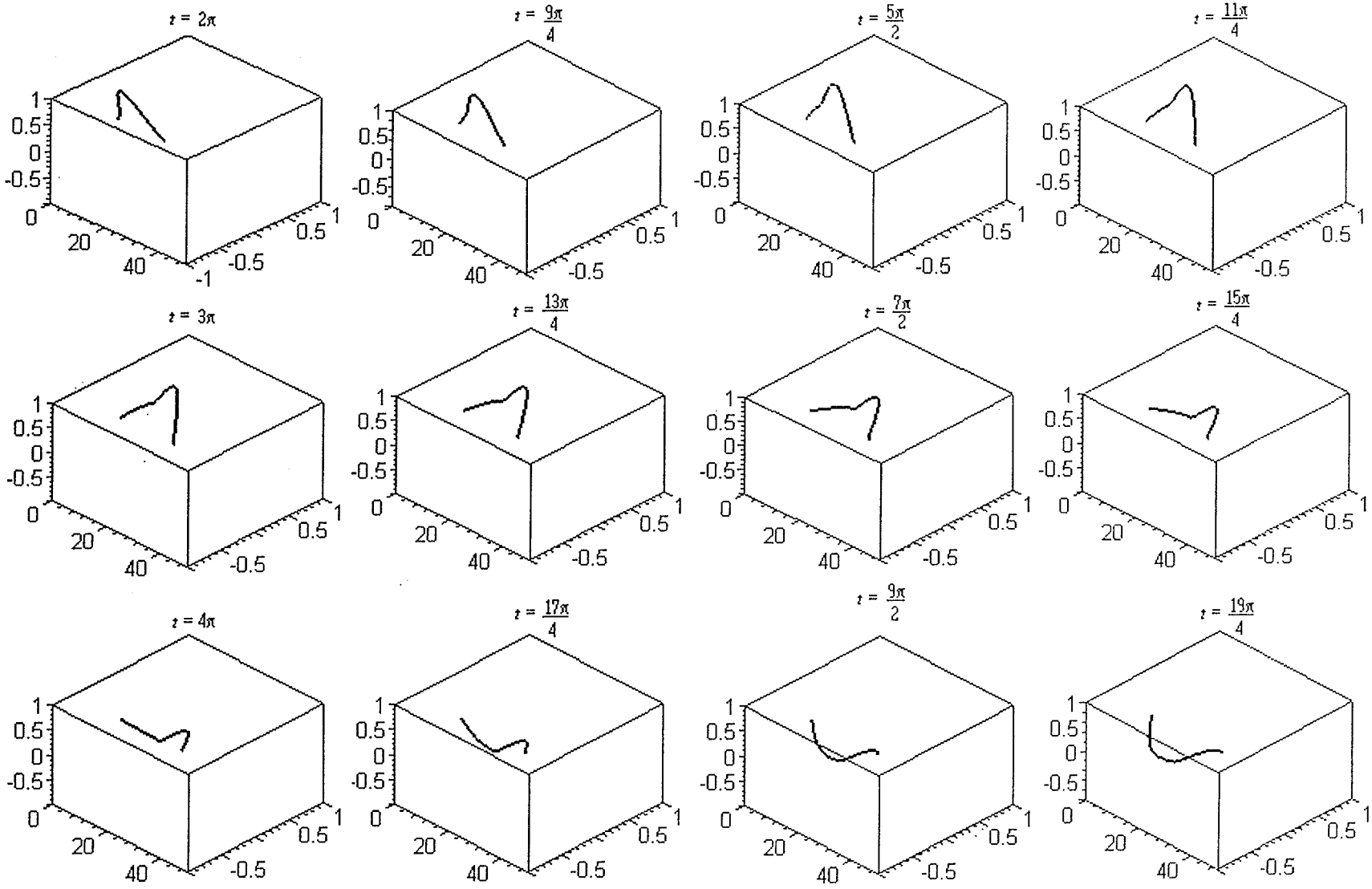
t = 2π
t = 9π/4
t = 5π/2
t = 11π/4
t = 3π
t = 13π/4
t = 7π/2
t = 15π/4
t = 4π
t = 17π/4
t = 9π/2
t = 19π/4

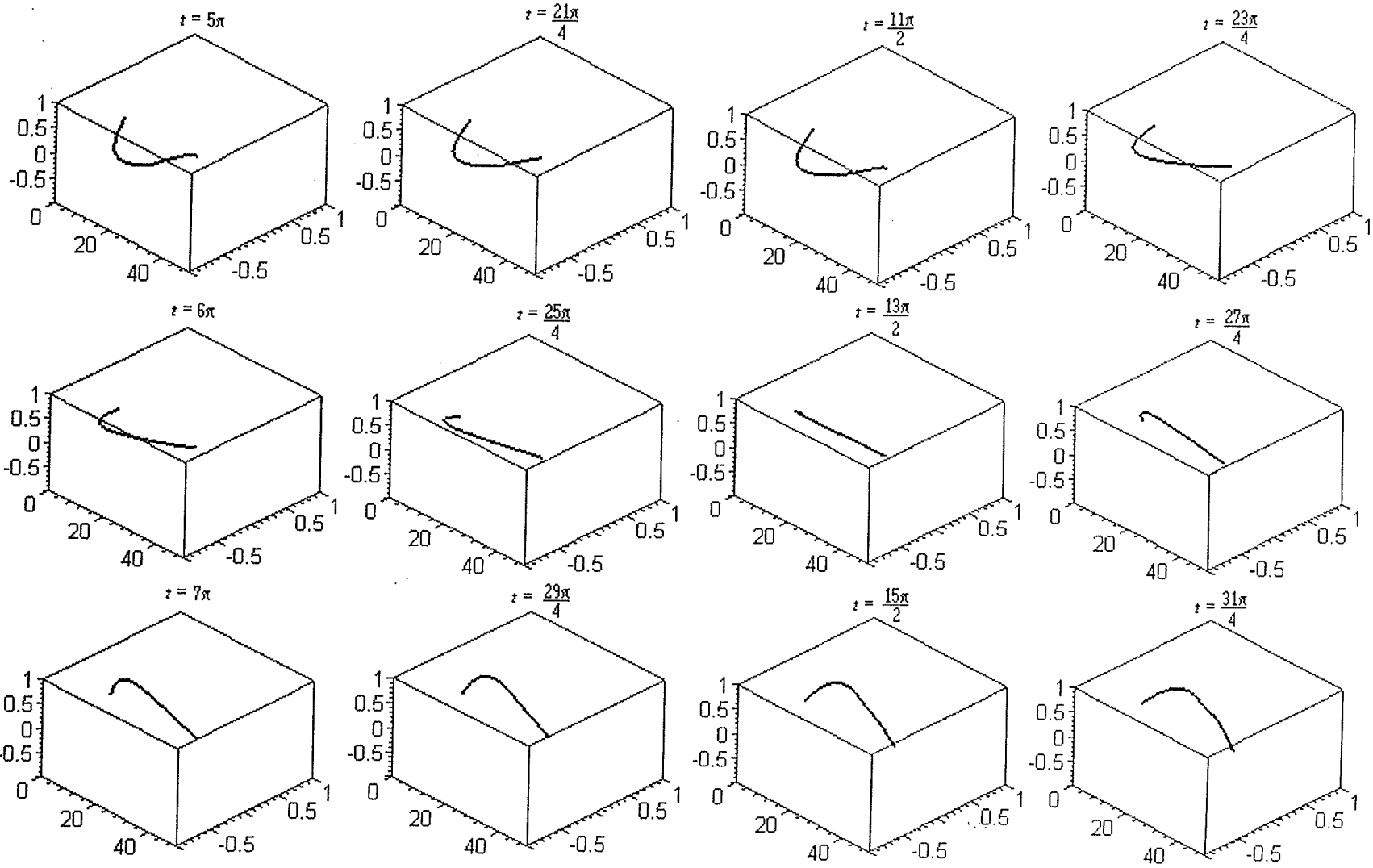
t = 5π
t = 21π/4
t = 11π/2
t = 23π/4
t = 6π
t = 25π/4
t = 13π/2
t = 27π/4
t = 7π
t = 29π/4
t = 15π/2
t = 31π/4
1
0.5
0
-0.5
0
20
40
-0.5
0.5
1

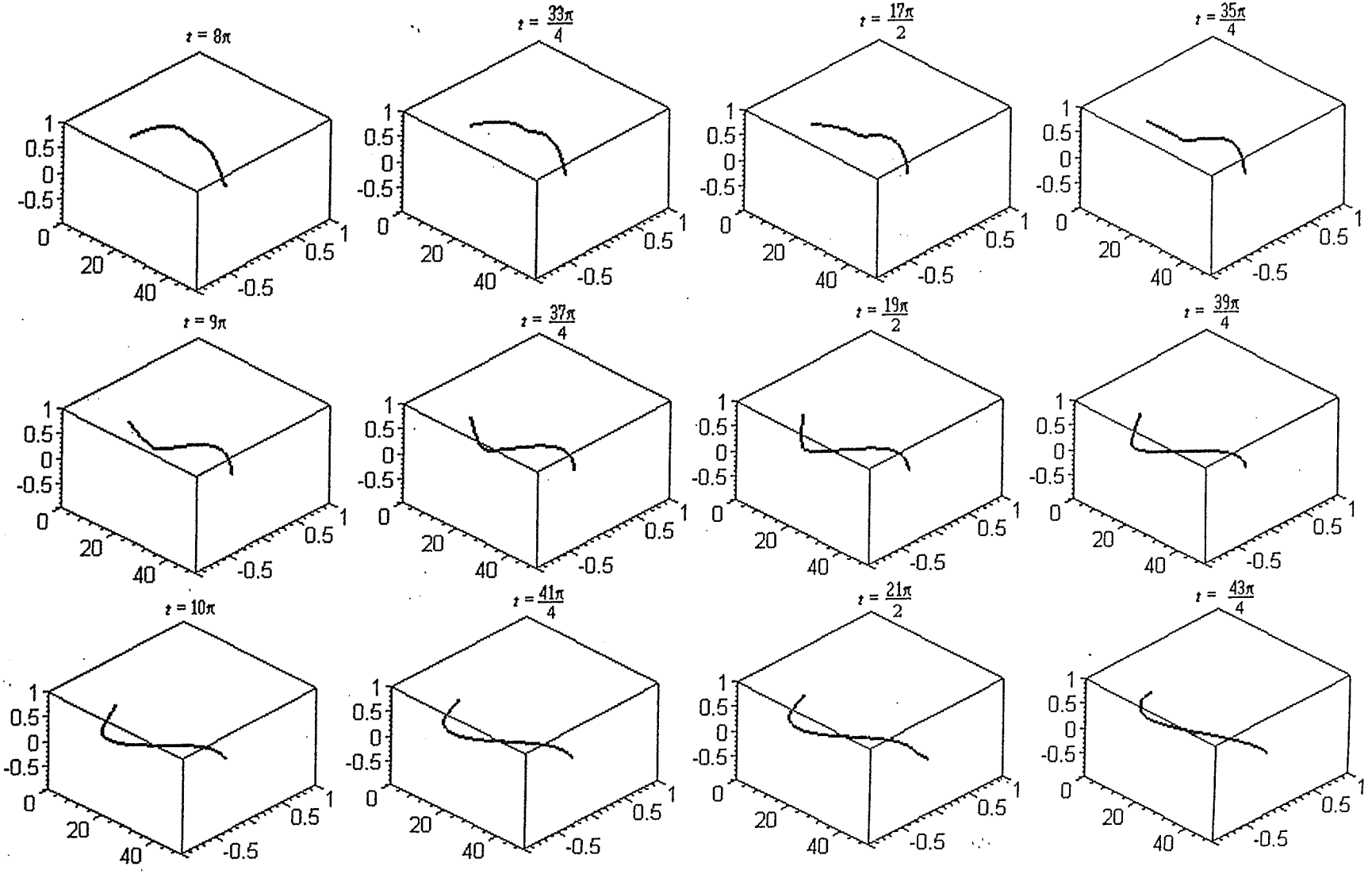
t = 8π
t = 33π/4
t = 17π/2
t = 35π/4
t = 9π
t = 37π/4
t = 19π/2
t = 39π/4
t = 10π
t = 41π/4
t = 21π/2
t = 43π/4
1
0.5
0
-0.5
0
20
40
-0.5
0.5
1

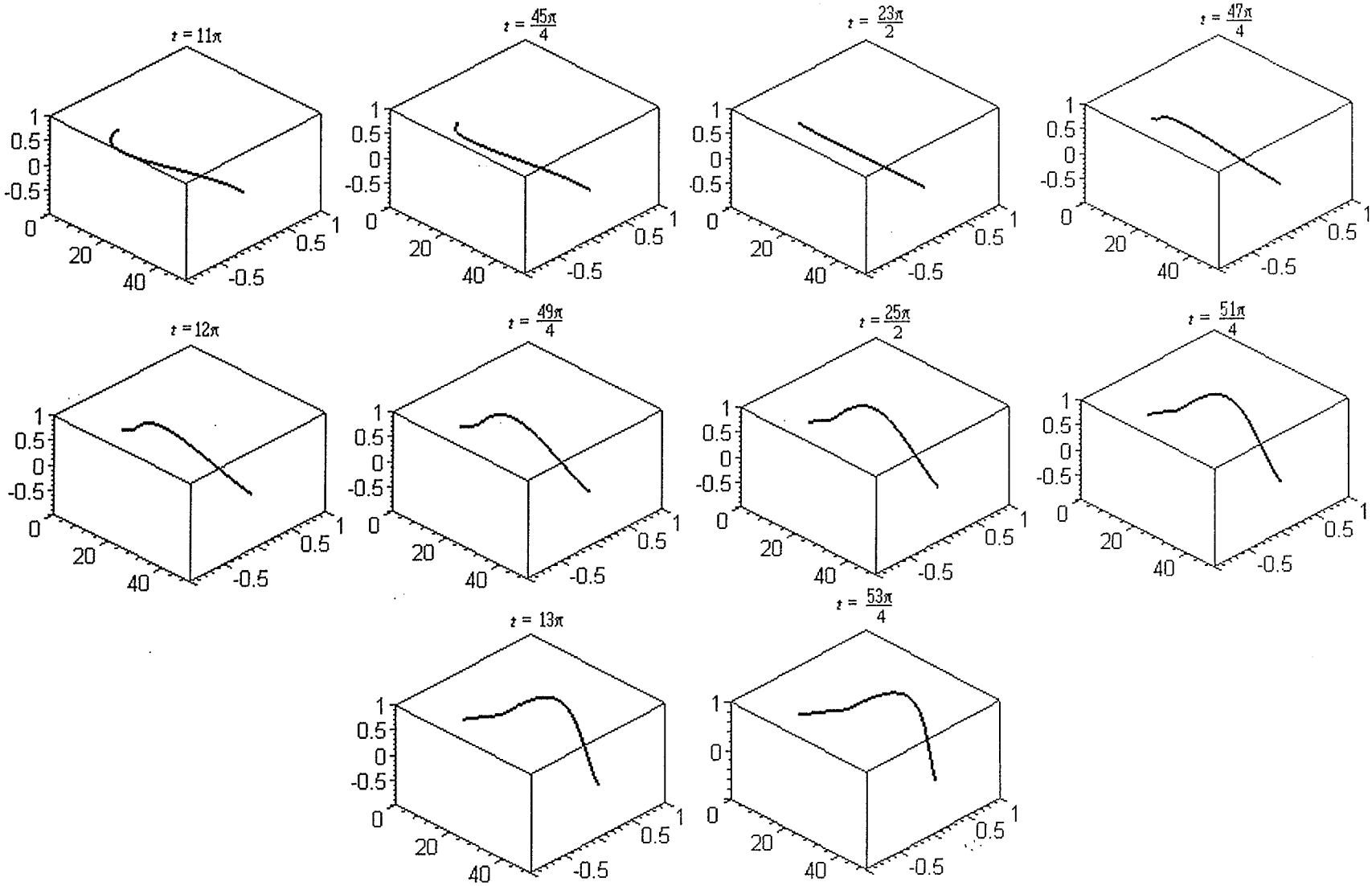
t = 11π
t = 45π/4
t = 23π/2
t = 47π/4
t = 12π
t = 49π/4
t = 25π/2
t = 51π/4
t = 13π
t = 53π/4

In order to confirm the validity of the above approximate solution, we repeat the analysis for the same example in the case when $N = 30$ (61 term Fourier series approximation).

Table 3.4.1b: Numerical Approximations of A_n, denoted by $\hat{A}_n$:

n	Re $\hat{A}_n$	Im $\hat{A}_n$
-30	-8.746255915E-05	-4.322650233E-05
-29	2.975465618E-05	1.001093228E-04
-28	5.703887250E-05	-9.646721125E-05
-27	-1.178210277E-04	2.559466688E-05
-26	1.066902722E-04	7.441169955E-05
-25	-1.947872239E-05	-1.394029489E-04
-24	-9.657930788E-05	1.184236478E-04
-23	1.661529662E-04	-1.058895944E-05
-22	-1.320642349E-04	-1.253694093E-04
-21	-2.337007117E-06	1.999937708E-04
-20	1.635834186E-04	-1.481648639E-04
-19	-2.438808624E-04	-2.132252600E-05
-18	1.675172864E-04	2.156960341E-04
-17	4.976197303E-05	-3.025643913E-04
-16	-2.892233278E-04	1.912922023E-04
-15	3.841096468E-04	9.368068823E-05
-14	-2.212834018E-04	-3.976084915E-04
-13	-1.645728103E-04	5.031943885E-04
-12	5.669243535E-04	-2.603393693E-04
-11	-6.890653040E-04	-2.865594548E-04
-10	3.130658770E-04	8.535576760E-04
-9	5.174810903E-04	-1.007688429E-03
-8	-1.399977936E-03	3.861559538E-04
-7	1.637234068E-03	1.027132062E-03
-6	-4.766864673E-04	-2.665430385E-03
-5	-2.524270468E-03	3.216852755E-03
-4	6.953698103E-03	-2.827354618E-04
-3	-9.135951470E-03	-1.143891178E-02
-2	-2.371310545E-02	3.879504385E-02

-1	6.846731080E-02	2.259885331E-01
0	-8.063593263E-02	0.000000000E+01
1	6.846731080E-02	-2.259885331E-01
2	-2.371310545E-02	-3.879504385E-02
3	-9.135951470E-03	1.143891178E-02
4	6.953698103E-03	2.827354618E-04
5	-2.524270468E-03	-3.216852755E-03
6	-4.766864673E-04	2.665430385E-03
7	1.637234068E-03	-1.027132062E-03
8	-1.399977936E-03	-3.861559538E-04
9	5.174810903E-04	1.007688429E-03
10	3.130658770E-04	-8.535576760E-04
11	-6.890653040E-04	2.865594548E-04
12	5.669243535E-04	2.603393693E-04
13	-1.645728103E-04	-5.031943885E-04
14	-2.212834018E-04	3.976084915E-04
15	3.841096468E-04	-9.368068823E-05
16	-2.892233278E-04	-1.912922023E-04
17	4.976197303E-05	3.025643913E-04
18	1.675172864E-04	-2.156960341E-04
19	-2.438808624E-04	2.132252600E-05
20	1.635834186E-04	1.481648639E-04
21	-2.337007117E-06	-1.999937708E-04
22	-1.320642349E-04	1.253694093E-04
23	1.661529662E-04	1.058895944E-05
24	-9.657930788E-05	-1.184236478E-04
25	-1.947872239E-05	1.394029489E-04
26	1.066902722E-04	-7.441169955E-05
27	-1.178210277E-04	-2.559466688E-05
28	5.703887250E-05	9.646721125E-05
29	2.975465618E-05	-1.001093228E-04
30	-8.746255915E-05	4.322650233E-05

Graphical representations for the resulting wave motion at a sequence of times over the interval $\left[0, \frac{53\pi}{4}\right]$ are shown in Figure 3.4.1b.

Figure 3.4.1b Graphical Illustration of Example 3.4.1 (61 Fourier series approximation)

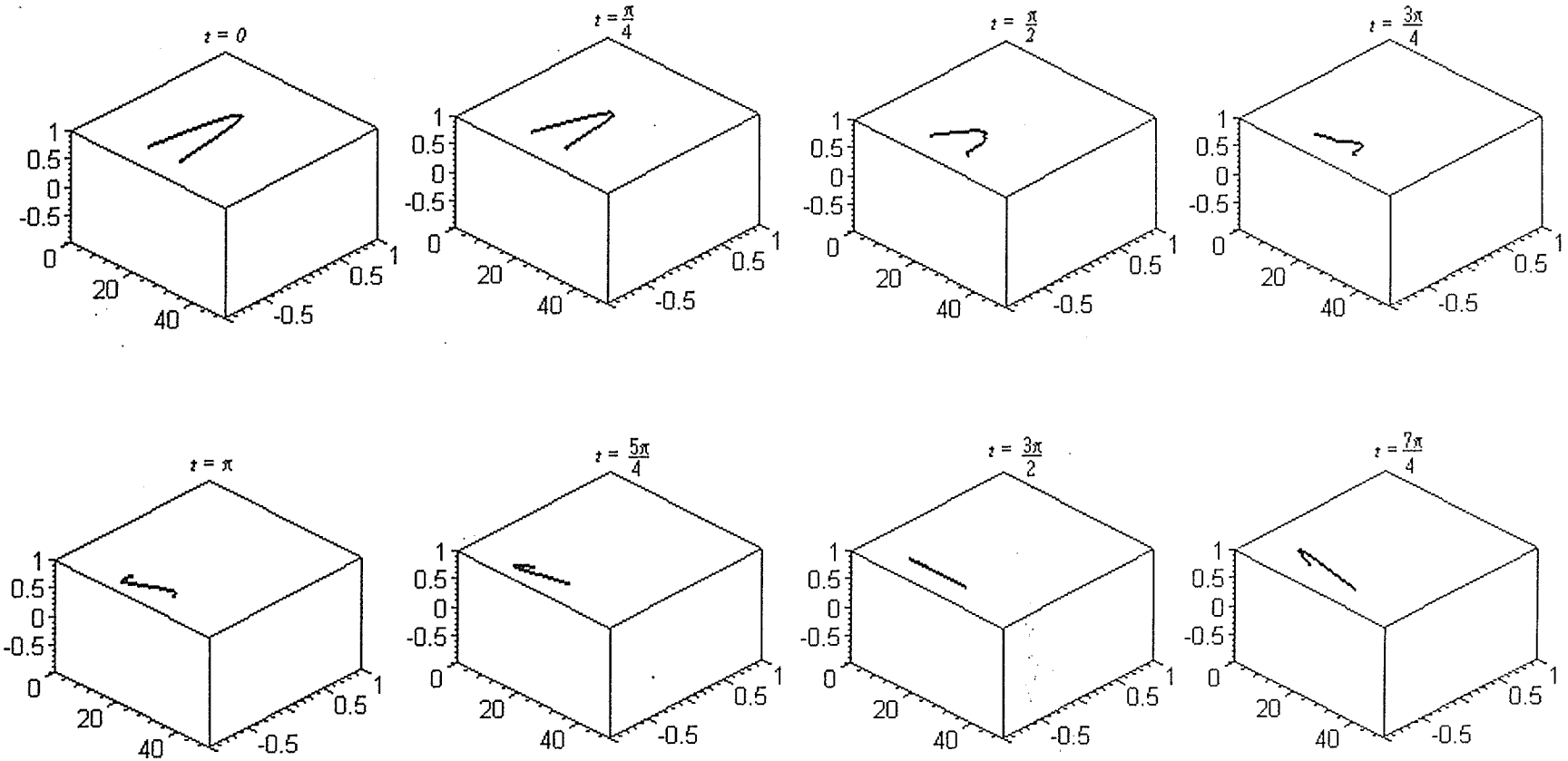

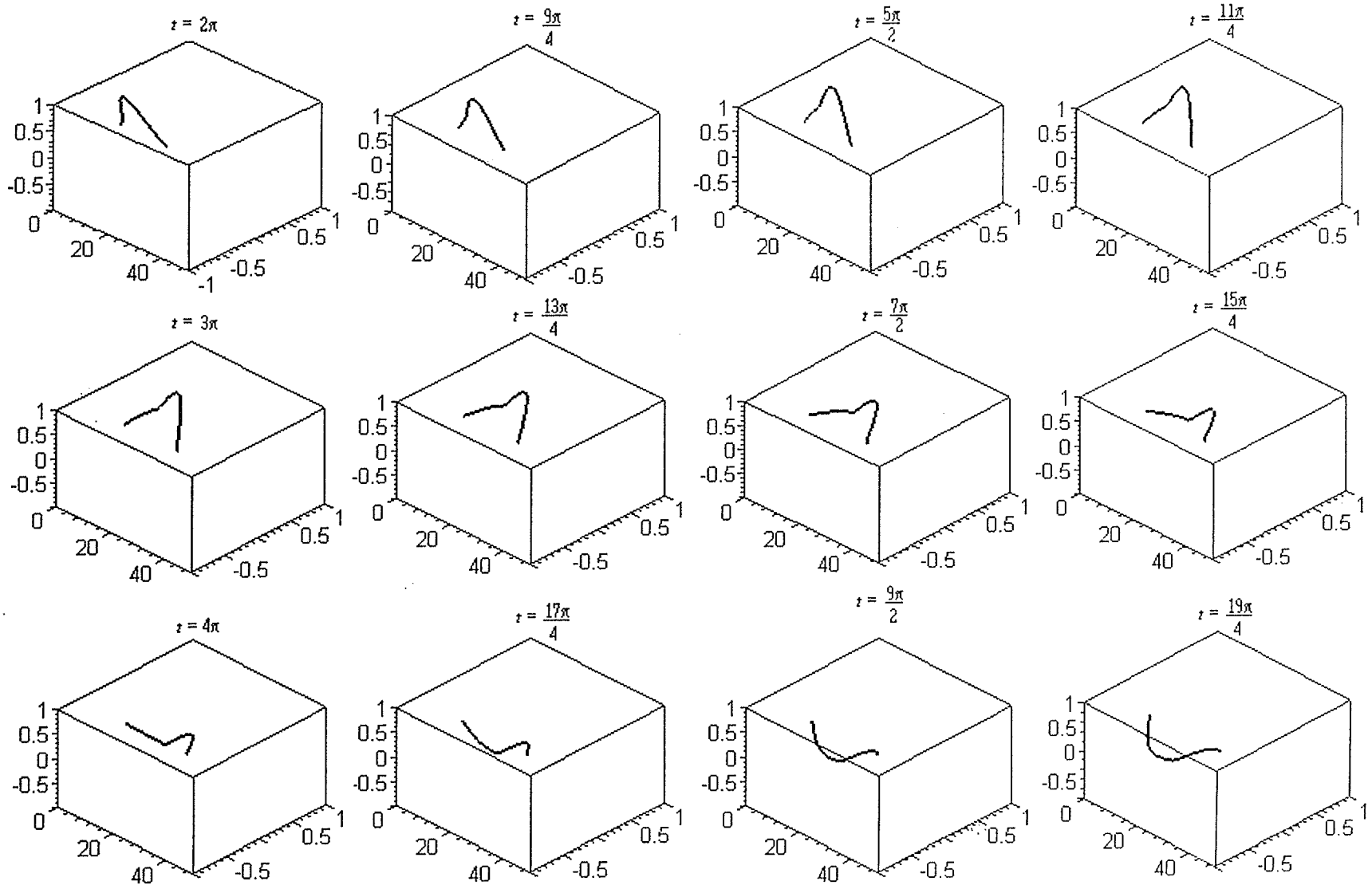
t = 2π
t = 9π/4
t = 5π/2
t = 11π/4
t = 3π
t = 13π/4
t = 7π/2
t = 15π/4
t = 4π
t = 17π/4
t = 9π/2
t = 19π/4

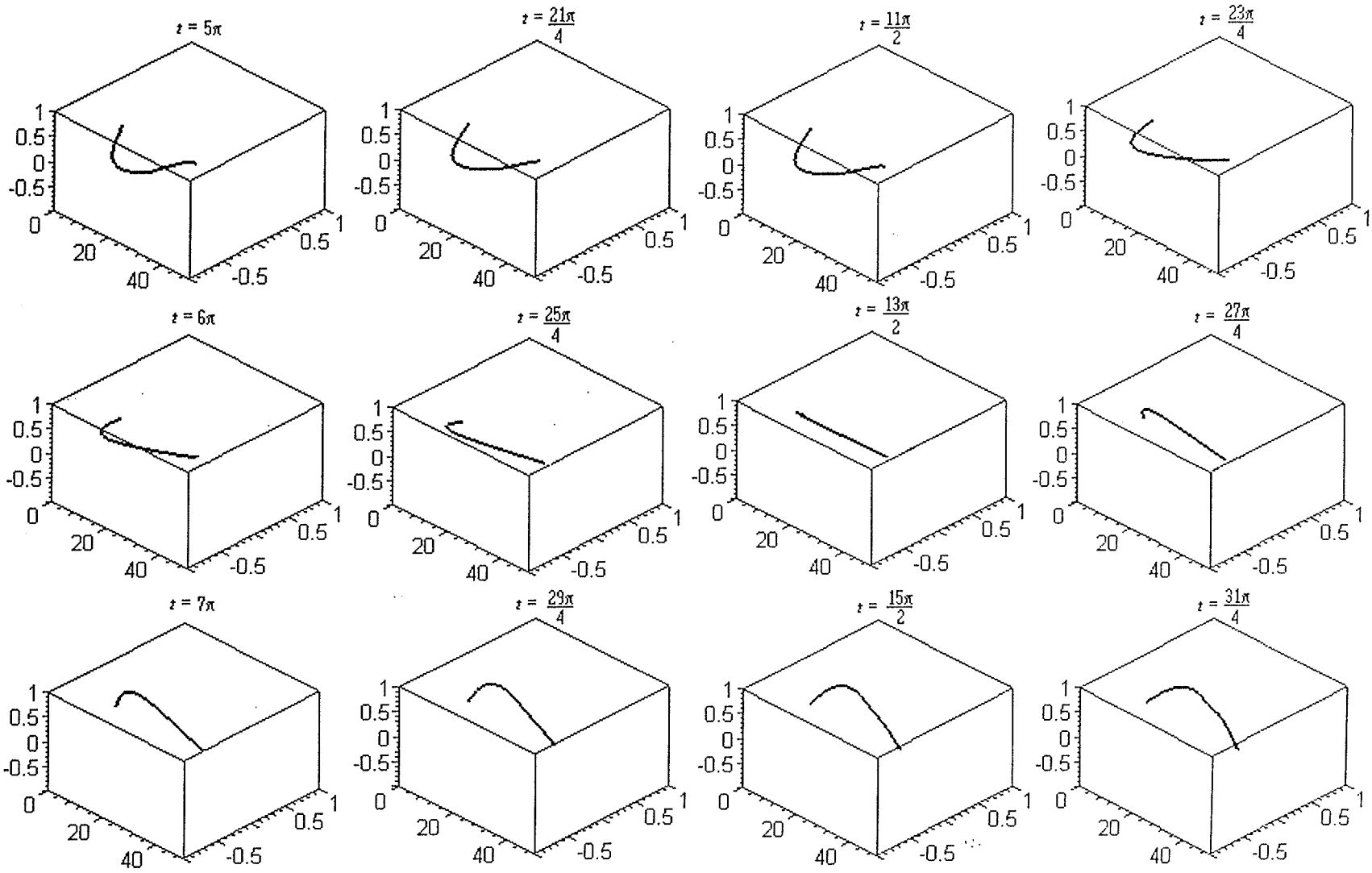
t = 5π
t = 21π/4
t = 11π/2
t = 23π/4
t = 6π
t = 25π/4
t = 13π/2
t = 27π/4
t = 7π
t = 29π/4
t = 15π/2
t = 31π/4
1
0.5
0
-0.5
0
20
40
0.5
1
-0.5

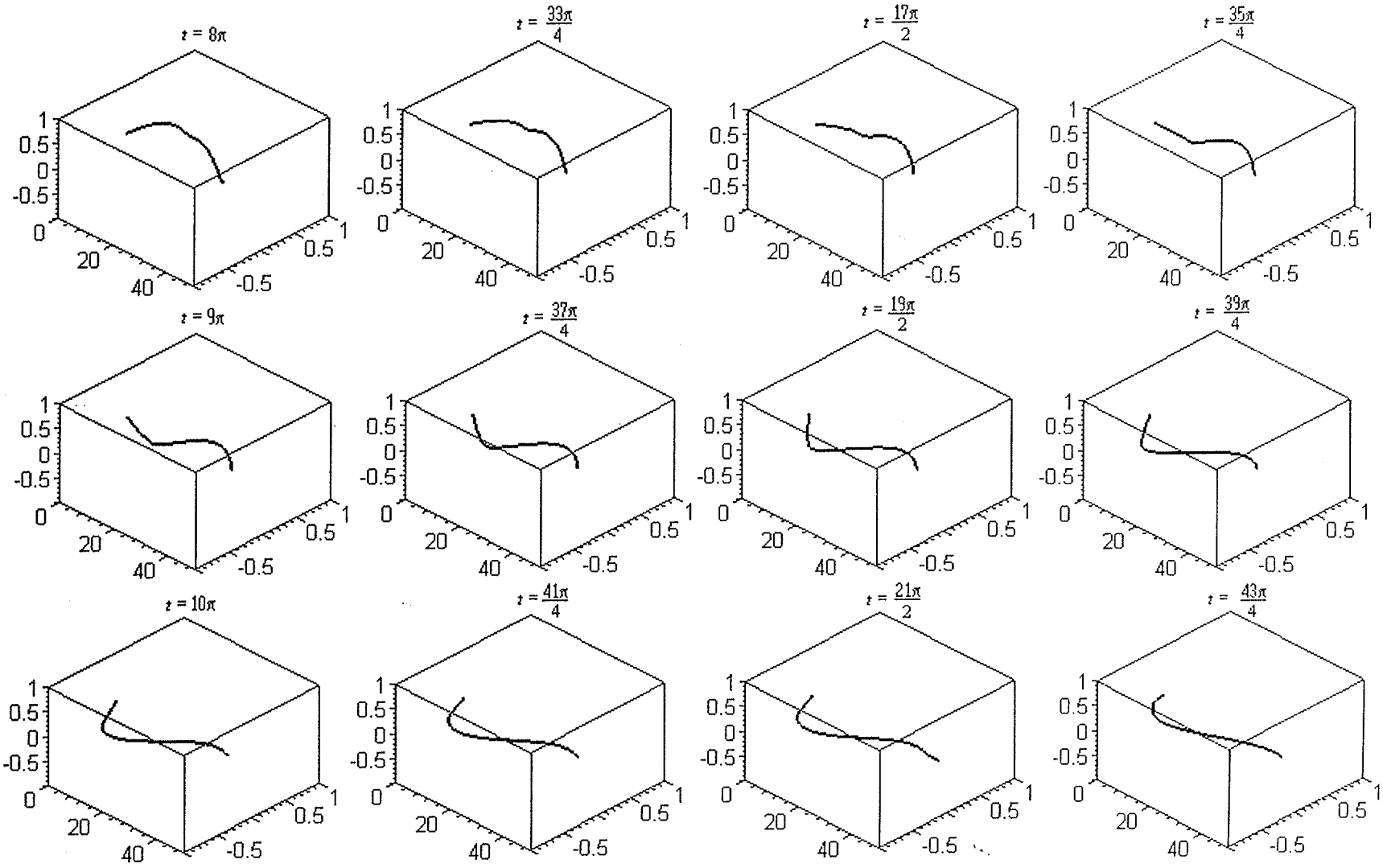
t = 8π
t = 33π/4
t = 17π/2
t = 35π/4
t = 9π
t = 37π/4
t = 19π/2
t = 39π/4
t = 10π
t = 41π/4
t = 21π/2
t = 43π/4
1
0.5
0
-0.5
0
20
40
-0.5
0.5
1

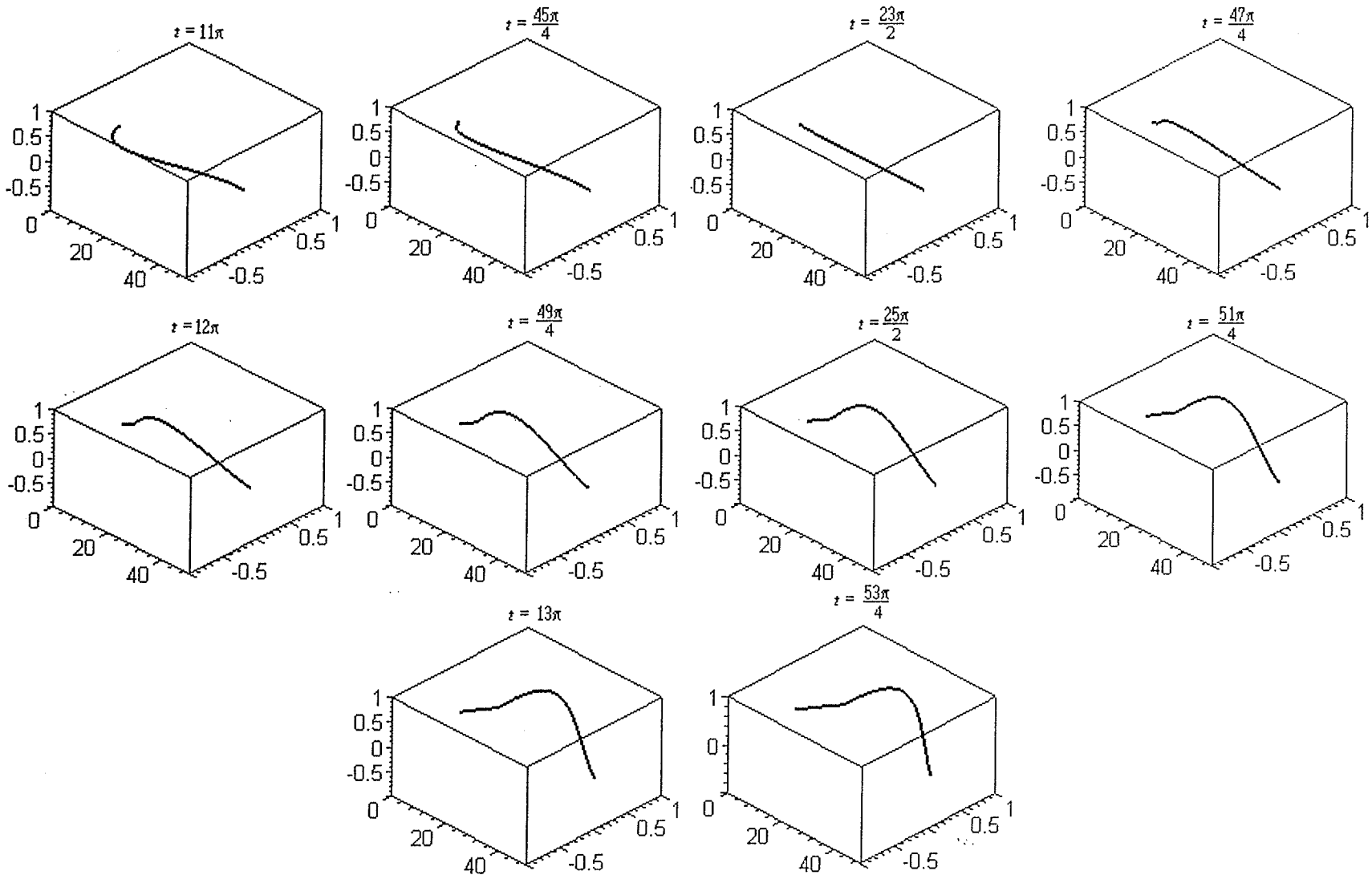
t = 11π
t = 45π/4
t = 23π/2
t = 47π/4
t = 12π
t = 49π/4
t = 25π/2
t = 51π/4
t = 13π
t = 53π/4
1
0.5
0
-0.5
0
20
40
-0.5
0.5
1

Observations:

1) The planar nature of the wave is evident and the amplitude of the rotating wave is between 0 and 1.
2) The lengthening of the wave is also evident.
3) There is a general tendency for $|A_n|$ and $|A_{-n}|$ to decrease as n increases, although not monotonically.
4) At times $t = \pi, \frac{17\pi}{4}, \frac{37\pi}{4}$ it appears as though the wave has transitioned from the first fundamental mode into the second fundamental mode; however, the transition is only temporary as the moving boundary prevents the wave from remaining in this mode.
5) No apparent differences between Figures 3.4.1a and 3.4.1b occur, thus, our truncation of the Fourier series (3.4.2) is reasonable.
6) It is a relatively straightforward matter to use the results of section 6.3 of [Qin] to obtain analytical expressions for the solution of Example 3.4.1. Indeed, if this is done, and the results are compared graphically with the preceding graphs, the only noticeable difference observed is the "smoothing of the corner" present in the analytic solution. This corner is a result of the choice of the initial- and boundary-conditions, which guarantee only that the solution is of class C^0. This smoothing in the above diagrams is, of course, a result of the truncation of the Fourier series representation of the solution of this problem.

Example 3.4.2:

As in the previous example, suppose $c=2,\ k=1,\ L=10$ and $\omega = 1/5$, so that

$$\left.\begin{aligned} &\frac{\partial^2 u_1}{\partial t^2} - \frac{2}{5}\frac{\partial u_2}{\partial t} - \frac{1}{25}u_1 = 4\frac{\partial^2 u_1}{\partial x^2}, \\ &\frac{\partial^2 u_2}{\partial t^2} + \frac{2}{5}\frac{\partial u_1}{\partial t} - \frac{1}{25}u_2 = 4\frac{\partial^2 u_2}{\partial x^2}, \end{aligned}\right\} \quad t \geq 0, \quad 0 \leq x \leq t+10 \qquad (3.4.7a)$$

with initial-conditions

$$\left.\begin{aligned} &u_1(x,0) = \sin\left(\frac{\pi x}{10}\right), \quad \frac{\partial u_1}{\partial t}(x,0) = 0, \\ &u_2(x,0) = 0, \qquad\quad \frac{\partial u_2}{\partial t}(x,0) = -\frac{3}{20}\sin\left(\frac{\pi x}{10}\right), \end{aligned}\right\} \quad \text{for } 0 \leq x \leq t+10 \qquad (3.4.7b)$$

and boundary-conditions:

$$u_1(0,t) = u_2(0,t) = u_1(t+10,t) = u_2(t+10,t) = 0, \quad \text{for } t \geq 0. \qquad (3.4.7c,d)$$

In this example, the initial-conditions are such that $g_2(x) \neq -\omega f_1(x)$. Rotational lag will occur and thus, the resulting wave will not remain planar, even though it is initially so.

Determination of the coefficients A_n once again can be done using numerical integration, and again we use $\hat{A}_n$ to denote the approximation to A_n. In particular, in this example

$$A_n = \frac{1}{4\ln(3)} \int_{\ln(1/2)}^{\ln(3/2)} \left[\hat{B}(\zeta) + 2\hat{\alpha}(\zeta)\right] e^{-i\lambda_n \zeta}\, d\zeta$$

with

$$\lambda_n = \frac{2n\pi}{\ln(3)}, \qquad \hat{B}(\zeta) = \frac{i}{2\pi}\left\{1 - \cos\left[2\pi\left(e^{\zeta} - 1\right)\right]\right., \qquad \hat{\alpha}(\zeta) = \sin\left[2\pi\left(e^{\zeta} - 1\right)\right].$$

First we will truncate the series (3.4.2) at $N = 15$.

Table 3.4.2a: Numerical Approximations of A_n, denoted by $\hat{A}_n$:

n	Re $\hat{A}_n$	Im $\hat{A}_n$
-15	3.796781200E-04	9.248942580E-05
-14	-2.186581090E-04	-3.925997968E-04
-13	-1.621910396E-04	4.965271073E-04
-12	5.586125570E-04	-2.568133940E-04
-11	-6.783500433E-04	-2.816958735E-04
-10	3.081687553E-04	8.385962385E-04
-9	5.067977698E-04	-9.887499158E-04
-8	-1.369506538E-03	3.791834580E-04
-7	1.598475863E-03	9.999882840E-04
-6	-4.676791040E-04	-2.589195588E-03
-5	-2.431951064E-03	3.115135770E-03
-4	6.668766970E-03	-2.968233065E-04
-3	-8.735995123E-03	-1.079554185E-02
-2	-2.177110206E-02	3.645545398E-02
-1	6.412634670E-02	2.067132766E-01
0	-8.063593263E-02	4.207215154E-02
1	7.280827488E-02	-2.452637896E-01
2	-2.565510880E-02	-4.113463373E-02
3	-9.535907813E-03	1.208228171E-02
4	7.238629238E-03	2.686476165E-04
5	-2.616589868E-03	-3.318569740E-03
6	-4.856938308E-04	2.741665183E-03
7	1.675992272E-03	-1.054275839E-03
8	-1.430449335E-03	-3.931284495E-04
9	5.281644108E-04	1.026626942E-03
10	3.179629990E-04	-8.685191135E-04
11	-6.997805645E-04	2.914230358E-04
12	5.752361505E-04	2.638653445E-04
13	-1.669545809E-04	-5.098616700E-04
14	-2.239086945E-04	4.026171863E-04
15	3.885411733E-04	-9.487195068E-05

Graphical representations for the resulting wave motion at a sequence of times over the interval $\left[0, \frac{53\pi}{4}\right]$ are shown in Figure 3.4.2a.

Figure 3.4.2a Graphical Illustration of Example 3.4.2 (31 term Fourier series approximation)

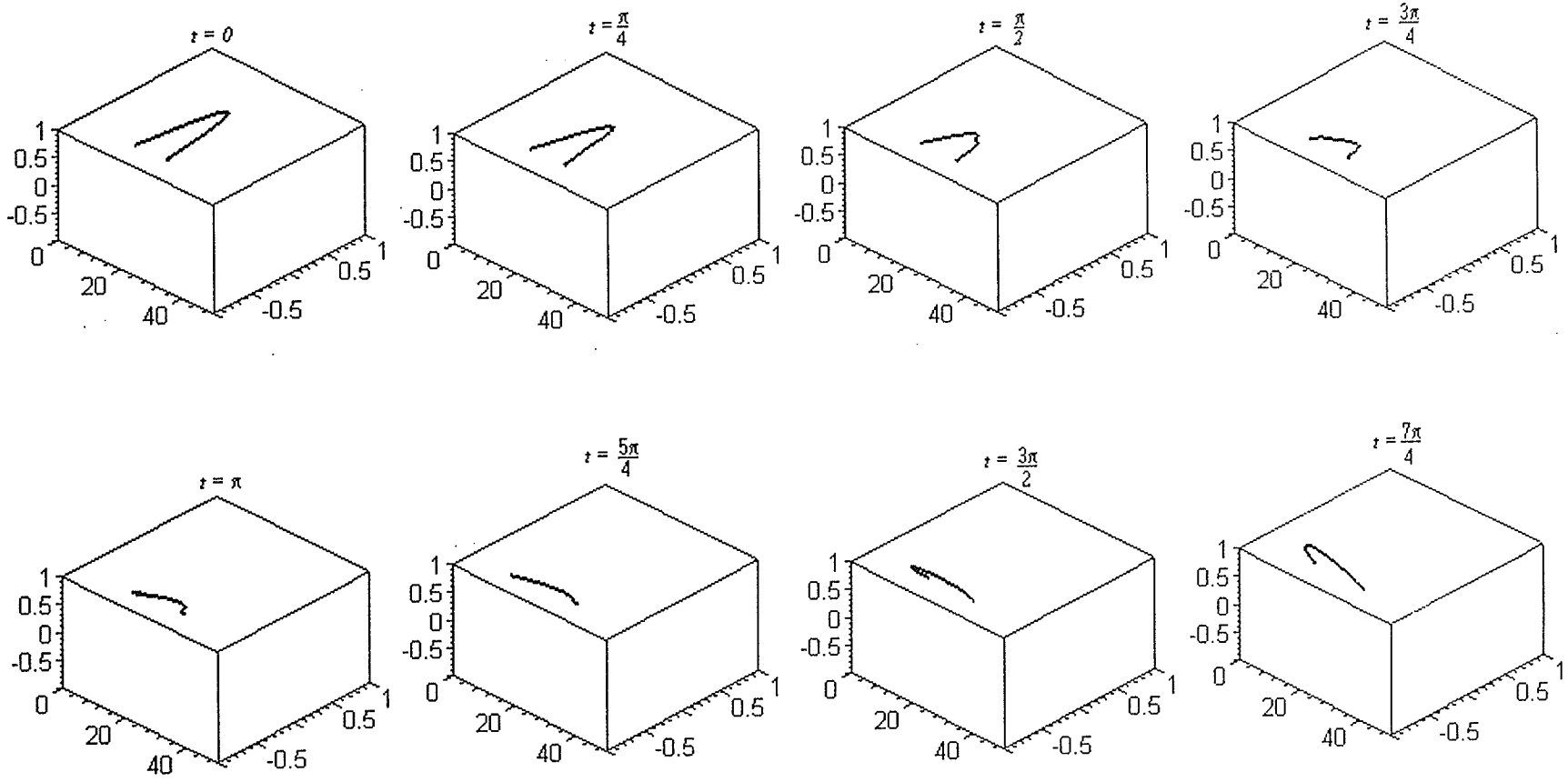

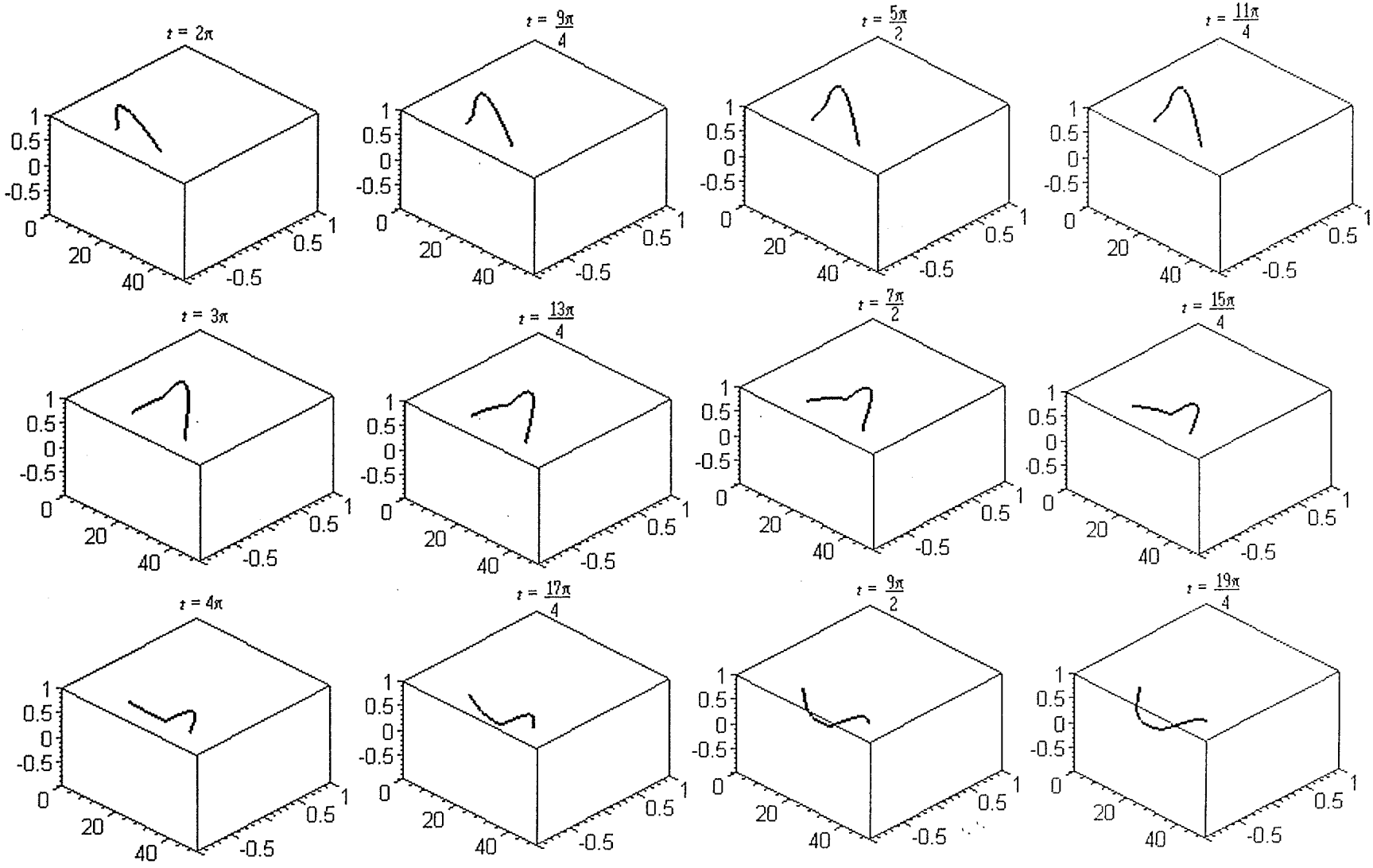
t = 2π
t = 9π/4
t = 5π/2
t = 11π/4
t = 3π
t = 13π/4
t = 7π/2
t = 15π/4
t = 4π
t = 17π/4
t = 9π/2
t = 19π/4
1
0.5
0
-0.5
0
20
40
-0.5
0.5
1

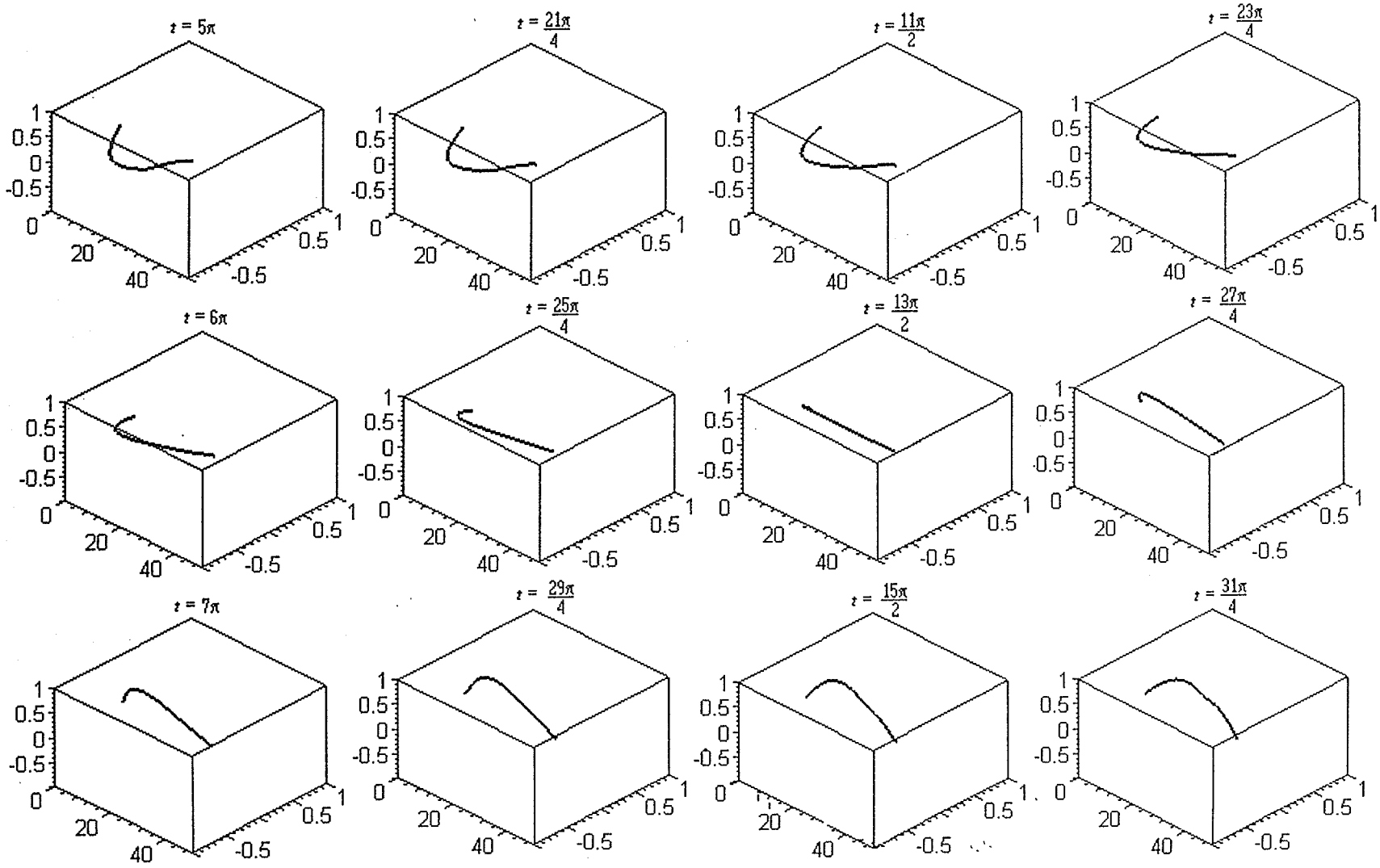
t = 5π
t = 21π/4
t = 11π/2
t = 23π/4
t = 6π
t = 25π/4
t = 13π/2
t = 27π/4
t = 7π
t = 29π/4
t = 15π/2
t = 31π/4

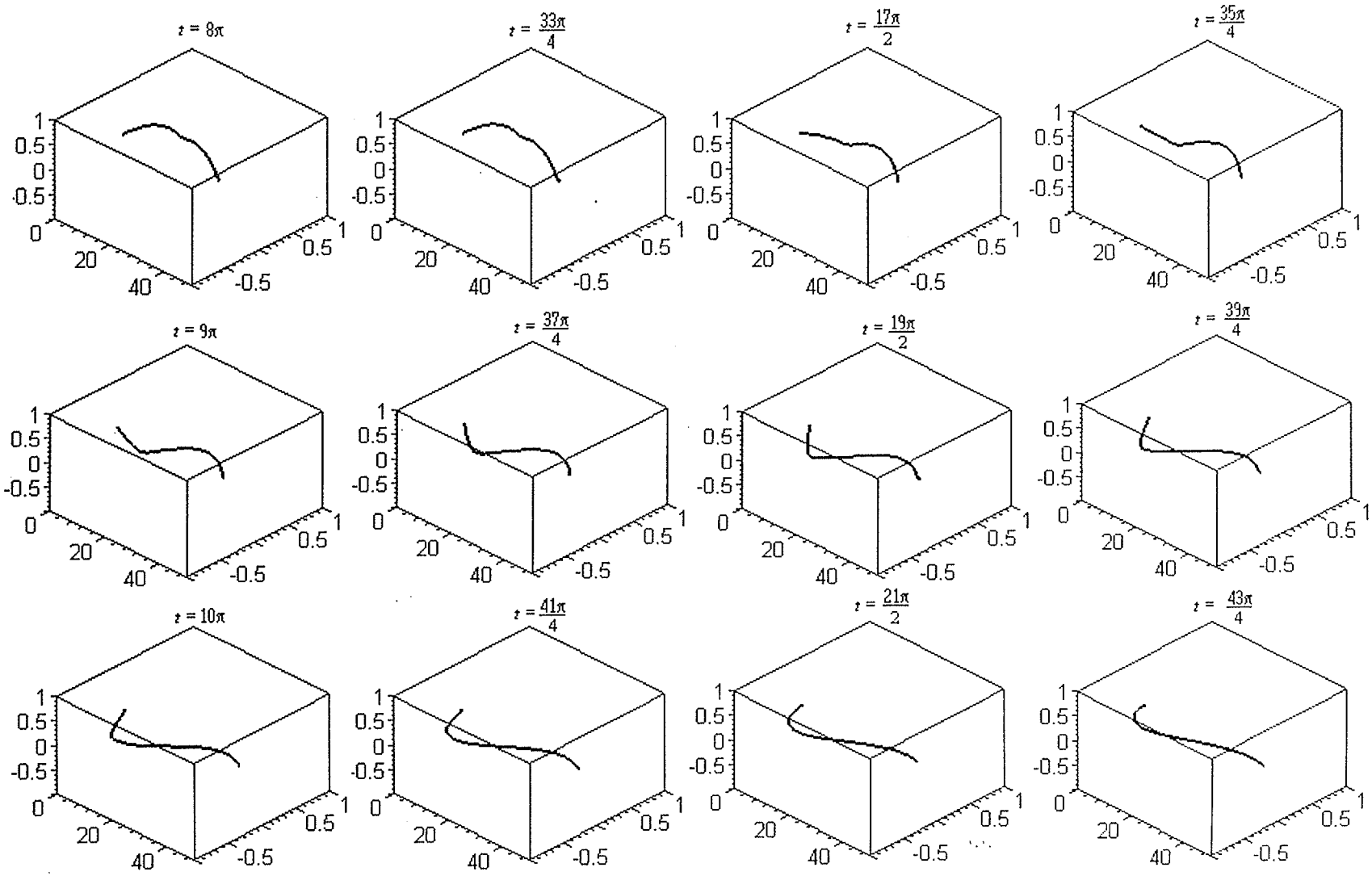
t = 8π
t = 33π/4
t = 17π/2
t = 35π/4
t = 9π
t = 37π/4
t = 19π/2
t = 39π/4
t = 10π
t = 41π/4
t = 21π/2
t = 43π/4
1
0.5
0
-0.5
0
20
40
-0.5
0.5
1

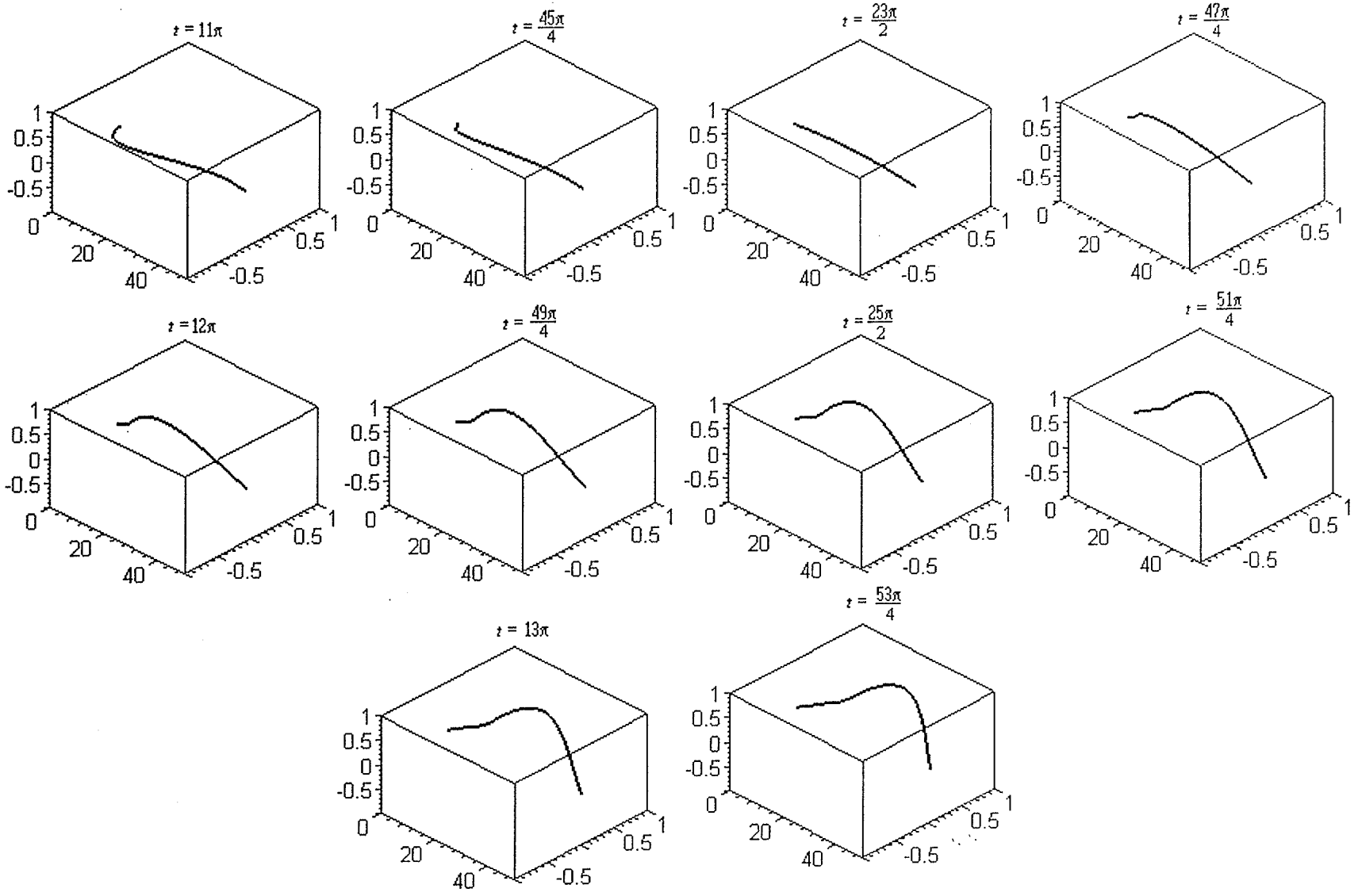
t = 11π
t = 45π/4
t = 23π/2
t = 47π/4
t = 12π
t = 49π/4
t = 25π/2
t = 51π/4
t = 13π
t = 53π/4
1
0.5
0
-0.5
0
20
40
-0.5
0.5
1

As was done in Example 3.4.1, we will extend our analysis to a 61 term Fourier series approximation and will consider the case when $N = 30$.

Table 3.4.2b: Numerical Approximations of A_n, denoted by $\hat{A}_n$:

n	Re $\hat{A}_n$	Im $\hat{A}_n$
-30	-8.695631745E-05	-4.296891193E-05
-29	2.958275185E-05	9.950430913E-05
-28	5.667563205E-05	-9.587004615E-05
-27	-1.170569592E-04	2.543903030E-05
-26	1.059806007E-04	7.390239675E-05
-25	-1.935634460E-05	-1.384276658E-04
-24	-9.586437973E-05	1.175726715E-04
-23	1.648910770E-04	-1.052781183E-05
-22	-1.310326856E-04	-1.243584520E-04
-21	-2.289882348E-06	1.983327947E-04
-20	1.621343372E-04	-1.468978539E-04
-19	-2.416465239E-04	-2.108558618E-05
-18	1.659358821E-04	2.135758559E-04
-17	4.918802618E-05	-2.994740285E-04
-16	-2.860297275E-04	1.892791473E-04
-15	3.796781200E-04	9.248942580E-05
-14	-2.186581090E-04	-3.925997968E-04
-13	-1.621910396E-04	4.965271073E-04
-12	5.586125570E-04	-2.568133940E-04
-11	-6.783500433E-04	-2.816958735E-04
-10	3.081687553E-04	8.385962385E-04
-9	5.067977698E-04	-9.887499158E-04
-8	-1.369506538E-03	3.791834580E-04
-7	1.598475863E-03	9.999882840E-04
-6	-4.676791040E-04	-2.589195588E-03
-5	-2.431951064E-03	3.115135770E-03
-4	6.668766970E-03	-2.968233065E-04
-3	-8.735995123E-03	-1.079554185E-02
-2	-2.177110206E-02	3.645545398E-02

-1	6.412634670E-02	2.067132766E-01
0	-8.063593263E-02	4.207215154E-02
1	7.280827488E-02	-2.452637896E-01
2	-2.565510880E-02	-4.113463373E-02
3	-9.535907813E-03	1.208228171E-02
4	7.238629238E-03	2.686476165E-04
5	-2.616589868E-03	-3.318569740E-03
6	-4.856938308E-04	2.741665183E-03
7	1.675992272E-03	-1.054275839E-03
8	-1.430449335E-03	-3.931284495E-04
9	5.281644108E-04	1.026626942E-03
10	3.179629990E-04	-8.685191135E-04
11	-6.997805645E-04	2.914230358E-04
12	5.752361505E-04	2.638653445E-04
13	-1.669545809E-04	-5.098616700E-04
14	-2.239086945E-04	4.026171863E-04
15	3.885411733E-04	-9.487195068E-05
16	-2.924169283E-04	-1.933052573E-04
17	5.033591985E-05	3.056547538E-04
18	1.690986906E-04	-2.178162122E-04
19	-2.461152007E-04	2.155946583E-05
20	1.650324999E-04	1.494318739E-04
21	-2.384131881E-06	-2.016547469E-04
22	-1.330957841E-04	1.263803667E-04
23	1.674148555E-04	1.065010705E-05
24	-9.729423605E-05	-1.192746241E-04
25	-1.960110017E-05	1.403782319E-04
26	1.073999437E-04	-7.492100240E-05
27	-1.185850962E-04	-2.575030343E-05
28	5.740211295E-05	9.706437635E-05
29	2.992656050E-05	-1.007143364E-04
30	-8.796880085E-05	4.348409270E-05

Graphical representations for the resulting wave motion at a sequence of times over the interval $\left[0, \frac{53\pi}{4}\right]$ are shown in Figure 3.4.2b.

Figure 3.4.2b Graphical Illustration of Example 3.4.2 (61 term Fourier series approximation)

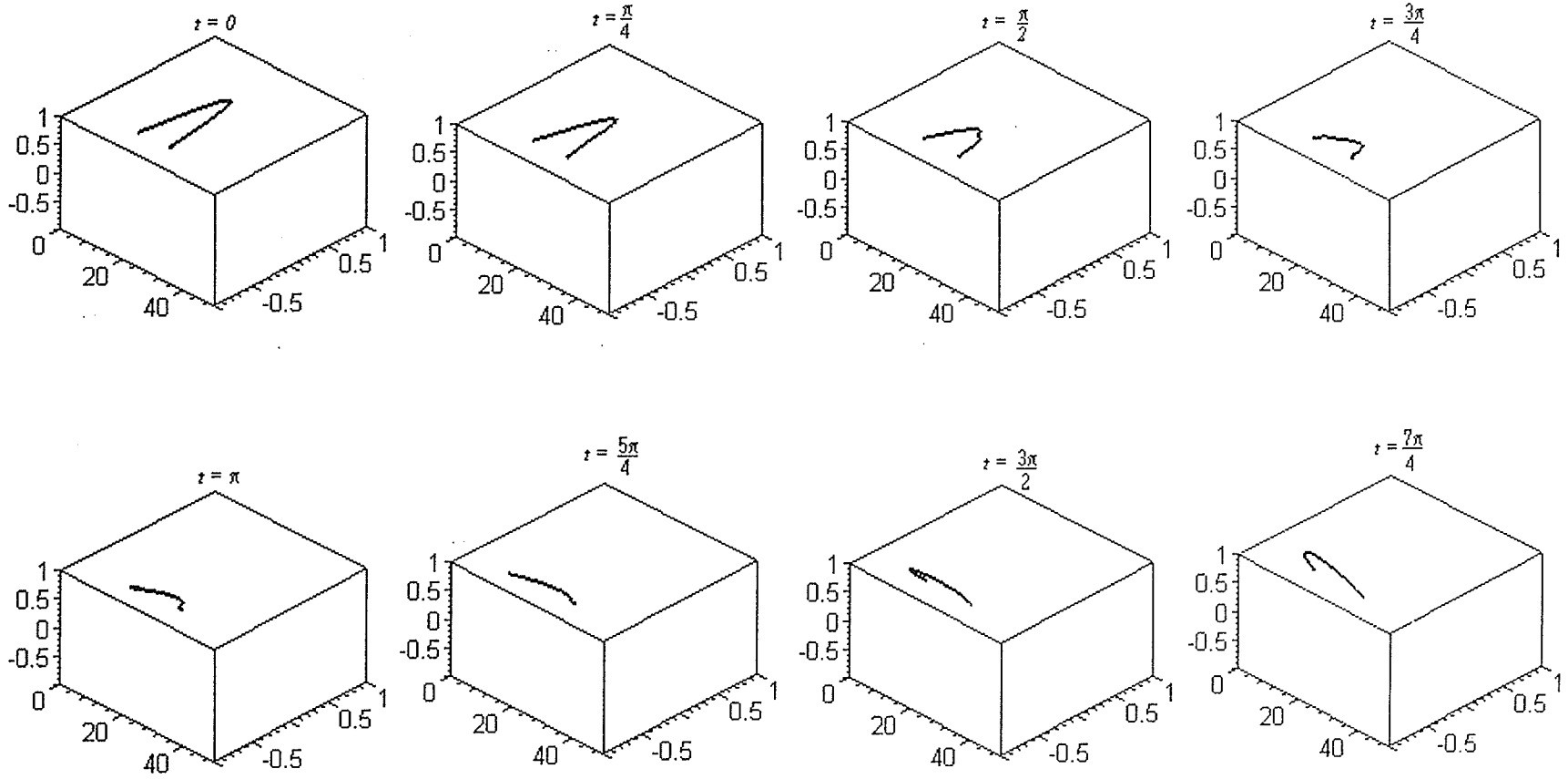

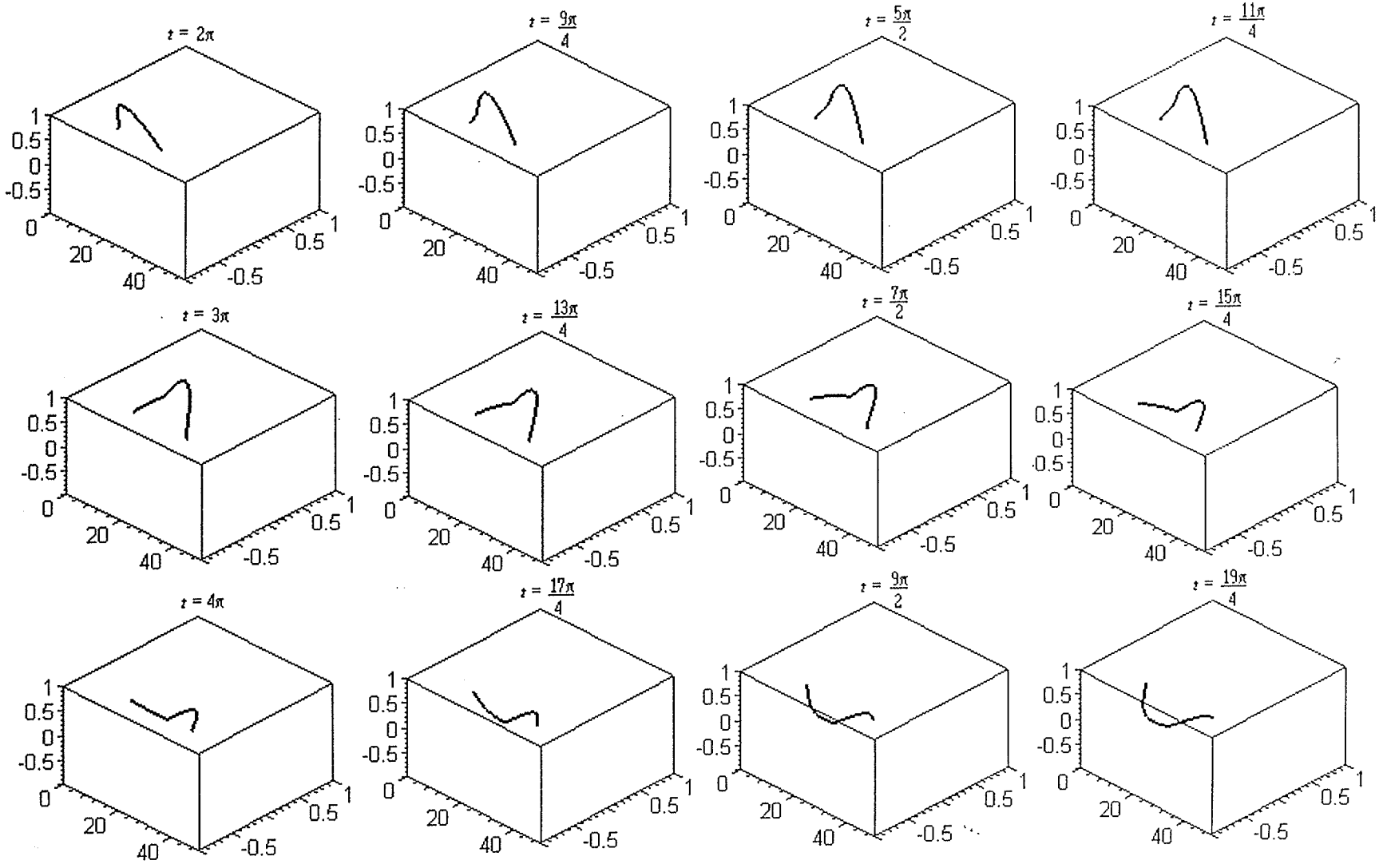
t = 2π
t = 9π/4
t = 5π/2
t = 11π/4
t = 3π
t = 13π/4
t = 7π/2
t = 15π/4
t = 4π
t = 17π/4
t = 9π/2
t = 19π/4

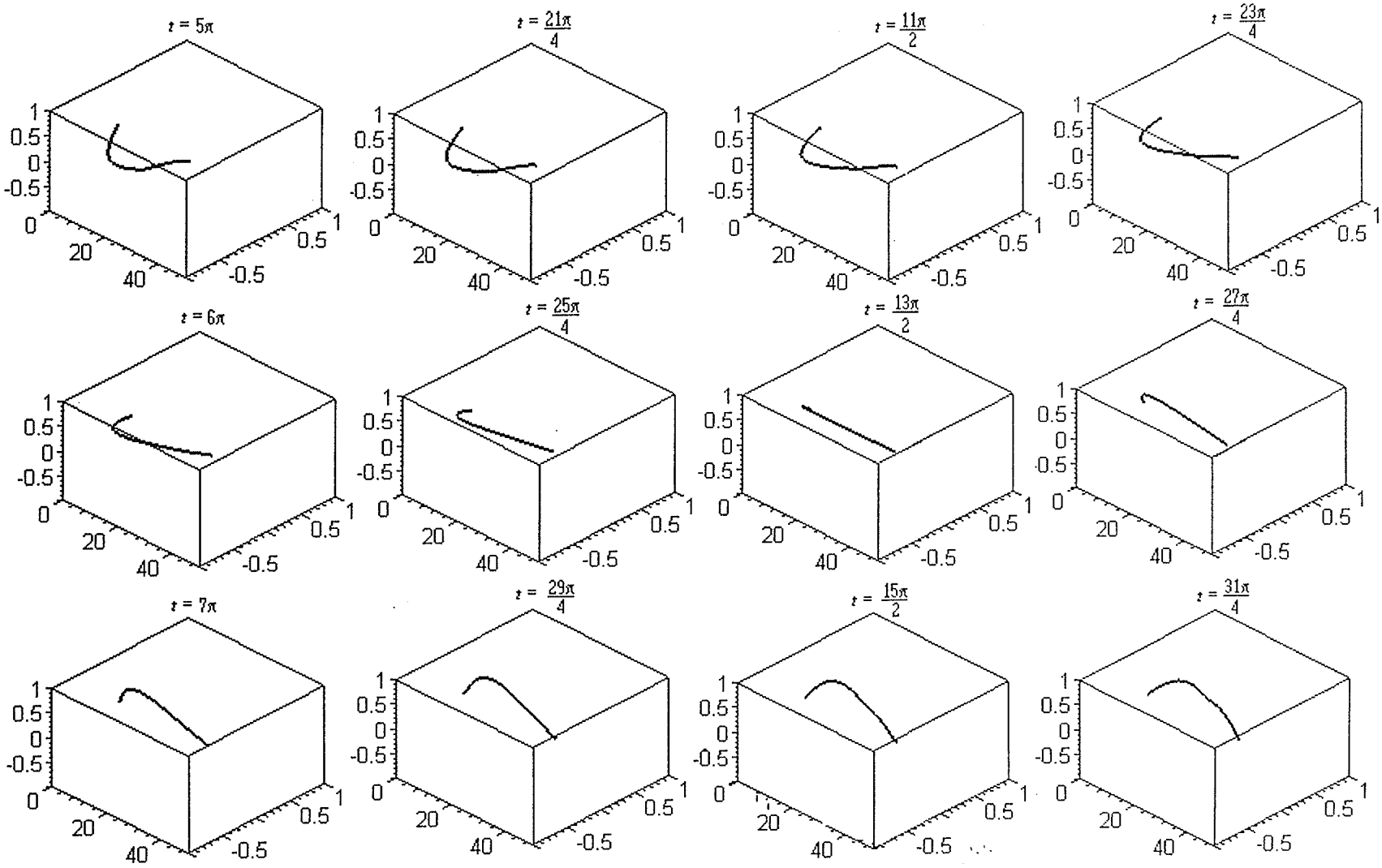
t = 5π
t = 21π/4
t = 11π/2
t = 23π/4
t = 6π
t = 25π/4
t = 13π/2
t = 27π/4
t = 7π
t = 29π/4
t = 15π/2
t = 31π/4

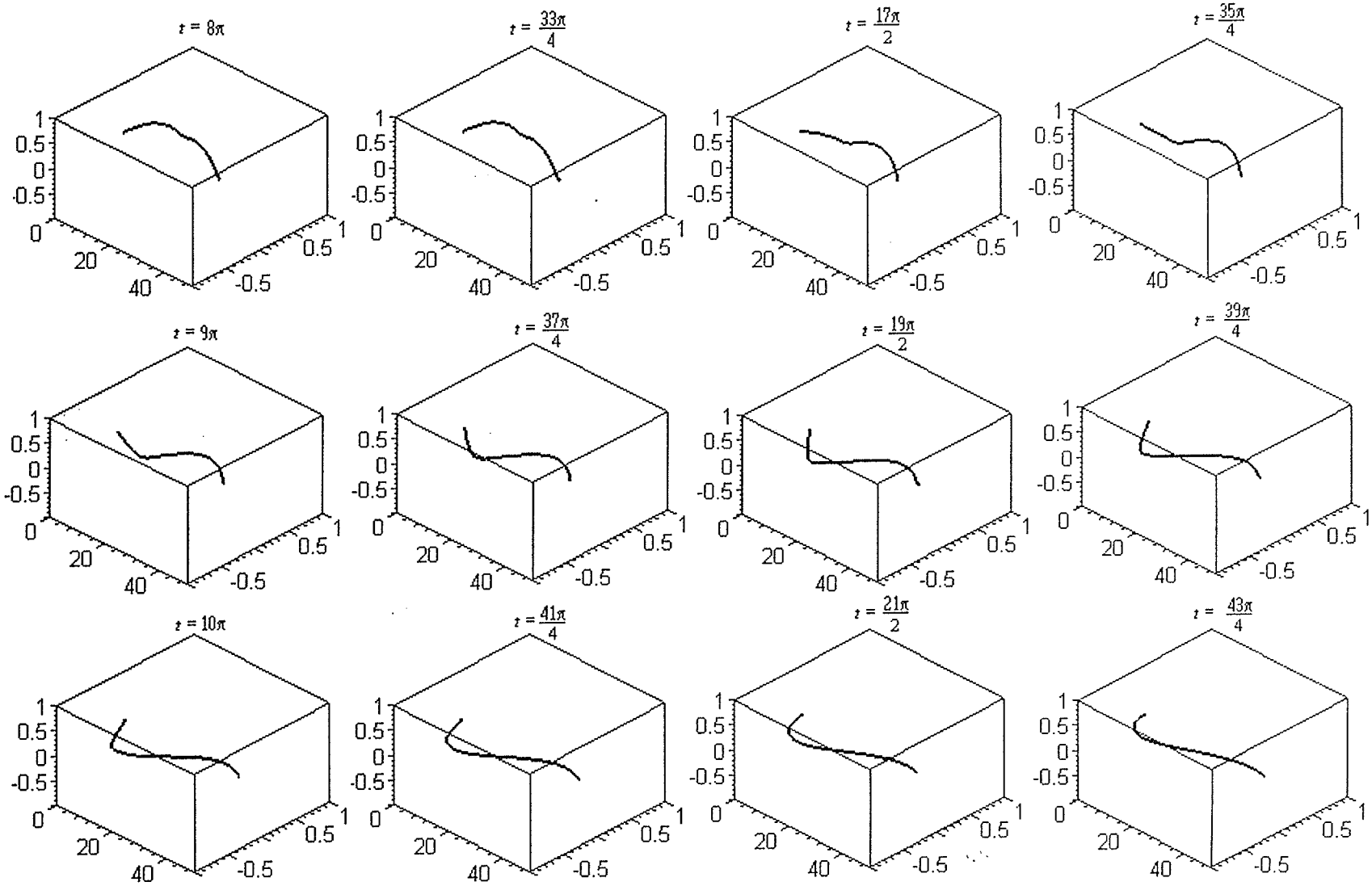
t = 8π
t = 33π/4
t = 17π/2
t = 35π/4
t = 9π
t = 37π/4
t = 19π/2
t = 39π/4
t = 10π
t = 41π/4
t = 21π/2
t = 43π/4
1
0.5
0
-0.5
0
20
40
-0.5
0.5
1

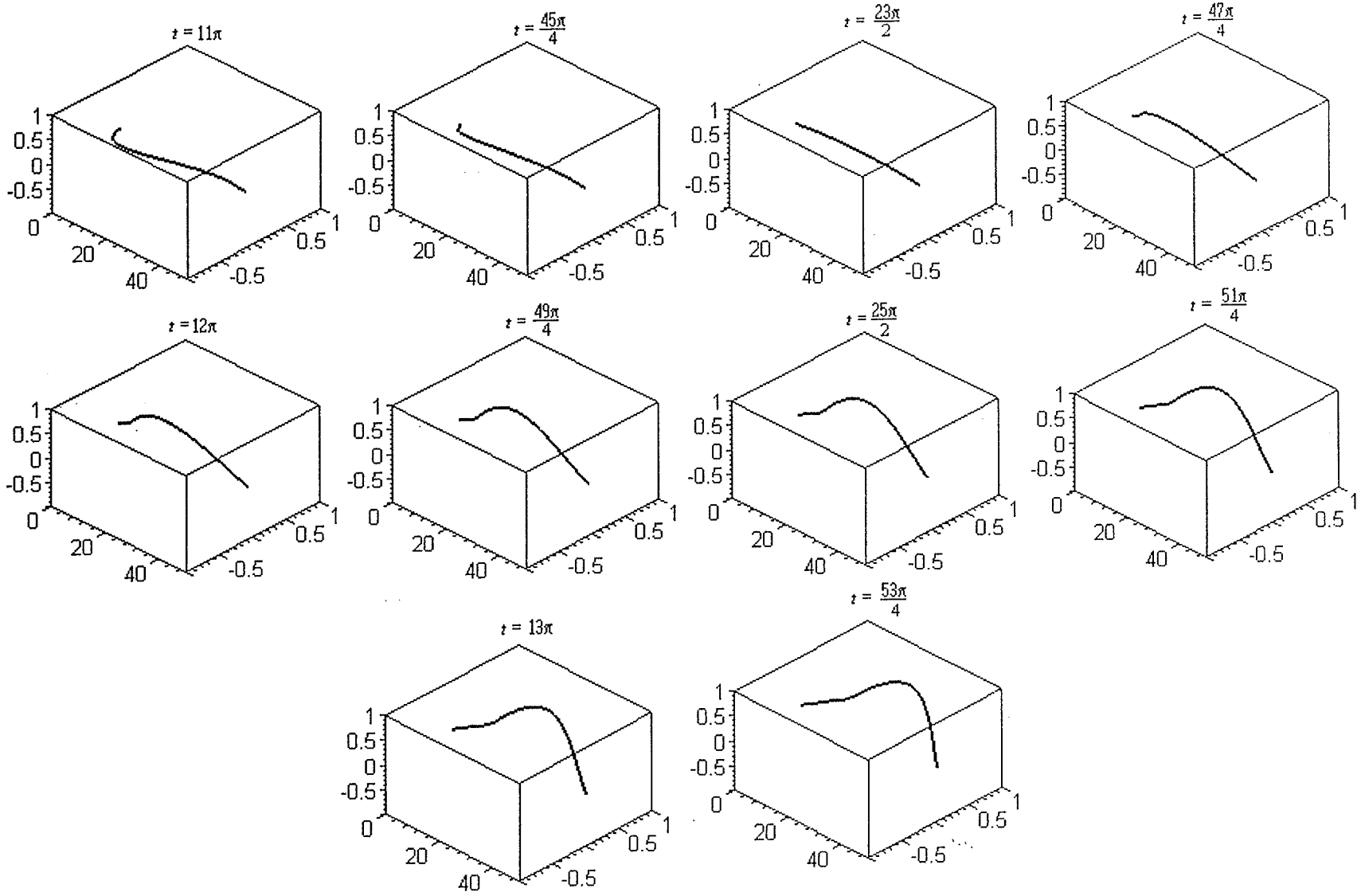
t = 11π
t = 45π/4
t = 23π/2
t = 47π/4
t = 12π
t = 49π/4
t = 25π/2
t = 51π/4
t = 13π
t = 53π/4
1
0.5
0
-0.5
0
20
40
-0.5
0.5
1

Observations: 1) The non-planar nature of the wave begins to become evident approximately at time $t = \frac{3\pi}{4}$ where the top portion of the wave begins to "topple over", and is extremely evident for times $t = \frac{5\pi}{4}, \frac{3\pi}{2}, \frac{9\pi}{4}, \frac{37\pi}{4}$.

2) The lengthening of wave is evident as was also seen in Example 3.4.1.

3) Once again, there is no noticeable difference between the graphical illustrations shown in Figures 3.4.2a and 3.4.2b, thus indicating a reasonable approximation of the solution through truncation of the Fourier series with minimal error.

Chapter 4

The Non-Homogeneous Problem

4.1 Introduction

In this chapter we will consider the IMBVP with general initial- and boundary-conditions and with the linear moving boundary $S(t) = kt + L$. All of the previous analysis and transformations from Chapter 2 hold, although, because we now consider non-zero boundary-conditions, the boundary transformation (2.3.1) causes the differential equation to be non-homogeneous.

4.2 The Non-Homogeneous IMBVP

As indicated in section 3.1, we restrict consideration to the special case of a linearly-moving endpoint, whose motion is described by the function

$$S(t) = kt + L \tag{4.2.1}$$

with k, L positive real constants and $k < c$. It is assumed throughout the sequel that at least one of the functions $p_1(t), p_2(t), q_1(t)$ or $q_2(t)$, appearing in (1.3.1c,d), is non-zero, so that

all of the transformations of Chapter 2 must now be considered. In particular, the Carrier-Greenspan transformation is given by (3.3.3), i.e.,

$$\xi = \frac{kx}{c(kt + L)}, \qquad \tau = \ln\left(\frac{kt + L}{L}\right), \tag{4.2.2}$$

with inverse given by (3.3.4), i.e.,

$$x = \frac{cL}{k}\xi e^{\tau}, \qquad t = \frac{L(e^{\tau} - 1)}{k}. \tag{4.2.3}$$

In addition, after all transformations of Chapter 2 have been performed, the IMBVP (1.3.1) assumes the form

$$(1 - \xi^2)\frac{\partial^2 \widetilde{Z}}{\partial \xi^2} + 2\xi\frac{\partial^2 \widetilde{Z}}{\partial \xi \partial \tau} - \frac{\partial^2 \widetilde{Z}}{\partial \tau^2} - 2\xi\frac{\partial \widetilde{Z}}{\partial \xi} + \frac{\partial \widetilde{Z}}{\partial \tau} = -\frac{L^2}{k^2}e^{2\tau}\widetilde{A}(\xi, \tau) \tag{4.2.4a}$$

with initial-conditions

$$\widetilde{Z}(\xi,0) = \widetilde{\alpha}(\xi), \qquad \frac{\partial \widetilde{Z}}{\partial \tau}(\xi,0) = \widetilde{\beta}^*(\xi), \qquad 0 \le \xi \le \frac{k}{c} \tag{4.2.4b}$$

and boundary-conditions

$$\widetilde{Z}(0, \tau) = \widetilde{Z}\left(\frac{k}{c}, \tau\right) = 0, \qquad \tau \ge 0 \tag{4.2.4c,d}$$

where

$$\widetilde{A}(\xi, \tau) = \frac{ck}{L^2}e^{-2\tau}\left[\left(\xi - \frac{k}{c}\right)\ddot{\widetilde{P}}(\tau) - \left(3\xi - \frac{k}{c}\right)\dot{\widetilde{P}}(\tau) + 2\xi\widetilde{P}(\tau)\right.$$

$$\left. - \xi\ddot{\widetilde{Q}}(\tau) + 3\xi\dot{\widetilde{Q}}(\tau) - 2\xi\widetilde{Q}(\tau)\right], \tag{4.2.5a}$$

in which, in accordance with (2.4.4), we define

$$\widetilde{\beta}^*(\xi) = \frac{L}{k}\widetilde{\beta}(\xi) + \xi\widetilde{\alpha}'(\xi), \tag{4.2.5b}$$

$$\tilde{\alpha}(\xi) = \alpha\left(\frac{cL}{k}\xi e^{\tau}\right)\Big|_{\tau=0} = \alpha\left(\frac{cL}{k}\xi\right), \tag{4.2.5c}$$

$$\tilde{\beta}(\xi) = \beta\left(\frac{cL}{k}\xi e^{\tau}\right)\Big|_{\tau=0} = \beta\left(\frac{cL}{k}\xi\right), \tag{4.2.5d}$$

$$\tilde{P}(\tau) = P\left(\frac{L(e^{\tau}-1)}{k}\right), \tag{4.2.5e}$$

$$\tilde{Q}(\tau) = Q\left(\frac{L(e^{\tau}-1)}{k}\right), \tag{4.2.5f}$$

and $\cdot \equiv \dfrac{d}{\partial\tau}$.

Following Greenspan [Gre], we seek a solution of the above IMBVP through the use of Laplace transforms (taken with respect to τ) defined, in the usual fashion, according to

$$\bar{Z}(\xi,s) = \mathcal{L}\left\{\tilde{Z}(\xi,\tau)\right\} = \int_0^{\infty} e^{-s\tau}\tilde{Z}(\xi,\tau)d\tau\,. \tag{4.2.6}$$

Operationally, ξ is held constant throughout this integration, so we may immediately write, by virtue of (4.2.4b) and (4.2.5),

$$\mathcal{L}\left\{\frac{\partial\tilde{Z}}{\partial\xi}\right\} = \frac{\partial\bar{Z}}{\partial\xi}(\xi,s),$$

$$\mathcal{L}\left\{\frac{\partial^2\tilde{Z}}{\partial\xi^2}\right\} = \frac{\partial^2\bar{Z}}{\partial\xi^2}(\xi,s),$$

$$\mathcal{L}\left\{\frac{\partial\tilde{Z}}{\partial\tau}\right\} = s\bar{Z}(\xi,s) - \tilde{Z}(\xi,0)$$

$$= s\bar{Z}(\xi,s) - \tilde{\alpha}(\xi),$$

$$\mathcal{L}\left\{\frac{\partial^2 \tilde{Z}}{\partial \tau^2}\right\} = s^2 \bar{Z}(\xi, s) - s\tilde{Z}(\xi,0) - \frac{\partial \tilde{Z}}{\partial \tau}(\xi,0)$$

$$= s^2 \bar{Z}(\xi, s) - s\tilde{\alpha}(\xi) - \tilde{\beta}^*(\xi),$$

$$\mathcal{L}\left\{\frac{\partial^2 \tilde{Z}}{\partial \xi \partial \tau}\right\} = s\frac{\partial \bar{Z}}{\partial \xi}(\xi, s) - \frac{\partial \tilde{Z}}{\partial \xi}(\xi,0)$$

$$= s\frac{\partial \bar{Z}}{\partial \xi}(\xi, s) - \tilde{\alpha}'(\xi).$$

Thus, upon taking Laplace transforms, (4.2.4a) essentially becomes an ordinary differential equation in ξ, depending on the parameter s, of the form

$$(1-\xi^2)\frac{\partial^2 \bar{Z}}{\partial \xi^2} + 2(s-1)\xi\frac{\partial \bar{Z}}{\partial \xi} - s(s-1)\bar{Z} = Y(\xi, s) \quad , \tag{4.2.7a}$$

in which

$$Y(\xi, s) = -\frac{L^2}{k^2}\bar{A}(\xi, s-2) + \xi\tilde{\alpha}'(\xi) + (1-s)\tilde{\alpha}(\xi) - \frac{L}{k}\tilde{\beta}(\xi) \ , \tag{4.2.7b}$$

and

$$\bar{A}(\xi, s) = \mathcal{L}\left\{\tilde{A}(\xi, \tau)\right\}. \tag{4.2.7c}$$

In an effort to solve (4.2.7a), we introduce the function

$$\phi(\xi, s) = \left(1-\xi^2\right)^{\frac{(1-s)}{2}}\bar{Z}(\xi, s), \tag{4.2.8}$$

and rewrite (4.2.7a) in the form

$$\frac{\partial^2 \phi}{\partial \xi^2}(\xi, s) + \frac{(1-s^2)}{(1-\xi^2)^2}\phi(\xi, s) = (1-\xi^2)^{\frac{-(s+1)}{2}}Y(\xi, s), \tag{4.2.9}$$

which may be regarded as a second order non-homogeneous ordinary differential equation in ξ, with variable coefficients and with s a parameter. To obtain a solution, we must first find a solution $\phi_h(\xi, s)$ to the homogeneous problem

$$\frac{\partial^2 \phi_h}{\partial \xi^2}(\xi, s) + \frac{(1-s^2)}{(1-\xi^2)^2}\phi_h(\xi, s) = 0. \tag{4.2.10}$$

Based on the form of the coefficient of $\phi_h(\xi, s)$, and using the analysis of Chapter 3 as a guide, we assume a solution of (4.2.10) of the form

$$\phi_h(\xi, s) = (1-\xi)^{\varepsilon}(1+\xi)^{\delta} \tag{4.2.11}$$

where ε, δ are constants yet to be determined. Substituting (4.2.11) into (4.2.10) yields

$$[\varepsilon(\varepsilon-1) - 2\varepsilon\delta + \delta(\delta-1) + (1-s^2)] + 2[\varepsilon(\varepsilon-1) - \delta(\delta-1)]\ \xi$$

$$+ [\varepsilon(\varepsilon-1) + 2\varepsilon\delta + \delta(\delta-1)]\ \xi^2 = 0.$$

For this equation to be satisfied, the coefficients of the various powers of ξ must be zero. This requirement produces a system of three non-linear equations in 2 unknowns, namely

$$\varepsilon(\varepsilon-1) - 2\varepsilon\delta + \delta(\delta-1) = -\ (1-s^2)$$

$$\varepsilon(\varepsilon-1) - \delta(\delta-1) = 0$$

$$\varepsilon(\varepsilon-1) + 2\varepsilon\delta + \delta(\delta-1) = 0$$

possessing only two distinct solutions of the form

$$\varepsilon = \varepsilon_1 \equiv \frac{1}{2}(1+s), \qquad \delta = \delta_1 \equiv \frac{1}{2}(1-s),$$

or

$$\varepsilon = \varepsilon_2 \equiv \frac{1}{2}(1-s), \qquad \delta = \delta_2 \equiv \frac{1}{2}(1+s).$$

Therefore, the general solution of (4.2.9) is given by

$$\phi_h(\xi,s)=\sqrt{1-\xi^2}\left[c_1(s)\left(\frac{1-\xi}{1+\xi}\right)^{s/2}+c_2(s)\left(\frac{1+\xi}{1-\xi}\right)^{s/2}\right], \tag{4.2.12}$$

in which $c_1(s)$, $c_2(s)$ are arbitrary functions of the parameter s.

To conclude the analysis of (4.2.9), it is necessary only to determine a particular solution $\phi_p(\xi,s)$ of (4.2.9). This may be accomplished by a number of techniques; in this case we choose to employ the method of variation of parameters [Zil p.195]. To this end, we assume

$$\phi_p(\xi,s)=\psi_1(\xi,s)\phi_1(\xi,s)+\psi_2(\xi,s)\phi_2(\xi,s), \tag{4.2.13}$$

in which

$$\phi_1(\xi,s)=\sqrt{1-\xi^2}\left(\frac{1-\xi}{1+\xi}\right)^{s/2}$$

and

$$\phi_2(\xi,s)=\sqrt{1-\xi^2}\left(\frac{1+\xi}{1-\xi}\right)^{s/2}.$$

One may immediately deduce that

$$\frac{\partial\phi_1}{\partial\xi}=-\frac{(\xi+s)}{\sqrt{1-\xi^2}}\left(\frac{1-\xi}{1+\xi}\right)^{s/2}$$

and

$$\frac{\partial\phi_2}{\partial\xi}=-\frac{(\xi-s)}{\sqrt{1-\xi^2}}\left(\frac{1+\xi}{1-\xi}\right)^{s/2}.$$

Moreover, it may be shown that

$$W(\phi_1(\xi,s),\phi_2(\xi,s)) \equiv \begin{vmatrix} \phi_1(\xi,s) & \phi_2(\xi,s) \\ \dfrac{\partial\phi_1}{\partial\xi}(\xi,s) & \dfrac{\partial\phi_2}{\partial\xi}(\xi,s) \end{vmatrix},$$

$$= 2s,$$

$$W_1(\phi_1(\xi,s),\phi_2(\xi,s)) \equiv \begin{vmatrix} 0 & \phi_2(\xi,s) \\ (1-\xi^2)^{\frac{-(s+1)}{2}} Y(\xi,s) & \dfrac{\partial\phi_2}{\partial\xi}(\xi,s) \end{vmatrix}$$

$$= -\frac{Y(\xi,s)}{(1-\xi)^s},$$

and

$$W_2(\phi_1(\xi,s),\phi_2(\xi,s)) \equiv \begin{vmatrix} \phi_1(\xi,s) & 0 \\ \dfrac{\partial\phi_1}{\partial\xi}(\xi,s) & (1-\xi^2)^{\frac{-(s+1)}{2}} Y(\xi,s) \end{vmatrix}$$

$$= \frac{Y(\xi,s)}{(1+\xi)^s},$$

so that we may write

$$\psi_1(\xi,s) = \int_0^{\xi} \frac{W_1}{W}\,d\xi = -\frac{1}{2s}\int_0^{\xi} \frac{Y(\xi,s)}{(1-\xi)^s}\,d\xi, \tag{4.2.14a}$$

and

$$\psi_2(\xi,s) = \int_0^{\xi} \frac{W_2}{W}\,d\xi = \frac{1}{2s}\int_0^{\xi} \frac{Y(\xi,s)}{(1+\xi)^s}\,d\xi. \tag{4.2.14b}$$

Finally, when (4.2.14) are substituted into (4.2.13), the general solution of (4.2.9) assumes the form

$$\phi(\xi, s) = \phi_h(\xi, s) + \phi_p(\xi, s)$$

$$= \sqrt{1-\xi^2}\left\{\left(\frac{1-\xi}{1+\xi}\right)^{s/2}\left[c_1(s) - \frac{1}{2s}\int_0^{\xi}\frac{Y(\xi, s)}{(1-\xi)^s}\,d\xi\right]\right.$$

$$\left. + \left(\frac{1+\xi}{1-\xi}\right)^{s/2}\left[c_2(s) + \frac{1}{2s}\int_0^{\xi}\frac{Y(\xi, s)}{(1+\xi)^s}\,d\xi\right]\right\} \qquad (4.2.15)$$

Furthermore, upon substitution of (4.2.15) into (4.2.8), we obtain

$$\bar{Z}(\xi, s) = (1-\xi)^s\left[c_1(s) - \frac{1}{2s}\int_0^{\xi}\frac{Y(\xi, s)}{(1-\xi)^s}\,d\xi\right]$$

$$+ (1+\xi)^s\left[c_2(s) + \frac{1}{2s}\int_0^{\xi}\frac{Y(\xi, s)}{(1+\xi)^s}\,d\xi\right]. \qquad (4.2.16)$$

The coefficients $c_1(s)$ and $c_2(s)$ may be evaluated through use of the boundary-conditions

$$\bar{Z}(0, s) = \bar{Z}\left(k/c, s\right) = 0$$

which respectively, provide the results that

$$c_1(s) + c_2(s) = 0$$

and

$$\left(1 - k/c\right)^s\left[c_1(s) - \frac{1}{2s}\int_0^{k/c}\frac{Y(\xi, s)}{(1-\xi)^s}\,d\xi\right] + \left(1 + k/c\right)^s\left[c_2(s) + \frac{1}{2s}\int_0^{k/c}\frac{Y(\xi, s)}{(1-\xi)^s}\,d\xi\right] = 0,$$

from which we conclude that

$$c_1(s) = -c_2(s)$$

$$= \frac{1}{2c\left[\left(1-k/c\right)^s - \left(1+k/c\right)^s\right]} \int_0^{k/c} \left[\frac{\left(1-k/c\right)^s}{(1-\xi)^s} - \frac{\left(1+k/c\right)^s}{(1+\xi)^s}\right] Y(\xi, s)d\xi \,. \qquad (4.2.17)$$

Substitution of (4.2.17) into (4.2.16) yields the general solution of (4.2.7a), whose form depends crucially on the nature of the function $Y(\xi, s)$ defined in (4.2.7b).

Finally, it is noted that to complete the determination of the solution of the IMBVP (1.3.1) it is necessary to find the inverse Laplace transform $\tilde{Z}(\xi, \tau) = \mathcal{L}^{-1}\{\bar{Z}(\xi, s)\}$, to which we then apply the sequence of transforms of Chapter 2 in reverse order, eventually obtaining the desired solutions $u_1(x,t)$ and $u_2(x,t)$. We will not display all of the results of this process, but do note that there are two very serious difficulties to be encountered in this process:

a) The function $Y(\xi, s)$, defined by (4.2.7b), depends on the initial- and boundary-conditions (1.3.1b – d), and hence on the moving boundary $S(t) = kt + L$. The determination of $c_1(s)$, $c_2(s)$ and $\bar{Z}(\xi, s)$, as exhibited in (4.2.17) and (4.2.16), depend on one's ability to integrate $\frac{Y(\xi, s)}{(1-\xi)^s}$ and $\frac{Y(\xi, s)}{(1+\xi)^s}$, both definitely and indefinitely, with respect to ξ. Since either of these may pose considerable difficulty, it may be difficult to successfully use this method to solve the IMBVP (1.3.1).

b) Moreover, even if one is successful in evaluating the above-mentioned integrals, it is then necessary to find the inverse Laplace transform of $\bar{Z}(\xi, s)$. This too may prove to be extremely difficult.

4.3 Solution for the Non-Homogeneous Problem

To demonstrate the process outlined in the previous section, we will consider the IMBVP (1.3.1), with one non-zero boundary-condition, so that we will now be dealing with a non-homogeneous form of the partial differential equation (2.3.2a).

Example 4.3.1:

Take $c=2,\ k=1,\ L=10$ and $\omega = \frac{1}{5}$:

$$\left.\begin{aligned} \frac{\partial^2 u_1}{\partial t^2} - \frac{2}{5}\frac{\partial u_2}{\partial t} - \frac{1}{25}u_1 &= 4\frac{\partial^2 u_1}{\partial x^2}, \\ \frac{\partial^2 u_2}{\partial t^2} + \frac{2}{5}\frac{\partial u_1}{\partial t} - \frac{1}{25}u_2 &= 4\frac{\partial^2 u_2}{\partial x^2}, \end{aligned}\right\} \quad t \geq 0, \quad 0 \leq x \leq t+10 \qquad (4.3.1a)$$

with initial-conditions

$$\left.\begin{aligned} u_1(x,0) &= 0, \quad \frac{\partial u_1}{\partial t}(x,0) = 0 \\ u_2(x,0) &= 0, \quad \frac{\partial u_2}{\partial t}(x,0) = 0 \end{aligned}\right\} \quad 0 \leq x \leq t+10 \qquad (4.3.1b)$$

and boundary-conditions

$$u_1(0,t) = \frac{1}{2}\left[1 - \cos\left(\frac{\pi t}{10}\right)\right], \qquad u_2(0,t) = 0, \qquad (4.3.1c)$$

$$u_1(t+10,t)=0, \qquad u_2(t+10,t)=0 \tag{4.3.1d}$$

for $t \geq 0$.

After applying all of the transformations from Chapter 2 equation (4.2.7a) becomes

$$(1-\xi^2)\frac{\partial^2 \overline{Z}}{\partial \xi^2}+2(s-1)\xi\frac{\partial \overline{Z}}{\partial \xi}-s(s-1)\overline{Z}=Y(\xi,s) \tag{4.3.2a}$$

in which, for reasons to be explained below, (4.2.7b) reduces to

$$Y(\xi,s)=-100\overline{A}(\xi,s-2). \tag{4.3.2b}$$

In addition, by virtue of (2.2.5) and (2.3.4), we find that

$$\alpha(x)=\frac{x}{10}P(0)-P(0)=0$$

$$\beta(x)=\frac{x}{10}P'(0)-\frac{x}{100}P(0)-P'(0)=0,$$

and through the implementation of the Carrier-Greenspan transformation (4.2.2), it is easily shown that (2.4.4) provide

$$\tilde{\alpha}(\xi)=\tilde{\alpha}'(\xi)=\tilde{\beta}(\xi)=\tilde{\beta}^*(\xi)=0.$$

Thus, equations (4.2.5) provide

$$\tilde{A}(\xi,\tau)=\frac{1}{50}e^{-2\tau}\left[\left(\xi-\frac{1}{2}\right)\ddot{\tilde{P}}(\tau)-\left(3\xi-\frac{1}{2}\right)\dot{\tilde{P}}(\tau)+2\xi\tilde{P}(\tau)\right] \tag{4.3.2c}$$

where

$$\begin{aligned}\tilde{P}(\tau)&=P\left(10(e^{\tau}-1)\right)\\&=\frac{1}{2}\left[1-\cos\left(\pi(e^{\tau}-1)\right)\right]e^{2i(e^{\tau}-1)},\end{aligned}$$

$$\dot{\tilde{P}}(\tau)=\pi e^{\tau}\left\{\frac{1}{2}\sin\left(\pi(e^{\tau}-1)\right)+i\left[1-\cos\left(\pi(e^{\tau}-1)\right)\right]\right\}e^{2i(e^{\tau}-1)},$$

and

$$\ddot{\tilde{P}}(\tau) = \pi^2 e^{2\tau}\left\{\frac{1}{2}\cos\left(\pi(e^{\tau}-1)\right)+ i\sin\left(\pi(e^{\tau}-1)\right)\right\}e^{2i\left(e^{\tau}-1\right)}$$

$$+ \pi e^{\tau}\left\{\frac{1}{2}\sin\left(\pi(e^{\tau}-1)\right)+ i\left[1-\cos\left(\pi(e^{\tau}-1)\right)\right]\right\}\left(1+2ie^{\tau}\right)\, e^{2i\left(e^{\tau}-1\right)}.$$

When these derivatives are substituted into (4.3.2c), it becomes apparent how difficult it is going to be to take the Laplace transform of $\tilde{A}(\xi,\tau)$ to obtain $\overline{A}(\xi,s)$ and subsequently $Y(\xi,s)$. However, one important observation which can be made is that $\tilde{A}(\xi,\tau)$ is linear in ξ, thus both $\overline{A}(\xi,s)$ and $Y(\xi,s)$ will also be linear in ξ. This fact will allow for the integrals in the solution (4.2.16) to be evaluated, assuming that the Laplace transform $\overline{A}(\xi,s)$ can be found. Unfortunately, even if this were to pose no difficulty, we would still be faced with having to find the inverse Laplace transform $\tilde{Z}(\xi,s)$ of (4.2.16).

In light of the simple initial- and boundary-data we have specified in this example, this method of using the Laplace transform to solve the non-homogeneous IMBVP is far from ideal. Based on this disappointing realization, we will revert to using d'Alembert's method so that analysis of this example may continue.

Using (6.3.16) – (6.3.22) of [Qin], in conjunction with Diagram 4.3.1 (adapted from [Qin p.138]), it may be shown that d'Alembert's method yields the following expressions for the real and imaginary parts ($\mathrm{Re}\,W(x,t)$ and $\mathrm{Im}\,W(x,t)$) of the solution $W(x,t)$ of the IMBVP (2.2.4), and with $S(t) = t + 10$:

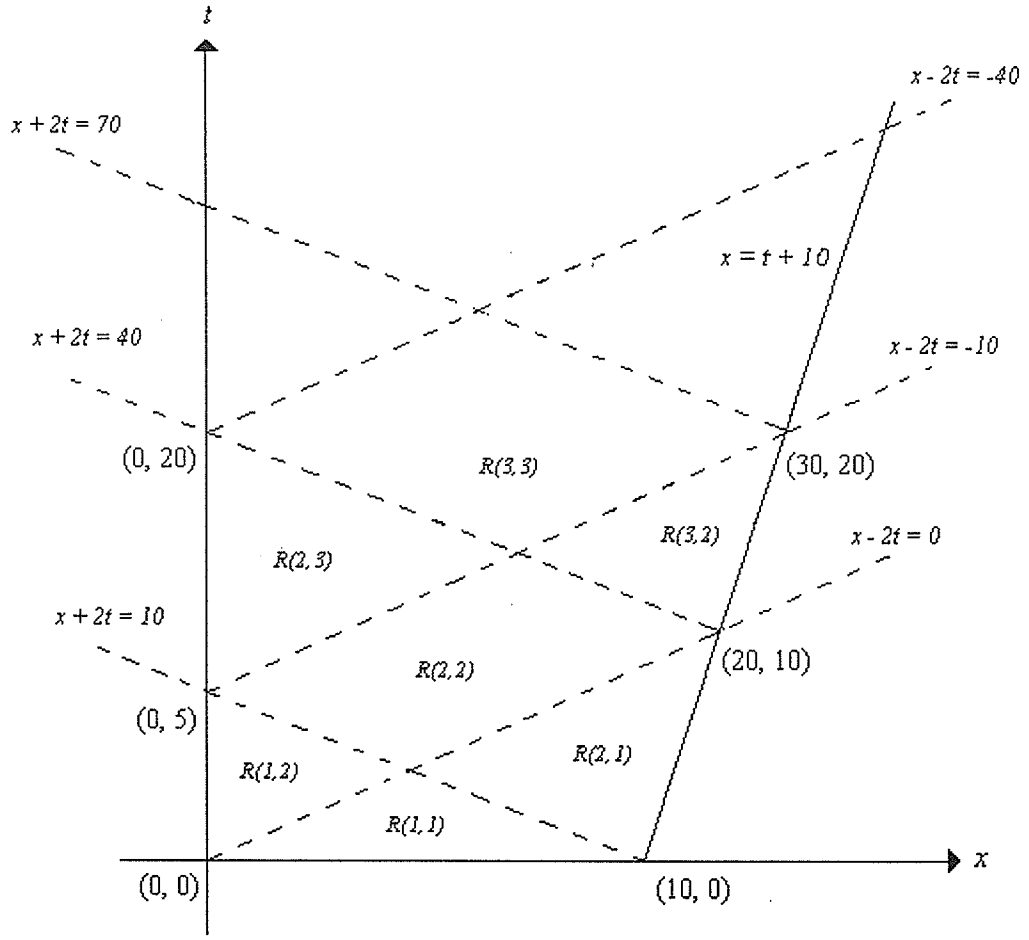

Diagram 4.3.1

For $0 \le t \le \frac{5}{2}$:

$$\operatorname{Re} W(x,t) = \begin{cases} p_1(t - x/2)\cos\left(\omega(t - x/2)\right), & 0 \le x \le 2t \\ 0, & 2t \le x \le 10 - 2t \\ 0, & 10 - 2t \le x \le t + 10 \end{cases}$$

$$\operatorname{Im} W(x,t) = \begin{cases} p_1(t - x/2)\sin\left(\omega(t - x/2)\right), & 0 \le x \le 2t \\ 0, & 2t \le x \le 10 - 2t \\ 0, & 10 - 2t \le x \le t + 10 \end{cases}$$

For $\frac{5}{2} \le t \le 5$:

$$\operatorname{Re} W(x,t) = \begin{cases} p_1(t - x/2)\cos\left(\omega(t - x/2)\right), & 0 \le x \le 10 - 2t \\ p_1(t - x/2)\cos\left(\omega(t - x/2)\right), & 10 - 2t \le x \le 2t \\ 0, & 2t \le x \le t + 10 \end{cases}$$

$$\operatorname{Im} W(x,t) = \begin{cases} p_1(t - x/2)\sin\left(\omega(t - x/2)\right), & 0 \le x \le 10 - 2t \\ p_1(t - x/2)\sin\left(\omega(t - x/2)\right), & 10 - 2t \le x \le 2t \\ 0, & 2t \le x \le t + 10 \end{cases}$$

For $5 \le t \le 10$:

$$\operatorname{Re} W(x,t) = \begin{cases} p_1(t - x/2)\cos\left(\omega(t - x/2)\right), & 0 \le x \le 2t - 10 \\ p_1(t - x/2)\cos\left(\omega(t - x/2)\right), & 2t - 10 \le x \le 2t \\ 0, & 2t \le x \le t + 10 \end{cases}$$

$$\operatorname{Im} W(x,t) = \begin{cases} p_1(t - x/2)\sin\left(\omega(t - x/2)\right), & 0 \le x \le 2t - 10 \\ p_1(t - x/2)\sin\left(\omega(t - x/2)\right), & 2t - 10 \le x \le 2t \\ 0, & 2t \le x \le t + 10 \end{cases}$$

For $10 \le t \le \frac{25}{2}$:

$$\operatorname{Re} W(x,t) = \begin{cases} p_1(t - x/2)\cos\left(\omega(t - x/2)\right), & 0 \le x \le 2t - 10 \\ p_1(t - x/2)\cos\left(\omega(t - x/2)\right), & 2t - 10 \le x \le 40 - 2t \\ p_1(t - x/2)\cos\left(\omega(t - x/2)\right) & \\ \quad + p_1\left(\frac{1}{6}(2t + x - 40)\right)\cos\left(\frac{\omega}{6}(2t + x - 40)\right), & 40 - 2t \le x \le t + 10 \end{cases}$$

$$\operatorname{Im} W(x,t) = \begin{cases} p_1(t - x/2)\sin\left(\omega(t - x/2)\right), & 0 \le x \le 2t - 10 \\ p_1(t - x/2)\sin\left(\omega(t - x/2)\right), & 2t - 10 \le x \le 40 - 2t \\ p_1(t - x/2)\sin\left(\omega(t - x/2)\right) & \\ \quad + p_1\left(\frac{1}{6}(2t + x - 40)\right)\sin\left(\frac{\omega}{6}(2t + x - 40)\right), & 40 - 2t \le x \le t + 10 \end{cases}$$

For $\frac{25}{2} \le t \le 20$:

$$\operatorname{Re} W(x,t) = \begin{cases} p_1(t - x/2)\cos\left(\omega(t - x/2)\right), & 0 \le x \le 40 - 2t \\ p_1(t - x/2)\cos\left(\omega(t - x/2)\right) & \\ \quad + p_1\left(\frac{1}{6}(2t + x - 40)\right)\cos\left(\frac{\omega}{6}(2t + x - 40)\right), & 40 - 2t \le x \le 2t - 10 \\ p_1(t - x/2)\cos\left(\omega(t - x/2)\right) & \\ \quad + p_1\left(\frac{1}{6}(2t + x - 40)\right)\cos\left(\frac{\omega}{6}(2t + x - 40)\right), & 2t - 10 \le x \le t + 10 \end{cases}$$

$$\operatorname{Im} W(x,t) = \begin{cases} p_1(t - x/2)\sin\left(\omega(t - x/2)\right), & 0 \le x \le 40 - 2t \\ p_1(t - x/2)\sin\left(\omega(t - x/2)\right) & \\ \quad + p_1\left(\frac{1}{6}(2t + x - 40)\right)\sin\left(\frac{\omega}{6}(2t + x - 40)\right), & 40 - 2t \le x \le 2t - 10 \\ p_1(t - x/2)\sin\left(\omega(t - x/2)\right) & \\ \quad + p_1\left(\frac{1}{6}(2t + x - 40)\right)\sin\left(\frac{\omega}{6}(2t + x - 40)\right), & 2t - 10 \le x \le t + 10. \end{cases}$$

Graphical representation of the solution of (4.3.1) is displayed in a manner similar to that used in Chapter 3, using the above analytical expressions to compute

$$u_1(x,t) = \cos(\omega t)\operatorname{Re} W(x,t) + \sin(\omega t)\operatorname{Im} W(x,t)$$

and

$$u_2(x,t) = -\sin(\omega t)\,\mathrm{Re}\,W(x,t) + \cos(\omega t)\,\mathrm{Im}\,W(x,t)$$

[Qin p.144].

Figure 4.3.1a illustrates the dynamics of the wave at a sequence of times over the interval $[0,20]$. With an unconstrained plot, as displayed in Figure 4.3.1a, the amplitude of the motion is highly exaggerated and at first glance appears to be unrealistic. However, in a constrained plot as exhibited in Figure 4.3.1b, the dynamics of the tether assumes a much more realistic form.

Figure 4.3.1a Graphical Illustration of Example 4.3.1 (unconstrained)

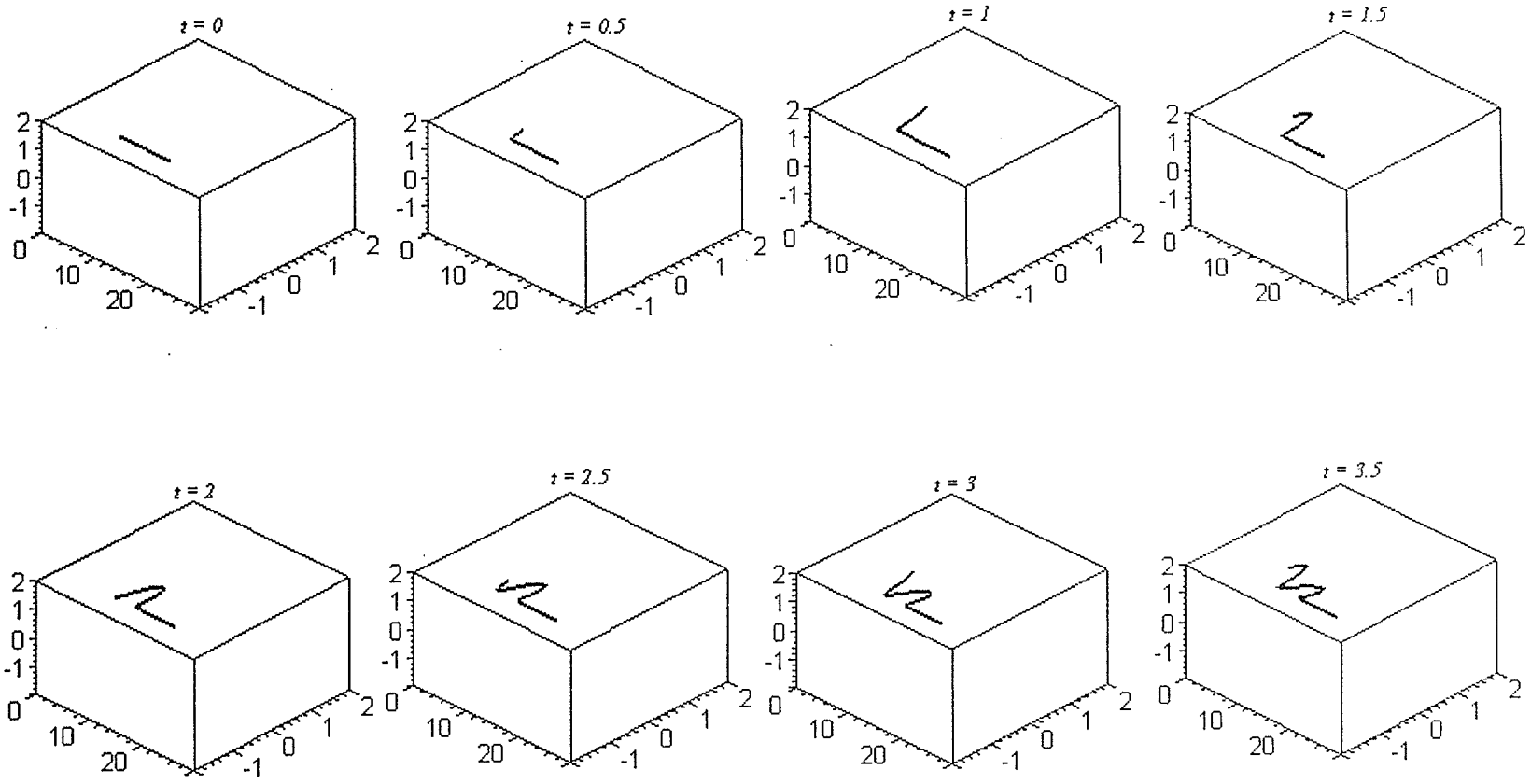

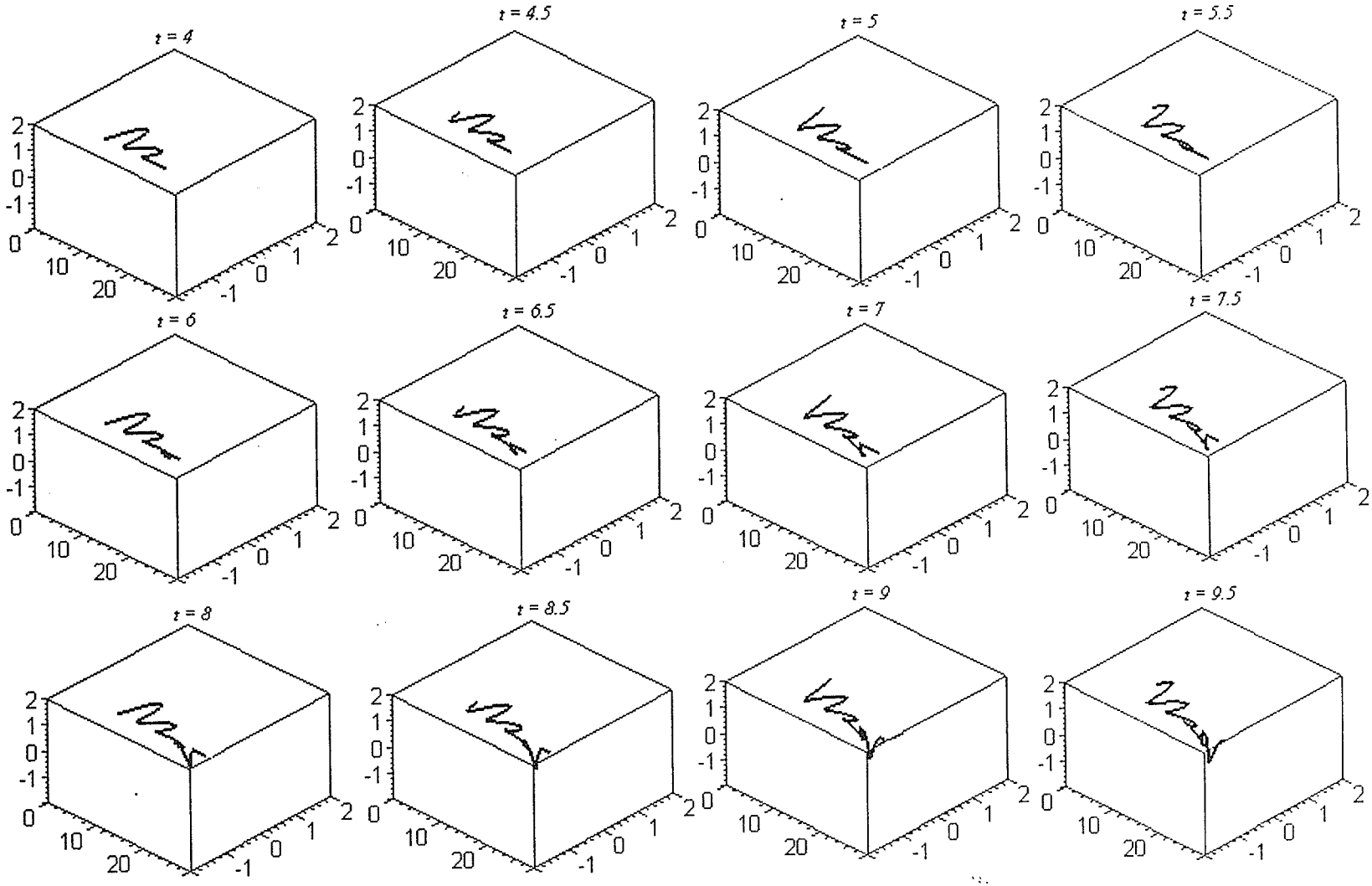
t = 4
t = 4.5
t = 5
t = 5.5
t = 6
t = 6.5
t = 7
t = 7.5
t = 8
t = 8.5
t = 9
t = 9.5

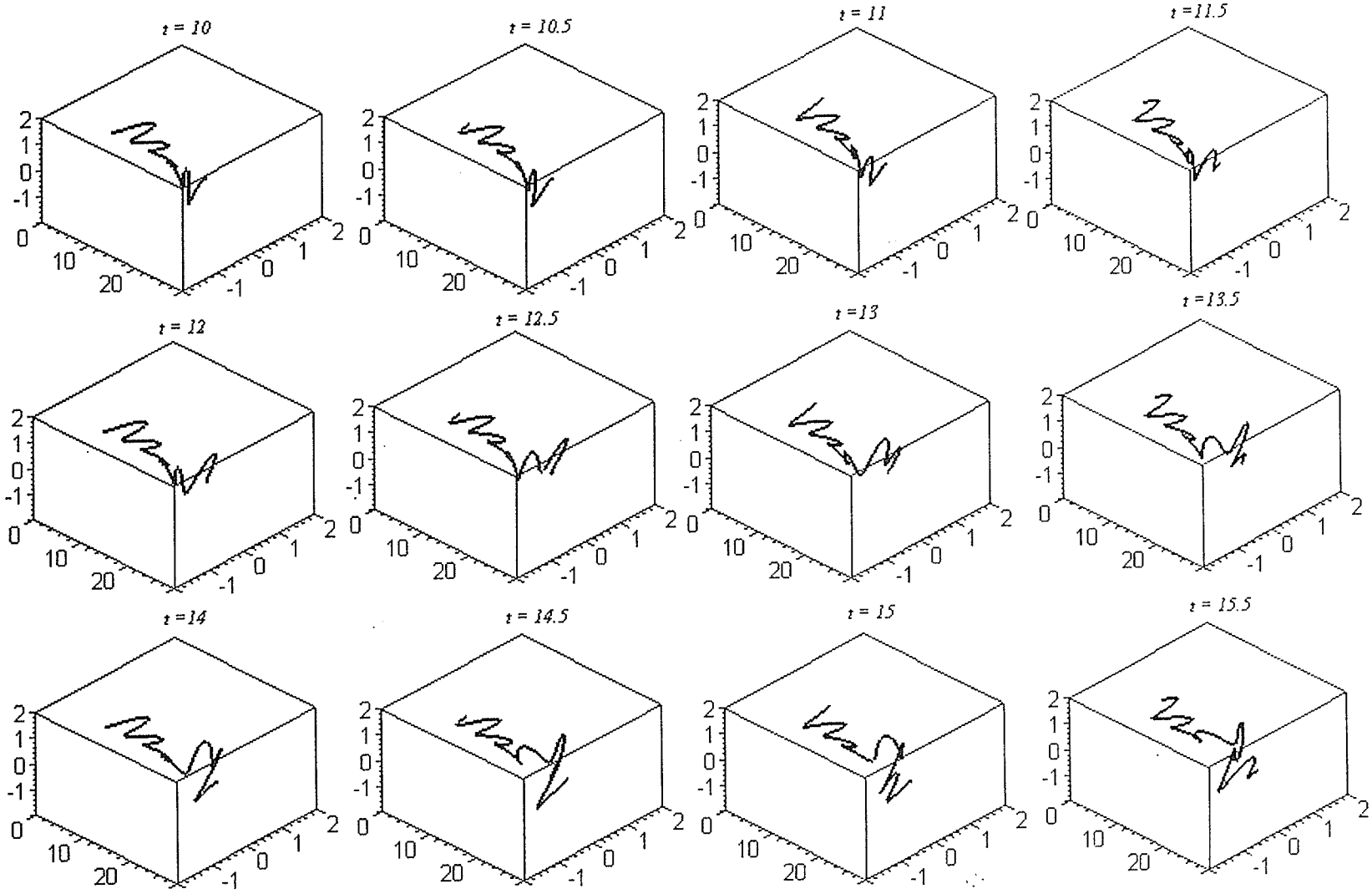
t = 10
t = 10.5
t = 11
t = 11.5
t = 12
t = 12.5
t = 13
t = 13.5
t = 14
t = 14.5
t = 15
t = 15.5

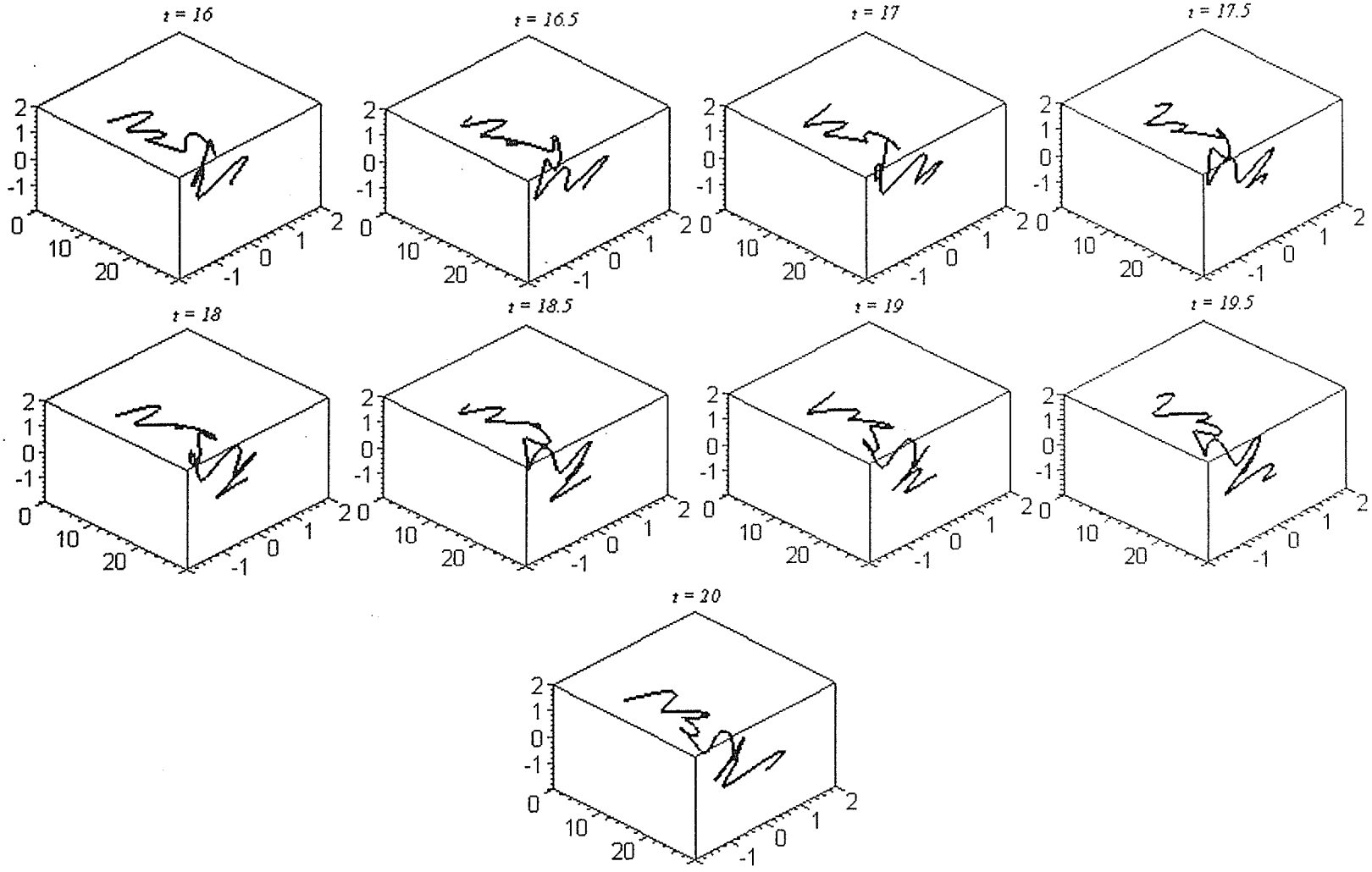
t = 16
t = 16.5
t = 17
t = 17.5
t = 18
t = 18.5
t = 19
t = 19.5
t = 20

Figure 4.3.1b Graphical Illustration of Example 4.3.1 (constrained)

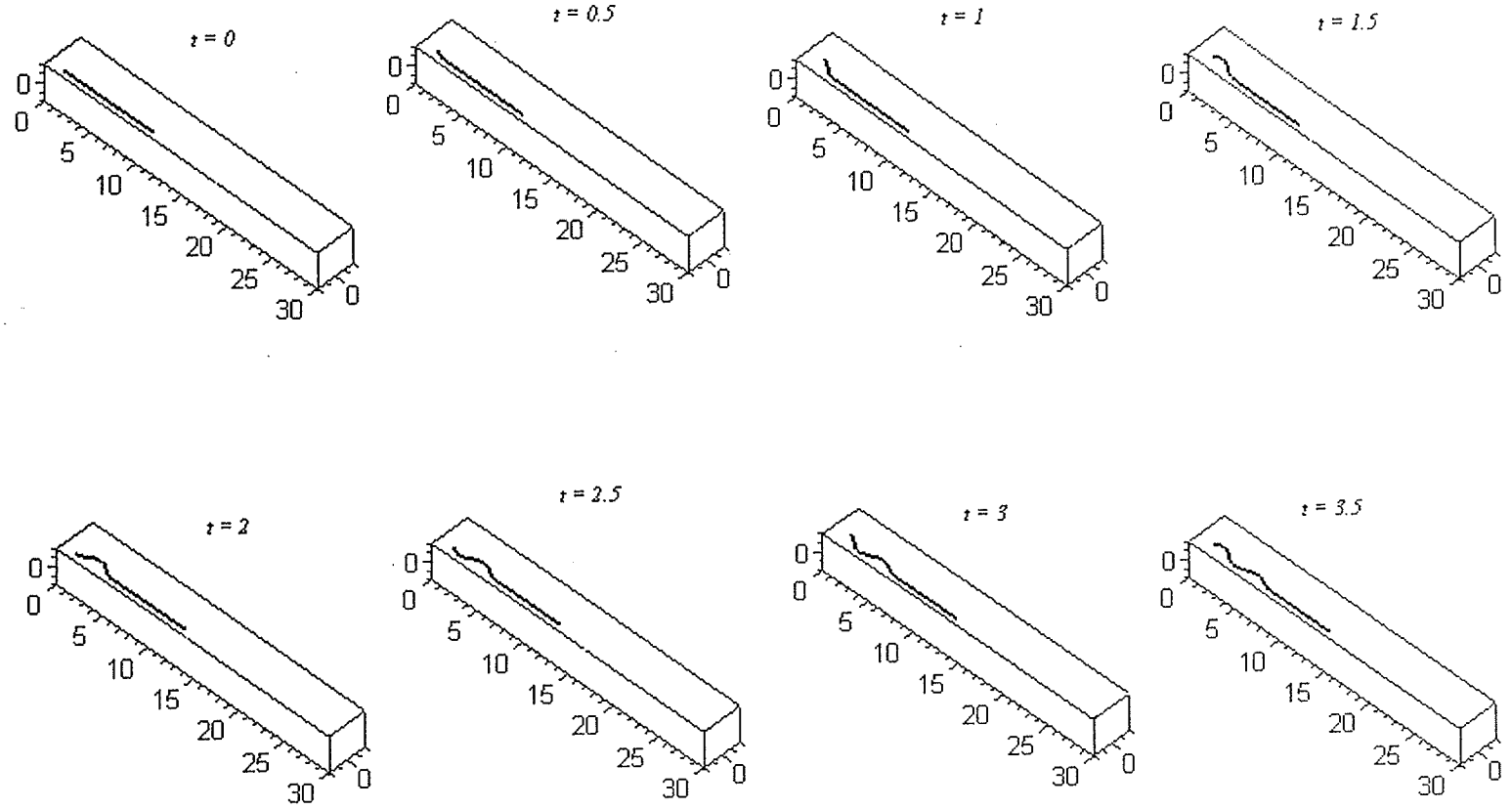

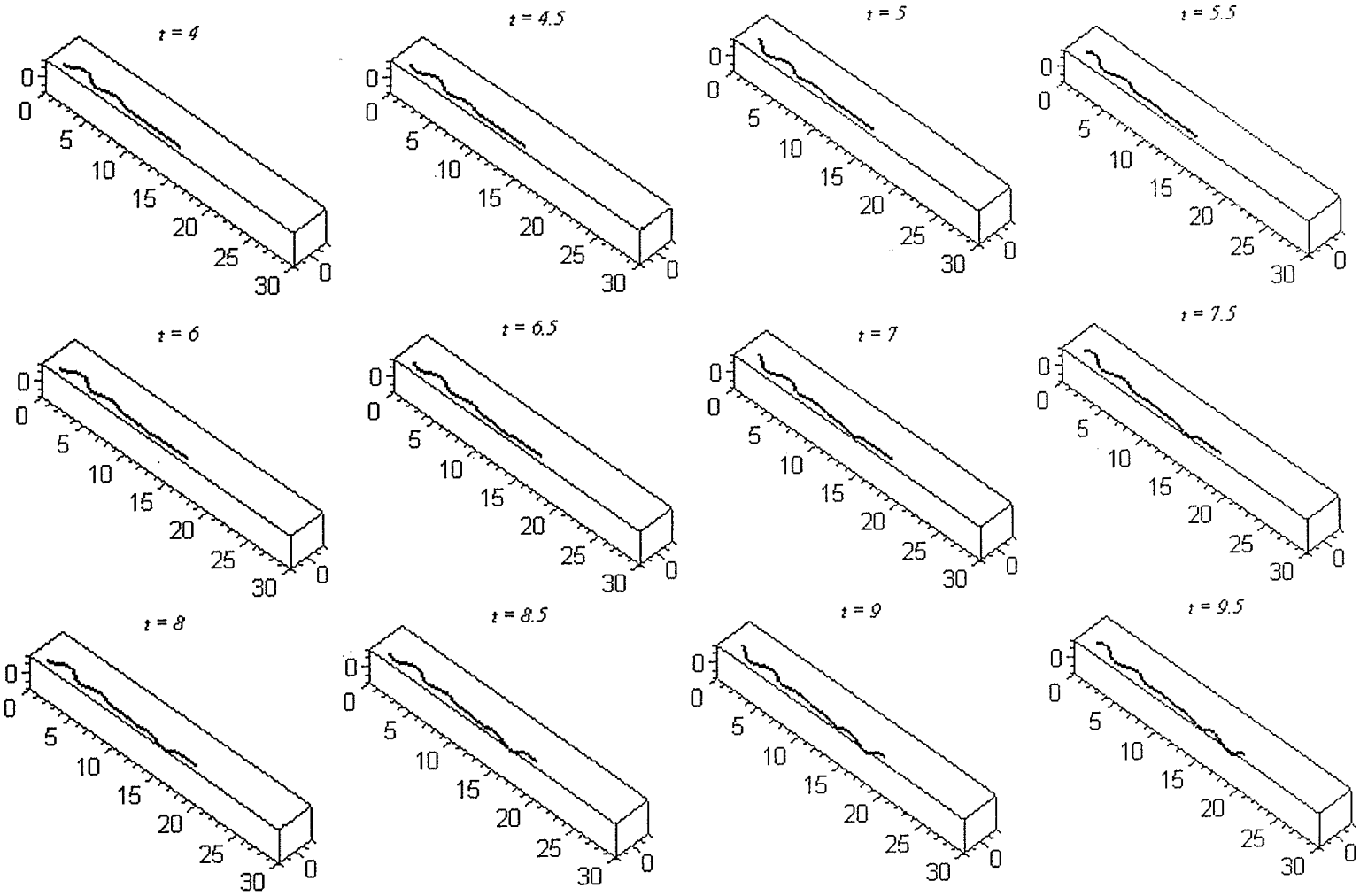
t = 4
t = 4.5
t = 5
t = 5.5
t = 6
t = 6.5
t = 7
t = 7.5
t = 8
t = 8.5
t = 9
t = 9.5
0
5
10
15
20
25
30

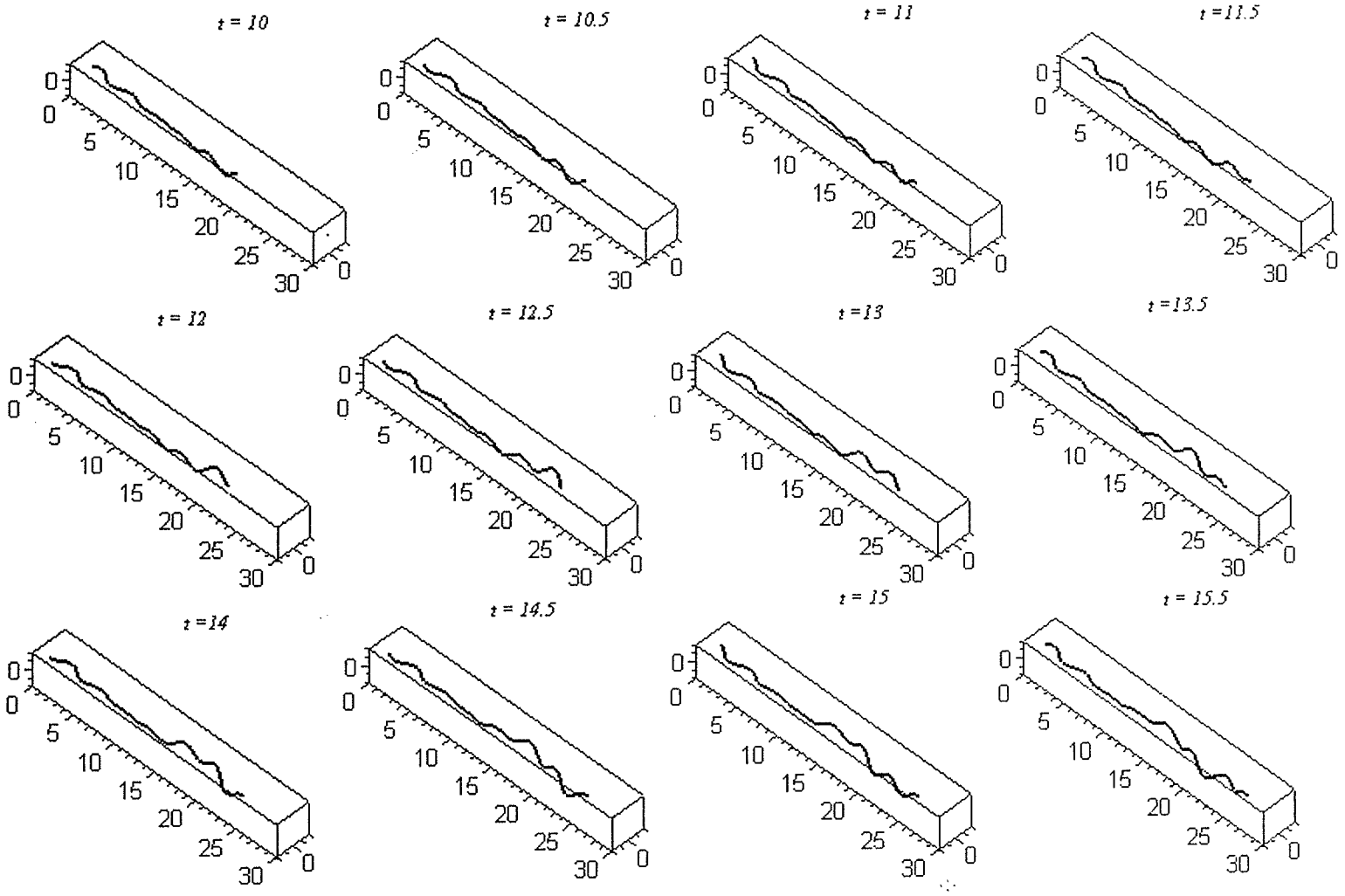
t = 10
t = 10.5
t = 11
t = 11.5
t = 12
t = 12.5
t = 13
t = 13.5
t = 14
t = 14.5
t = 15
t = 15.5
0
5
10
15
20
25
30

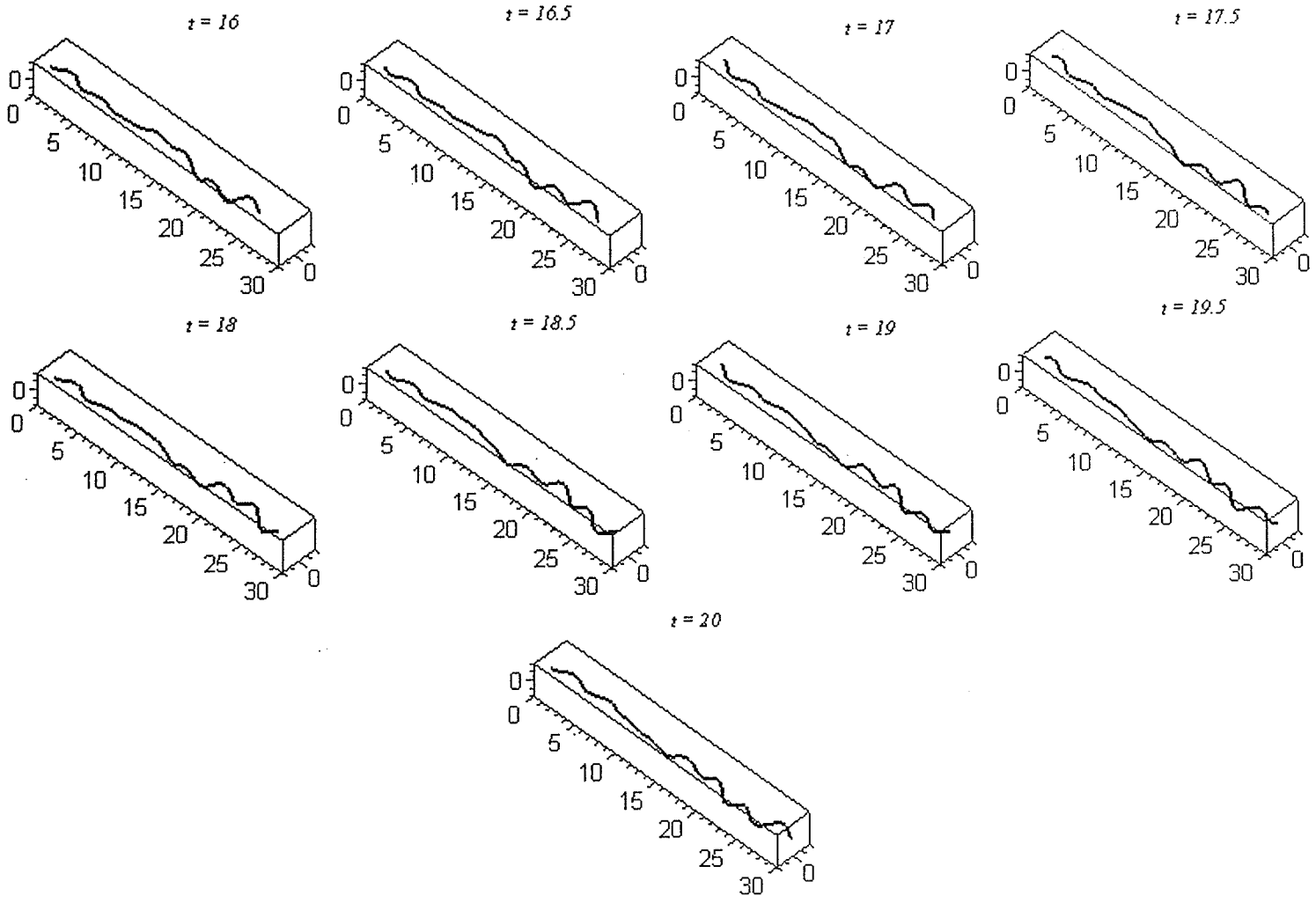
t = 16
t = 16.5
t = 17
t = 17.5
t = 18
t = 18.5
t = 19
t = 19.5
t = 20
0
5
10
15
20
25
30

Observations: 1) The lengthening of the string is evident.

2) Even though the "driving force" applied at the end of the string is purely planar, the resulting rotating wave transmitted along the string is non-planar, as a consequence of the rotation of the string.

3) Had the "driving force" applied at the end of the string been required to rotate at the same rate as the string (through appropriate choices of $p_1(t)$ and $p_2(t)$), the resulting wave transmitted along the string would have been a rotating planar wave.

Conclusions and Directions for Future Work

The transformations presented in Chapter 2, when applied to the homogeneous problem investigated in Chapter 3, yielded a method of solution which could be used as an alternative to the d'Alembert method investigated by Qin [Qin]. However, the extension of this method to the non-homogeneous problem gave rise to significant difficulties largely associated with the use of the Laplace transform. These difficulties are illustrated through the use of an example involving quite possibly the simplest initial- and boundary-conditions one could impose. Although analysis of Chapter 4 is mathematically correct, it is of little practical use as a result of the difficulties. This discovery leaves us with d'Alembert's method as the only practical analytical technique for a solution of the non-homogeneous IMBVP.

With the above conclusions in mind, possible extensions of our analysis may include:

1) Extension of the results of Chapter 3 for the homogeneous IMBVP to include the case of a general moving boundary (i.e., one for which $S(t)$ is not required to be a linear function).
2) Inclusion of some technique, other than the use of Laplace transforms, in the case of the non-homogeneous IMBVP of Chapter 4 in two cases:
    i) when $S(t) = kt + L$
    ii) when $S(t)$ is allowed to be a general function.

3) The use of some appropriately chose "wavelet basis" in the investigation of wave dynamics problems, beginning with the simple one-dimensional wave equation and continuing with extensions of it.

References

[Arf] G. Arfken; *Mathematical Methods for Physicists (2nd Edition),* Academic Press, Inc., New York, p. 632, 1970.

[Ber 1] T. G. Berry; *Preliminary Report: Tether Dynamics Analysis for Project Oedipus,* Report ER 87821/B, 1987, Bristol Aerospace Limited, Winnipeg, Manitoba.

[Ber 2] T. G. Berry; *Tether Motion Rotational Equilibrium Mode Analysis for Project Oedipus,* Report ER 88735/A, 1988, Bristol Aerospace Limited, Winnipeg, Manitoba.

[Ber 3] T. G. Berry; *Final Report: The Tether Dynamics Study for Project Oedipus,* Report ER 88782/A, 1988, Bristol Aerospace Limited, Winnipeg, Manitoba.

[Ber 4] T. G. Berry, J. J. Williams; Analytical Solutions for a Model of a Spinning Tether, *Proceedings of the Fourth International Conference on Tethers in Space* (Apr. 10-14, 1995), pp. 1341-1352, Smithsonian Institution, Washington D.C.

[Ber 5] T. G. Berry; *Final report: Wave Propagation/Tether Dynamics Analysis for Project Oedipus,* Report ER 88781/A, 1995, Bristol Aerospace Limited, Winnipeg, Manitoba.

[Car] C. F. Carrier; The Spaghetti Problem, *Am. Math Monthly.* 56 (1949), pp. 669-672.

[Chu] R. V. Churchill; *Fourier Series and Boundary Value Problems (2nd Edition),* McGraw-Hill Inc., New York, 1963.

[Cor] N. C. Corbett; *Initial Boundary Value Problems Associated with the Wave Equation,* M.Sc. Thesis, University of Manitoba, 1991.

[Gre] H. P. Greenspan; A String Problem, *J. Math. Anal. App.*, **6** (1963), pp. 339-348.

[Leb] N. N. Lebedev; *Special Functions and their Applications,* Dover Publications Inc., New York, pp. 162-164, 1972.

[Myi] T. Myint-U; *Partial Differential Equations for Scientists and Engineers (3rd Edition),* P T R Prentice-Hall, Inc., 1987.

[Qin] J. Qin; *Initial Boundary Value Problems Associated with a Spinning String,* M.Sc. Thesis, University of Manitoba, 1997.

[Ste] J. Stewart; *Single Variable Calculus (2nd Edition),* Brooks/Cole Publishing, California, p. 351, 1991.

[Tet] *Tethers In Space Handbook (2nd Edition),* National Aeronautics and Space Administration Office of Space Flight Advanced Program Development, NASA Headquarters, Washington DC, 1989.

[Zau] E. Zauderer; *Partial Differential Equations of Applied Mathematics (2nd Edition),* John Wiley & Sons, INC., 1998.

[Zil] D. G. Zill, M. C. Cullen; *Differential Equations with Boundary-Value Problems (3rd Edition),* PWS-KENT Publishing Company, Boston, 1993.

Appendix A

Computer Program for Chapter 3 Examples

The following is the Maple V Release 5 computer code for the examples of the homogeneous problems generated in Chapter 3. The only input required from the user is the assignment of the constants c, ω, L, k, and N, and the definition of the initial-conditions $f_1(x)$, $f_2(x)$, $g_1(x)$ and $g_2(x)$. Recall that in Chapter 3, $p_1(t)$, $p_2(t)$, $q_1(t)$ and $q_2(t)$ were all taken to be zero.

```
> restart;
  with(plots):
  c:=2;
  w:=1/5;
  L:=10;
  k:=1;
  N:=15;
  H:=Heaviside:
  lambdan:=n->2*n*Pi/ln((1+k/c)/(1-k/c)):
> f1:=x->sin(Pi*x/10);
  f2:=x->0;
  g1:=x->0;
  g2:=x->-w*f1(x);
  S:=t->k*t+L;
> xe:=(exp(z)-1)*c*L/k:
> REAlphaHat:=z->f1(z):
  IMAlphaHat:=z->f2(z):
  REBHat:=z->int(g1(x)-w*f2(x),x=0..z):
  IMBHat:=z->int(g2(x)+w*f1(x),x=0..z):
  RER:=z->c*REAlphaHat(xe)+REBHat(xe):
  IMR:=z->c*IMAlphaHat(xe)+IMBHat(xe):
> a:=ln(1-k/c):
  b:=ln(1+k/c):
  d:=ln((c+k)/(c-k)):
  REAn:=n->(1/(2*c*d))*int(RER(z)*cos(lambdan(n)*z)+IMR(z)*sin(lambd
  an(n)*z),z=a..b):
  IMAn:=n->(1/(2*c*d))*int(IMR(z)*cos(lambdan(n)*z)-RER(z)*sin(lambd
  an(n)*z),z=a..b):
> CosArg:=(n,s)->cos(lambdan(n)*ln(s)):
  SinArg:=(n,s)->sin(lambdan(n)*ln(s)):
  arg1:=1+k*(x+c*t)/(c*L):
  arg2:=1-k*(x-c*t)/(c*L):
> REZ:=(x,t,n)->REAn(n)*(CosArg(n,arg1)-CosArg(n,arg2))-IMAn(n)*(Sin
  Arg(n,arg1)-SinArg(n,arg2)):
  IMZ:=(x,t,n)->REAn(n)*(SinArg(n,arg1)-SinArg(n,arg2))+IMAn(n)*(Cos
  Arg(n,arg1)-CosArg(n,arg2)):
> RZ:=evalf(REZ(x,t,-N)):
  IZ:=evalf(IMZ(x,t,-N)):
  M:=2*N:
  for i from 1 to M do
  RZ:=RZ+evalf(REZ(x,t,i-N)):
  IZ:=IZ+evalf(IMZ(x,t,i-N)) od:
> for j from -N to N do
```

```
  REAn(j):=evalf(REAn(j));
  IMAn(j):=evalf(IMAn(j)) od;
> u1:=(x,t)->cos(w*t)*RZ+sin(w*t)*IZ:u1=u1(x,t);
  u2:=(x,t)->cos(w*t)*IZ-sin(w*t)*RZ:u2=u2(x,t);
> tval:=0:
  fns:=subs(t=tval,[x,u1(x,t)*(1-H(x-(k*t+L))),u2(x,t)*(1-H(x-(k*t+L
  )))]):
  plot1:=spacecurve(fns,numpoints=150,axes=boxed,thickness=2,x=0..50
  ,view=[0..50,-1..1,-1..1]):
  tval:=evalf(Pi/4):
  fns:=subs(t=tval,[x,u1(x,t)*(1-H(x-(k*t+L))),u2(x,t)*(1-H(x-(k*t+L
  )))]):
  plot2:=spacecurve(fns,numpoints=150,axes=boxed,thickness=2,x=0..50
  ,view=[0..50,-1..1,-1..1]):
  tval:=evalf(2*Pi/4):
  fns:=subs(t=tval,[x,u1(x,t)*(1-H(x-(k*t+L))),u2(x,t)*(1-H(x-(k*t+L
  )))]):
  plot3:=spacecurve(fns,numpoints=150,axes=boxed,thickness=2,x=0..50
  ,view=[0..50,-1..1,-1..1]):
  tval:=evalf(3*Pi/4):
  fns:=subs(t=tval,[x,u1(x,t)*(1-H(x-(k*t+L))),u2(x,t)*(1-H(x-(k*t+L
  )))]):
  plot4:=spacecurve(fns,numpoints=150,axes=boxed,thickness=2,x=0..50
  ,view=[0..50,-1..1,-1..1]):
  tval:=evalf(4*Pi/4):
  fns:=subs(t=tval,[x,u1(x,t)*(1-H(x-(k*t+L))),u2(x,t)*(1-H(x-(k*t+L
  )))]):
  plot5:=spacecurve(fns,numpoints=150,axes=boxed,thickness=2,x=0..50
  ,view=[0..50,-1..1,-1..1]):
  tval:=evalf(5*Pi/4):
  fns:=subs(t=tval,[x,u1(x,t)*(1-H(x-(k*t+L))),u2(x,t)*(1-H(x-(k*t+L
  )))]):
  plot6:=spacecurve(fns,numpoints=150,axes=boxed,thickness=2,x=0..50
  ,view=[0..50,-1..1,-1..1]):
  tval:=evalf(6*Pi/4):
  fns:=subs(t=tval,[x,u1(x,t)*(1-H(x-(k*t+L))),u2(x,t)*(1-H(x-(k*t+L
  )))]):
  plot7:=spacecurve(fns,numpoints=150,axes=boxed,thickness=2,x=0..50
  ,view=[0..50,-1..1,-1..1]):
  tval:=evalf(7*Pi/4):
  fns:=subs(t=tval,[x,u1(x,t)*(1-H(x-(k*t+L))),u2(x,t)*(1-H(x-(k*t+L
  )))]):
  plot8:=spacecurve(fns,numpoints=150,axes=boxed,thickness=2,x=0..50
```

```
,view=[0..50,-1..1,-1..1]):
tval:=evalf(8*Pi/4):
fns:=subs(t=tval,[x,u1(x,t)*(1-H(x-(k*t+L))),u2(x,t)*(1-H(x-(k*t+L
))))]):
plot9:=spacecurve(fns,numpoints=150,axes=boxed,thickness=2,x=0..50
,view=[0..50,-1..1,-1..1]):
tval:=evalf(9*Pi/4):
fns:=subs(t=tval,[x,u1(x,t)*(1-H(x-(k*t+L))),u2(x,t)*(1-H(x-(k*t+L
))))]):
plot10:=spacecurve(fns,numpoints=150,axes=boxed,thickness=2,x=0..5
0,view=[0..50,-1..1,-1..1]):
tval:=evalf(10*Pi/4):
fns:=subs(t=tval,[x,u1(x,t)*(1-H(x-(k*t+L))),u2(x,t)*(1-H(x-(k*t+L
))))]):
plot11:=spacecurve(fns,numpoints=150,axes=boxed,thickness=2,x=0..5
0,view=[0..50,-1..1,-1..1]):
tval:=evalf(11*Pi/4):
fns:=subs(t=tval,[x,u1(x,t)*(1-H(x-(k*t+L))),u2(x,t)*(1-H(x-(k*t+L
))))]):
plot12:=spacecurve(fns,numpoints=150,axes=boxed,thickness=2,x=0..5
0,view=[0..50,-1..1,-1..1]):
tval:=evalf(12*Pi/4):
fns:=subs(t=tval,[x,u1(x,t)*(1-H(x-(k*t+L))),u2(x,t)*(1-H(x-(k*t+L
))))]):
plot13:=spacecurve(fns,numpoints=150,axes=boxed,thickness=2,x=0..5
0,view=[0..50,-1..1,-1..1]):
tval:=evalf(13*Pi/4):
fns:=subs(t=tval,[x,u1(x,t)*(1-H(x-(k*t+L))),u2(x,t)*(1-H(x-(k*t+L
))))]):
plot14:=spacecurve(fns,numpoints=150,axes=boxed,thickness=2,x=0..5
0,view=[0..50,-1..1,-1..1]):
tval:=evalf(14*Pi/4):
fns:=subs(t=tval,[x,u1(x,t)*(1-H(x-(k*t+L))),u2(x,t)*(1-H(x-(k*t+L
))))]):
plot15:=spacecurve(fns,numpoints=150,axes=boxed,thickness=2,x=0..5
0,view=[0..50,-1..1,-1..1]):
tval:=evalf(15*Pi/4):
fns:=subs(t=tval,[x,u1(x,t)*(1-H(x-(k*t+L))),u2(x,t)*(1-H(x-(k*t+L
))))]):
plot16:=spacecurve(fns,numpoints=150,axes=boxed,thickness=2,x=0..5
0,view=[0..50,-1..1,-1..1]):
tval:=evalf(16*Pi/4):
fns:=subs(t=tval,[x,u1(x,t)*(1-H(x-(k*t+L))),u2(x,t)*(1-H(x-(k*t+L
```

```
))))]):
plot17:=spacecurve(fns,numpoints=150,axes=boxed,thickness=2,x=0..5
0,view=[0..50,-1..1,-1..1]):
tval:=evalf(17*Pi/4):
fns:=subs(t=tval,[x,u1(x,t)*(1-H(x-(k*t+L))),u2(x,t)*(1-H(x-(k*t+L
))))]):
plot18:=spacecurve(fns,numpoints=150,axes=boxed,thickness=2,x=0..5
0,view=[0..50,-1..1,-1..1]):
tval:=evalf(18*Pi/4):
fns:=subs(t=tval,[x,u1(x,t)*(1-H(x-(k*t+L))),u2(x,t)*(1-H(x-(k*t+L
))))]):
plot19:=spacecurve(fns,numpoints=150,axes=boxed,thickness=2,x=0..5
0,view=[0..50,-1..1,-1..1]):
tval:=evalf(19*Pi/4):
fns:=subs(t=tval,[x,u1(x,t)*(1-H(x-(k*t+L))),u2(x,t)*(1-H(x-(k*t+L
))))]):
plot20:=spacecurve(fns,numpoints=150,axes=boxed,thickness=2,x=0..5
0,view=[0..50,-1..1,-1..1]):
tval:=evalf(20*Pi/4):
fns:=subs(t=tval,[x,u1(x,t)*(1-H(x-(k*t+L))),u2(x,t)*(1-H(x-(k*t+L
))))]):
plot21:=spacecurve(fns,numpoints=150,axes=boxed,thickness=2,x=0..5
0,view=[0..50,-1..1,-1..1]):
tval:=evalf(21*Pi/4):
fns:=subs(t=tval,[x,u1(x,t)*(1-H(x-(k*t+L))),u2(x,t)*(1-H(x-(k*t+L
))))]):
plot22:=spacecurve(fns,numpoints=150,axes=boxed,thickness=2,x=0..5
0,view=[0..50,-1..1,-1..1]):
tval:=evalf(22*Pi/4):
fns:=subs(t=tval,[x,u1(x,t)*(1-H(x-(k*t+L))),u2(x,t)*(1-H(x-(k*t+L
))))]):
plot23:=spacecurve(fns,numpoints=150,axes=boxed,thickness=2,x=0..5
0,view=[0..50,-1..1,-1..1]):
tval:=evalf(23*Pi/4):
fns:=subs(t=tval,[x,u1(x,t)*(1-H(x-(k*t+L))),u2(x,t)*(1-H(x-(k*t+L
))))]):
plot24:=spacecurve(fns,numpoints=150,axes=boxed,thickness=2,x=0..5
0,view=[0..50,-1..1,-1..1]):
tval:=evalf(24*Pi/4):
fns:=subs(t=tval,[x,u1(x,t)*(1-H(x-(k*t+L))),u2(x,t)*(1-H(x-(k*t+L
))))]):
plot25:=spacecurve(fns,numpoints=150,axes=boxed,thickness=2,x=0..5
0,view=[0..50,-1..1,-1..1]):
```

```
tval:=evalf(25*Pi/4):
fns:=subs(t=tval,[x,u1(x,t)*(1-H(x-(k*t+L))),u2(x,t)*(1-H(x-(k*t+L
)))]):
plot26:=spacecurve(fns,numpoints=150,axes=boxed,thickness=2,x=0..5
0,view=[0..50,-1..1,-1..1]):
tval:=evalf(26*Pi/4):
fns:=subs(t=tval,[x,u1(x,t)*(1-H(x-(k*t+L))),u2(x,t)*(1-H(x-(k*t+L
)))]):
plot27:=spacecurve(fns,numpoints=150,axes=boxed,thickness=2,x=0..5
0,view=[0..50,-1..1,-1..1]):
tval:=evalf(27*Pi/4):
fns:=subs(t=tval,[x,u1(x,t)*(1-H(x-(k*t+L))),u2(x,t)*(1-H(x-(k*t+L
)))]):
plot28:=spacecurve(fns,numpoints=150,axes=boxed,thickness=2,x=0..5
0,view=[0..50,-1..1,-1..1]):
tval:=evalf(28*Pi/4):
fns:=subs(t=tval,[x,u1(x,t)*(1-H(x-(k*t+L))),u2(x,t)*(1-H(x-(k*t+L
)))]):
plot29:=spacecurve(fns,numpoints=150,axes=boxed,thickness=2,x=0..5
0,view=[0..50,-1..1,-1..1]):
tval:=evalf(29*Pi/4):
fns:=subs(t=tval,[x,u1(x,t)*(1-H(x-(k*t+L))),u2(x,t)*(1-H(x-(k*t+L
)))]):
plot30:=spacecurve(fns,numpoints=150,axes=boxed,thickness=2,x=0..5
0,view=[0..50,-1..1,-1..1]):
tval:=evalf(30*Pi/4):
fns:=subs(t=tval,[x,u1(x,t)*(1-H(x-(k*t+L))),u2(x,t)*(1-H(x-(k*t+L
)))]):
plot31:=spacecurve(fns,numpoints=150,axes=boxed,thickness=2,x=0..5
0,view=[0..50,-1..1,-1..1]):
tval:=evalf(31*Pi/4):
fns:=subs(t=tval,[x,u1(x,t)*(1-H(x-(k*t+L))),u2(x,t)*(1-H(x-(k*t+L
)))]):
plot32:=spacecurve(fns,numpoints=150,axes=boxed,thickness=2,x=0..5
0,view=[0..50,-1..1,-1..1]):
tval:=evalf(32*Pi/4):
fns:=subs(t=tval,[x,u1(x,t)*(1-H(x-(k*t+L))),u2(x,t)*(1-H(x-(k*t+L
)))]):
plot33:=spacecurve(fns,numpoints=150,axes=boxed,thickness=2,x=0..5
0,view=[0..50,-1..1,-1..1]):
tval:=evalf(33*Pi/4):
fns:=subs(t=tval,[x,u1(x,t)*(1-H(x-(k*t+L))),u2(x,t)*(1-H(x-(k*t+L
)))]):
```

```
plot34:=spacecurve(fns,numpoints=150,axes=boxed,thickness=2,x=0..5
0,view=[0..50,-1..1,-1..1]):
tval:=evalf(34*Pi/4):
fns:=subs(t=tval,[x,u1(x,t)*(1-H(x-(k*t+L))),u2(x,t)*(1-H(x-(k*t+L
)))]):
plot35:=spacecurve(fns,numpoints=150,axes=boxed,thickness=2,x=0..5
0,view=[0..50,-1..1,-1..1]):
tval:=evalf(35*Pi/4):
fns:=subs(t=tval,[x,u1(x,t)*(1-H(x-(k*t+L))),u2(x,t)*(1-H(x-(k*t+L
)))]):
plot36:=spacecurve(fns,numpoints=150,axes=boxed,thickness=2,x=0..5
0,view=[0..50,-1..1,-1..1]):
tval:=evalf(36*Pi/4):
fns:=subs(t=tval,[x,u1(x,t)*(1-H(x-(k*t+L))),u2(x,t)*(1-H(x-(k*t+L
)))]):
plot37:=spacecurve(fns,numpoints=150,axes=boxed,thickness=2,x=0..5
0,view=[0..50,-1..1,-1..1]):
tval:=evalf(37*Pi/4):
fns:=subs(t=tval,[x,u1(x,t)*(1-H(x-(k*t+L))),u2(x,t)*(1-H(x-(k*t+L
)))]):
plot38:=spacecurve(fns,numpoints=150,axes=boxed,thickness=2,x=0..5
0,view=[0..50,-1..1,-1..1]):
tval:=evalf(38*Pi/4):
fns:=subs(t=tval,[x,u1(x,t)*(1-H(x-(k*t+L))),u2(x,t)*(1-H(x-(k*t+L
)))]):
plot39:=spacecurve(fns,numpoints=150,axes=boxed,thickness=2,x=0..5
0,view=[0..50,-1..1,-1..1]):
tval:=evalf(39*Pi/4):
fns:=subs(t=tval,[x,u1(x,t)*(1-H(x-(k*t+L))),u2(x,t)*(1-H(x-(k*t+L
)))]):
plot40:=spacecurve(fns,numpoints=150,axes=boxed,thickness=2,x=0..5
0,view=[0..50,-1..1,-1..1]):
tval:=evalf(40*Pi/4):
fns:=subs(t=tval,[x,u1(x,t)*(1-H(x-(k*t+L))),u2(x,t)*(1-H(x-(k*t+L
)))]):
plot41:=spacecurve(fns,numpoints=150,axes=boxed,thickness=2,x=0..5
0,view=[0..50,-1..1,-1..1]):
tval:=evalf(41*Pi/4):
fns:=subs(t=tval,[x,u1(x,t)*(1-H(x-(k*t+L))),u2(x,t)*(1-H(x-(k*t+L
)))]):
plot42:=spacecurve(fns,numpoints=150,axes=boxed,thickness=2,x=0..5
0,view=[0..50,-1..1,-1..1]):
tval:=evalf(42*Pi/4):
```

```
fns:=subs(t=tval,[x,u1(x,t)*(1-H(x-(k*t+L))),u2(x,t)*(1-H(x-(k*t+L
)))]):
plot43:=spacecurve(fns,numpoints=150,axes=boxed,thickness=2,x=0..5
0,view=[0..50,-1..1,-1..1]):
tval:=evalf(43*Pi/4):
fns:=subs(t=tval,[x,u1(x,t)*(1-H(x-(k*t+L))),u2(x,t)*(1-H(x-(k*t+L
)))]):
plot44:=spacecurve(fns,numpoints=150,axes=boxed,thickness=2,x=0..5
0,view=[0..50,-1..1,-1..1]):
tval:=evalf(44*Pi/4):
fns:=subs(t=tval,[x,u1(x,t)*(1-H(x-(k*t+L))),u2(x,t)*(1-H(x-(k*t+L
)))]):
plot45:=spacecurve(fns,numpoints=150,axes=boxed,thickness=2,x=0..5
0,view=[0..50,-1..1,-1..1]):
tval:=evalf(45*Pi/4):
fns:=subs(t=tval,[x,u1(x,t)*(1-H(x-(k*t+L))),u2(x,t)*(1-H(x-(k*t+L
)))]):
plot46:=spacecurve(fns,numpoints=150,axes=boxed,thickness=2,x=0..5
0,view=[0..50,-1..1,-1..1]):
tval:=evalf(46*Pi/4):
fns:=subs(t=tval,[x,u1(x,t)*(1-H(x-(k*t+L))),u2(x,t)*(1-H(x-(k*t+L
)))]):
plot47:=spacecurve(fns,numpoints=150,axes=boxed,thickness=2,x=0..5
0,view=[0..50,-1..1,-1..1]):
tval:=evalf(47*Pi/4):
fns:=subs(t=tval,[x,u1(x,t)*(1-H(x-(k*t+L))),u2(x,t)*(1-H(x-(k*t+L
)))]):
plot48:=spacecurve(fns,numpoints=150,axes=boxed,thickness=2,x=0..5
0,view=[0..50,-1..1,-1..1]):
tval:=evalf(48*Pi/4):
fns:=subs(t=tval,[x,u1(x,t)*(1-H(x-(k*t+L))),u2(x,t)*(1-H(x-(k*t+L
)))]):
plot49:=spacecurve(fns,numpoints=150,axes=boxed,thickness=2,x=0..5
0,view=[0..50,-1..1,-1..1]):
tval:=evalf(49*Pi/4):
fns:=subs(t=tval,[x,u1(x,t)*(1-H(x-(k*t+L))),u2(x,t)*(1-H(x-(k*t+L
)))]):
plot50:=spacecurve(fns,numpoints=150,axes=boxed,thickness=2,x=0..5
0,view=[0..50,-1..1,-1..1]):
tval:=evalf(50*Pi/4):
fns:=subs(t=tval,[x,u1(x,t)*(1-H(x-(k*t+L))),u2(x,t)*(1-H(x-(k*t+L
)))]):
plot51:=spacecurve(fns,numpoints=150,axes=boxed,thickness=2,x=0..5
```

```
   0,view=[0..50,-1..1,-1..1]):
   tval:=evalf(51*Pi/4):
   fns:=subs(t=tval,[x,u1(x,t)*(1-H(x-(k*t+L))),u2(x,t)*(1-H(x-(k*t+L
   )))]):
   plot52:=spacecurve(fns,numpoints=150,axes=boxed,thickness=2,x=0..5
   0,view=[0..50,-1..1,-1..1]):
   tval:=evalf(52*Pi/4):
   fns:=subs(t=tval,[x,u1(x,t)*(1-H(x-(k*t+L))),u2(x,t)*(1-H(x-(k*t+L
   )))]):
   plot53:=spacecurve(fns,numpoints=150,axes=boxed,thickness=2,x=0..5
   0,view=[0..50,-1..1,-1..1]):
   tval:=evalf(53*Pi/4):
   fns:=subs(t=tval,[x,u1(x,t)*(1-H(x-(k*t+L))),u2(x,t)*(1-H(x-(k*t+L
   )))]):
   plot54:=spacecurve(fns,numpoints=150,axes=boxed,thickness=2,x=0..5
   0,view=[0..50,-1..1,-1..1]):
> display([plot1,plot2,plot3,plot4,plot5,plot6,plot7,plot8,plot9,plo
   t10,plot11,plot12,plot13,plot14,plot15,plot16,plot17,plot18,plot19
   ,plot20,plot21,plot22,plot23,plot24,plot25,plot26,plot27,plot28,pl
   ot29,plot30,plot31,plot32,plot33,plot34,plot35,plot36,plot37,plot3
   8,plot39,plot40,plot41,plot42,plot43,plot44,plot45,plot46,plot47,p
   lot48,plot49,plot50,plot51,plot52,plot53,plot54],insequence=true);
>
```

Appendix B

Computer Program for Chapter 4 Example

The following is the Maple V Release 5 computer code for the example presented in Chapter 4 pertaining to the non-homogeneous IMBVP solved by way of d'Alembert's method. The program can be easily modified if the user wishes to consider a non-zero boundary-condition other than $p_1(t) = \frac{1}{2}\left[1 - \cos(\pi t)\right]$ but assumes that

$p_2(t) = q_1(t) = q_2(t) = 0$.

```
> restart;
  with(plots):
  H:=Heaviside:
  omega:=1/5:
  p1:=t->0.5*(1-cos(Pi*t));
> ReW1:=(x,t)->p1(t-x/2)*cos(omega*(t-x/2))*(H(x)-H(x-2*t));
  ImW1:=(x,t)->p1(t-x/2)*sin(omega*(t-x/2))*(H(x)-H(x-2*t));
  ReW2:=(x,t)->p1(t-x/2)*cos(omega*(t-x/2))*(H(x)-H(x-10+2*t))+p1(t-
  x/2)*cos(omega*(t-x/2))*(H(x-10+2*t)-H(x-2*t));
  ImW2:=(x,t)->p1(t-x/2)*sin(omega*(t-x/2))*(H(x)-H(x-10+2*t))+p1(t-
  x/2)*sin(omega*(t-x/2))*(H(x-10+2*t)-H(x-2*t));
  ReW3:=(x,t)->p1(t-x/2)*cos(omega*(t-x/2))*(H(x)-H(x-2*t+10))+p1(t-
  x/2)*cos(omega*(t-x/2))*(H(x-2*t+10)-H(x-2*t));
  ImW3:=(x,t)->p1(t-x/2)*sin(omega*(t-x/2))*(H(x)-H(x-2*t+10))+p1(t-
  x/2)*sin(omega*(t-x/2))*(H(x-2*t+10)-H(x-2*t));
  ReW4:=(x,t)->p1(t-x/2)*cos(omega*(t-x/2))*(H(x)-H(x-2*t+10))+p1(t-
  x/2)*cos(omega*(t-x/2))*(H(x-2*t+10)-H(x-40+2*t))+(p1(t-x/2)*cos(o
  mega*(t-x/2))-p1(x/6-20/3+t/3)*cos(omega*(x/6-20/3+t/3)))*(H(x-40+
  2*t)-H(x-t-10));
  ImW4:=(x,t)->p1(t-x/2)*sin(omega*(t-x/2))*(H(x)-H(x-2*t+10))+p1(t-
  x/2)*sin(omega*(t-x/2))*(H(x-2*t+10)-H(x-40+2*t))+(p1(t-x/2)*sin(o
  mega*(t-x/2))-p1(x/6-20/3+t/3)*sin(omega*(x/6-20/3+t/3)))*(H(x-40+
  2*t)-H(x-t-10));
  ReW5:=(x,t)->p1(t-x/2)*cos(omega*(t-x/2))*(H(x)-H(x-40+2*t))+(p1(t
  -x/2)*cos(omega*(t-x/2))-p1(x/6-20/3+t/3)*cos(omega*(x/6-20/3+t/3)
  ))*(H(x-40+2*t)-H(x-2*t+10))+(p1(t-x/2)*cos(omega*(t-x/2))-p1(x/6-
  20/3+t/3)*cos(omega*(x/6-20/3+t/3)))*(H(x-2*t+10)-H(x-t-10));
  ImW5:=(x,t)->p1(t-x/2)*sin(omega*(t-x/2))*(H(x)-H(x-40+2*t))+(p1(t
  -x/2)*sin(omega*(t-x/2))-p1(x/6-20/3+t/3)*sin(omega*(x/6-20/3+t/3)
  ))*(H(x-40+2*t)-H(x-2*t+10))+(p1(t-x/2)*sin(omega*(t-x/2))-p1(x/6-
  20/3+t/3)*sin(omega*(x/6-20/3+t/3)))*(H(x-2*t+10)-H(x-t-10));
> tval:=0:
  u1:=(x,t)->(cos(omega*t)*ReW1(x,t)+sin(omega*t)*ImW1(x,t)):
  u2:=(x,t)->(-sin(omega*t)*ReW1(x,t)+cos(omega*t)*ImW1(x,t)):
  fns:=subs(t=tval,[x,u1(x,t)*(1-H(x-(t+10))),u2(x,t)*(1-H(x-(t+10))
  )]):
  plot1:=spacecurve(fns,numpoints=150,axes=boxed,thickness=2,x=0..30
  ,view=[0..30,-2..2,-2..2]):
  tval:=0.5:
  u1:=(x,t)->(cos(omega*t)*ReW1(x,t)+sin(omega*t)*ImW1(x,t)):
  u2:=(x,t)->(-sin(omega*t)*ReW1(x,t)+cos(omega*t)*ImW1(x,t)):
  fns:=subs(t=tval,[x,u1(x,t)*(1-H(x-(t+10))),u2(x,t)*(1-H(x-(t+10))
  )]):
```

```
plot2:=spacecurve(fns,numpoints=150,axes=boxed,thickness=2,x=0..30
,view=[0..30,-2..2,-2..2]):
tval:=1:
u1:=(x,t)->(cos(omega*t)*ReW1(x,t)+sin(omega*t)*ImW1(x,t)):
u2:=(x,t)->(-sin(omega*t)*ReW1(x,t)+cos(omega*t)*ImW1(x,t)):
fns:=subs(t=tval,[x,u1(x,t)*(1-H(x-(t+10))),u2(x,t)*(1-H(x-(t+10))
)]):
plot3:=spacecurve(fns,numpoints=150,axes=boxed,thickness=2,x=0..30
,view=[0..30,-2..2,-2..2]):
tval:=1.5:
u1:=(x,t)->(cos(omega*t)*ReW1(x,t)+sin(omega*t)*ImW1(x,t)):
u2:=(x,t)->(-sin(omega*t)*ReW1(x,t)+cos(omega*t)*ImW1(x,t)):
fns:=subs(t=tval,[x,u1(x,t)*(1-H(x-(t+10))),u2(x,t)*(1-H(x-(t+10))
)]):
plot4:=spacecurve(fns,numpoints=150,axes=boxed,thickness=2,x=0..30
,view=[0..30,-2..2,-2..2]):
tval:=2:
u1:=(x,t)->(cos(omega*t)*ReW1(x,t)+sin(omega*t)*ImW1(x,t)):
u2:=(x,t)->(-sin(omega*t)*ReW1(x,t)+cos(omega*t)*ImW1(x,t)):
fns:=subs(t=tval,[x,u1(x,t)*(1-H(x-(t+10))),u2(x,t)*(1-H(x-(t+10))
)]):
plot5:=spacecurve(fns,numpoints=150,axes=boxed,thickness=2,x=0..30
,view=[0..30,-2..2,-2..2]):
tval:=2.5:
u1:=(x,t)->(cos(omega*t)*ReW1(x,t)+sin(omega*t)*ImW1(x,t)):
u2:=(x,t)->(-sin(omega*t)*ReW1(x,t)+cos(omega*t)*ImW1(x,t)):
fns:=subs(t=tval,[x,u1(x,t)*(1-H(x-(t+10))),u2(x,t)*(1-H(x-(t+10))
)]):
plot6:=spacecurve(fns,numpoints=150,axes=boxed,thickness=2,x=0..30
,view=[0..30,-2..2,-2..2]):
tval:=3:
u1:=(x,t)->(cos(omega*t)*ReW2(x,t)+sin(omega*t)*ImW2(x,t)):
u2:=(x,t)->(-sin(omega*t)*ReW2(x,t)+cos(omega*t)*ImW2(x,t)):
fns:=subs(t=tval,[x,u1(x,t)*(1-H(x-(t+10))),u2(x,t)*(1-H(x-(t+10))
)]):
plot7:=spacecurve(fns,numpoints=150,axes=boxed,thickness=2,x=0..30
,view=[0..30,-2..2,-2..2]):
tval:=3.5:
u1:=(x,t)->(cos(omega*t)*ReW2(x,t)+sin(omega*t)*ImW2(x,t)):
u2:=(x,t)->(-sin(omega*t)*ReW2(x,t)+cos(omega*t)*ImW2(x,t)):
fns:=subs(t=tval,[x,u1(x,t)*(1-H(x-(t+10))),u2(x,t)*(1-H(x-(t+10))
)]):
plot8:=spacecurve(fns,numpoints=150,axes=boxed,thickness=2,x=0..30
```

```
,view=[0..30,-2..2,-2..2]):
tval:=4:
u1:=(x,t)->(cos(omega*t)*ReW2(x,t)+sin(omega*t)*ImW2(x,t)):
u2:=(x,t)->(-sin(omega*t)*ReW2(x,t)+cos(omega*t)*ImW2(x,t)):
fns:=subs(t=tval,[x,u1(x,t)*(1-H(x-(t+10))),u2(x,t)*(1-H(x-(t+10))
)]):
plot9:=spacecurve(fns,numpoints=150,axes=boxed,thickness=2,x=0..30
,view=[0..30,-2..2,-2..2]):
tval:=4.5:
u1:=(x,t)->(cos(omega*t)*ReW2(x,t)+sin(omega*t)*ImW2(x,t)):
u2:=(x,t)->(-sin(omega*t)*ReW2(x,t)+cos(omega*t)*ImW2(x,t)):
fns:=subs(t=tval,[x,u1(x,t)*(1-H(x-(t+10))),u2(x,t)*(1-H(x-(t+10))
)]):
plot10:=spacecurve(fns,numpoints=150,axes=boxed,thickness=2,x=0..3
0,view=[0..30,-2..2,-2..2]):
tval:=5:
u1:=(x,t)->(cos(omega*t)*ReW2(x,t)+sin(omega*t)*ImW2(x,t)):
u2:=(x,t)->(-sin(omega*t)*ReW2(x,t)+cos(omega*t)*ImW2(x,t)):
fns:=subs(t=tval,[x,u1(x,t)*(1-H(x-(t+10))),u2(x,t)*(1-H(x-(t+10))
)]):
plot11:=spacecurve(fns,numpoints=150,axes=boxed,thickness=2,x=0..3
0,view=[0..30,-2..2,-2..2]):
tval:=5.5:
u1:=(x,t)->(cos(omega*t)*ReW3(x,t)+sin(omega*t)*ImW3(x,t)):
u2:=(x,t)->(-sin(omega*t)*ReW3(x,t)+cos(omega*t)*ImW3(x,t)):
fns:=subs(t=tval,[x,u1(x,t)*(1-H(x-(t+10))),u2(x,t)*(1-H(x-(t+10))
)]):
plot12:=spacecurve(fns,numpoints=150,axes=boxed,thickness=2,x=0..3
0,view=[0..30,-2..2,-2..2]):
tval:=6:
u1:=(x,t)->(cos(omega*t)*ReW3(x,t)+sin(omega*t)*ImW3(x,t)):
u2:=(x,t)->(-sin(omega*t)*ReW3(x,t)+cos(omega*t)*ImW3(x,t)):
fns:=subs(t=tval,[x,u1(x,t)*(1-H(x-(t+10))),u2(x,t)*(1-H(x-(t+10))
)]):
plot13:=spacecurve(fns,numpoints=150,axes=boxed,thickness=2,x=0..3
0,view=[0..30,-2..2,-2..2]):
tval:=6.5:
u1:=(x,t)->(cos(omega*t)*ReW3(x,t)+sin(omega*t)*ImW3(x,t)):
u2:=(x,t)->(-sin(omega*t)*ReW3(x,t)+cos(omega*t)*ImW3(x,t)):
fns:=subs(t=tval,[x,u1(x,t)*(1-H(x-(t+10))),u2(x,t)*(1-H(x-(t+10))
)]):
plot14:=spacecurve(fns,numpoints=150,axes=boxed,thickness=2,x=0..3
0,view=[0..30,-2..2,-2..2]):
```

```
tval:=7:
u1:=(x,t)->(cos(omega*t)*ReW3(x,t)+sin(omega*t)*ImW3(x,t)):
u2:=(x,t)->(-sin(omega*t)*ReW3(x,t)+cos(omega*t)*ImW3(x,t)):
fns:=subs(t=tval,[x,u1(x,t)*(1-H(x-(t+10))),u2(x,t)*(1-H(x-(t+10))
)]):
plot15:=spacecurve(fns,numpoints=150,axes=boxed,thickness=2,x=0..3
0,view=[0..30,-2..2,-2..2]):
tval:=7.5:
u1:=(x,t)->(cos(omega*t)*ReW3(x,t)+sin(omega*t)*ImW3(x,t)):
u2:=(x,t)->(-sin(omega*t)*ReW3(x,t)+cos(omega*t)*ImW3(x,t)):
fns:=subs(t=tval,[x,u1(x,t)*(1-H(x-(t+10))),u2(x,t)*(1-H(x-(t+10))
)]):
plot16:=spacecurve(fns,numpoints=150,axes=boxed,thickness=2,x=0..3
0,view=[0..30,-2..2,-2..2]):
tval:=8:
u1:=(x,t)->(cos(omega*t)*ReW3(x,t)+sin(omega*t)*ImW3(x,t)):
u2:=(x,t)->(-sin(omega*t)*ReW3(x,t)+cos(omega*t)*ImW3(x,t)):
fns:=subs(t=tval,[x,u1(x,t)*(1-H(x-(t+10))),u2(x,t)*(1-H(x-(t+10))
)]):
plot17:=spacecurve(fns,numpoints=150,axes=boxed,thickness=2,x=0..3
0,view=[0..30,-2..2,-2..2]):
tval:=8.5:
u1:=(x,t)->(cos(omega*t)*ReW3(x,t)+sin(omega*t)*ImW3(x,t)):
u2:=(x,t)->(-sin(omega*t)*ReW3(x,t)+cos(omega*t)*ImW3(x,t)):
fns:=subs(t=tval,[x,u1(x,t)*(1-H(x-(t+10))),u2(x,t)*(1-H(x-(t+10))
)]):
plot18:=spacecurve(fns,numpoints=150,axes=boxed,thickness=2,x=0..3
0,view=[0..30,-2..2,-2..2]):
tval:=9:
u1:=(x,t)->(cos(omega*t)*ReW3(x,t)+sin(omega*t)*ImW3(x,t)):
u2:=(x,t)->(-sin(omega*t)*ReW3(x,t)+cos(omega*t)*ImW3(x,t)):
fns:=subs(t=tval,[x,u1(x,t)*(1-H(x-(t+10))),u2(x,t)*(1-H(x-(t+10))
)]):
plot19:=spacecurve(fns,numpoints=150,axes=boxed,thickness=2,x=0..3
0,view=[0..30,-2..2,-2..2]):
tval:=9.5:
u1:=(x,t)->(cos(omega*t)*ReW3(x,t)+sin(omega*t)*ImW3(x,t)):
u2:=(x,t)->(-sin(omega*t)*ReW3(x,t)+cos(omega*t)*ImW3(x,t)):
fns:=subs(t=tval,[x,u1(x,t)*(1-H(x-(t+10))),u2(x,t)*(1-H(x-(t+10))
)]):
plot20:=spacecurve(fns,numpoints=150,axes=boxed,thickness=2,x=0..3
0,view=[0..30,-2..2,-2..2]):
tval:=10:
```

```
u1:=(x,t)->(cos(omega*t)*ReW3(x,t)+sin(omega*t)*ImW3(x,t)):
u2:=(x,t)->(-sin(omega*t)*ReW3(x,t)+cos(omega*t)*ImW3(x,t)):
fns:=subs(t=tval,[x,u1(x,t)*(1-H(x-(t+10))),u2(x,t)*(1-H(x-(t+10))
)]):
plot21:=spacecurve(fns,numpoints=150,axes=boxed,thickness=2,x=0..3
0,view=[0..30,-2..2,-2..2]):
tval:=10.5:
u1:=(x,t)->(cos(omega*t)*ReW4(x,t)+sin(omega*t)*ImW4(x,t)):
u2:=(x,t)->(-sin(omega*t)*ReW4(x,t)+cos(omega*t)*ImW4(x,t)):
fns:=subs(t=tval,[x,u1(x,t)*(1-H(x-(t+10))),u2(x,t)*(1-H(x-(t+10))
)]):
plot22:=spacecurve(fns,numpoints=150,axes=boxed,thickness=2,x=0..3
0,view=[0..30,-2..2,-2..2]):
tval:=11:
u1:=(x,t)->(cos(omega*t)*ReW4(x,t)+sin(omega*t)*ImW4(x,t)):
u2:=(x,t)->(-sin(omega*t)*ReW4(x,t)+cos(omega*t)*ImW4(x,t)):
fns:=subs(t=tval,[x,u1(x,t)*(1-H(x-(t+10))),u2(x,t)*(1-H(x-(t+10))
)]):
plot23:=spacecurve(fns,numpoints=150,axes=boxed,thickness=2,x=0..3
0,view=[0..30,-2..2,-2..2]):
tval:=11.5:
u1:=(x,t)->(cos(omega*t)*ReW4(x,t)+sin(omega*t)*ImW4(x,t)):
u2:=(x,t)->(-sin(omega*t)*ReW4(x,t)+cos(omega*t)*ImW4(x,t)):
fns:=subs(t=tval,[x,u1(x,t)*(1-H(x-(t+10))),u2(x,t)*(1-H(x-(t+10))
)]):
plot24:=spacecurve(fns,numpoints=150,axes=boxed,thickness=2,x=0..3
0,view=[0..30,-2..2,-2..2]):
tval:=12:
u1:=(x,t)->(cos(omega*t)*ReW4(x,t)+sin(omega*t)*ImW4(x,t)):
u2:=(x,t)->(-sin(omega*t)*ReW4(x,t)+cos(omega*t)*ImW4(x,t)):
fns:=subs(t=tval,[x,u1(x,t)*(1-H(x-(t+10))),u2(x,t)*(1-H(x-(t+10))
)]):
plot25:=spacecurve(fns,numpoints=150,axes=boxed,thickness=2,x=0..3
0,view=[0..30,-2..2,-2..2]):
tval:=12.5:
u1:=(x,t)->(cos(omega*t)*ReW4(x,t)+sin(omega*t)*ImW4(x,t)):
u2:=(x,t)->(-sin(omega*t)*ReW4(x,t)+cos(omega*t)*ImW4(x,t)):
fns:=subs(t=tval,[x,u1(x,t)*(1-H(x-(t+10))),u2(x,t)*(1-H(x-(t+10))
)]):
plot26:=spacecurve(fns,numpoints=150,axes=boxed,thickness=2,x=0..3
0,view=[0..30,-2..2,-2..2]):
tval:=13:
u1:=(x,t)->(cos(omega*t)*ReW5(x,t)+sin(omega*t)*ImW5(x,t)):
```

```
u2:=(x,t)->(-sin(omega*t)*ReW5(x,t)+cos(omega*t)*ImW5(x,t)):
fns:=subs(t=tval,[x,u1(x,t)*(1-H(x-(t+10))),u2(x,t)*(1-H(x-(t+10))
)]):
plot27:=spacecurve(fns,numpoints=150,axes=boxed,thickness=2,x=0..3
0,view=[0..30,-2..2,-2..2]):
tval:=13.5:
u1:=(x,t)->(cos(omega*t)*ReW5(x,t)+sin(omega*t)*ImW5(x,t)):
u2:=(x,t)->(-sin(omega*t)*ReW5(x,t)+cos(omega*t)*ImW5(x,t)):
fns:=subs(t=tval,[x,u1(x,t)*(1-H(x-(t+10))),u2(x,t)*(1-H(x-(t+10))
)]):
plot28:=spacecurve(fns,numpoints=150,axes=boxed,thickness=2,x=0..3
0,view=[0..30,-2..2,-2..2]):
tval:=14:
u1:=(x,t)->(cos(omega*t)*ReW5(x,t)+sin(omega*t)*ImW5(x,t)):
u2:=(x,t)->(-sin(omega*t)*ReW5(x,t)+cos(omega*t)*ImW5(x,t)):
fns:=subs(t=tval,[x,u1(x,t)*(1-H(x-(t+10))),u2(x,t)*(1-H(x-(t+10))
)]):
plot29:=spacecurve(fns,numpoints=150,axes=boxed,thickness=2,x=0..3
0,view=[0..30,-2..2,-2..2]):
tval:=14.5:
u1:=(x,t)->(cos(omega*t)*ReW5(x,t)+sin(omega*t)*ImW5(x,t)):
u2:=(x,t)->(-sin(omega*t)*ReW5(x,t)+cos(omega*t)*ImW5(x,t)):
fns:=subs(t=tval,[x,u1(x,t)*(1-H(x-(t+10))),u2(x,t)*(1-H(x-(t+10))
)]):
plot30:=spacecurve(fns,numpoints=150,axes=boxed,thickness=2,x=0..3
0,view=[0..30,-2..2,-2..2]):
tval:=15:
u1:=(x,t)->(cos(omega*t)*ReW5(x,t)+sin(omega*t)*ImW5(x,t)):
u2:=(x,t)->(-sin(omega*t)*ReW5(x,t)+cos(omega*t)*ImW5(x,t)):
fns:=subs(t=tval,[x,u1(x,t)*(1-H(x-(t+10))),u2(x,t)*(1-H(x-(t+10))
)]):
plot31:=spacecurve(fns,numpoints=150,axes=boxed,thickness=2,x=0..3
0,view=[0..30,-2..2,-2..2]):
tval:=15.5:
u1:=(x,t)->(cos(omega*t)*ReW5(x,t)+sin(omega*t)*ImW5(x,t)):
u2:=(x,t)->(-sin(omega*t)*ReW5(x,t)+cos(omega*t)*ImW5(x,t)):
fns:=subs(t=tval,[x,u1(x,t)*(1-H(x-(t+10))),u2(x,t)*(1-H(x-(t+10))
)]):
plot32:=spacecurve(fns,numpoints=150,axes=boxed,thickness=2,x=0..3
0,view=[0..30,-2..2,-2..2]):
tval:=16:
u1:=(x,t)->(cos(omega*t)*ReW5(x,t)+sin(omega*t)*ImW5(x,t)):
u2:=(x,t)->(-sin(omega*t)*ReW5(x,t)+cos(omega*t)*ImW5(x,t)):
```

```
fns:=subs(t=tval,[x,u1(x,t)*(1-H(x-(t+10))),u2(x,t)*(1-H(x-(t+10))
)]):
plot33:=spacecurve(fns,numpoints=150,axes=boxed,thickness=2,x=0..3
0,view=[0..30,-2..2,-2..2]):
tval:=16.5:
u1:=(x,t)->(cos(omega*t)*ReW5(x,t)+sin(omega*t)*ImW5(x,t)):
u2:=(x,t)->(-sin(omega*t)*ReW5(x,t)+cos(omega*t)*ImW5(x,t)):
fns:=subs(t=tval,[x,u1(x,t)*(1-H(x-(t+10))),u2(x,t)*(1-H(x-(t+10))
)]):
plot34:=spacecurve(fns,numpoints=150,axes=boxed,thickness=2,x=0..3
0,view=[0..30,-2..2,-2..2]):
tval:=17:
u1:=(x,t)->(cos(omega*t)*ReW5(x,t)+sin(omega*t)*ImW5(x,t)):
u2:=(x,t)->(-sin(omega*t)*ReW5(x,t)+cos(omega*t)*ImW5(x,t)):
fns:=subs(t=tval,[x,u1(x,t)*(1-H(x-(t+10))),u2(x,t)*(1-H(x-(t+10))
)]):
plot35:=spacecurve(fns,numpoints=150,axes=boxed,thickness=2,x=0..3
0,view=[0..30,-2..2,-2..2]):
tval:=17.5:
u1:=(x,t)->(cos(omega*t)*ReW5(x,t)+sin(omega*t)*ImW5(x,t)):
u2:=(x,t)->(-sin(omega*t)*ReW5(x,t)+cos(omega*t)*ImW5(x,t)):
fns:=subs(t=tval,[x,u1(x,t)*(1-H(x-(t+10))),u2(x,t)*(1-H(x-(t+10))
)]):
plot36:=spacecurve(fns,numpoints=150,axes=boxed,thickness=2,x=0..3
0,view=[0..30,-2..2,-2..2]):
tval:=18:
u1:=(x,t)->(cos(omega*t)*ReW5(x,t)+sin(omega*t)*ImW5(x,t)):
u2:=(x,t)->(-sin(omega*t)*ReW5(x,t)+cos(omega*t)*ImW5(x,t)):
fns:=subs(t=tval,[x,u1(x,t)*(1-H(x-(t+10))),u2(x,t)*(1-H(x-(t+10))
)]):
plot37:=spacecurve(fns,numpoints=150,axes=boxed,thickness=2,x=0..3
0,view=[0..30,-2..2,-2..2]):
tval:=18.5:
u1:=(x,t)->(cos(omega*t)*ReW5(x,t)+sin(omega*t)*ImW5(x,t)):
u2:=(x,t)->(-sin(omega*t)*ReW5(x,t)+cos(omega*t)*ImW5(x,t)):
fns:=subs(t=tval,[x,u1(x,t)*(1-H(x-(t+10))),u2(x,t)*(1-H(x-(t+10))
)]):
plot38:=spacecurve(fns,numpoints=150,axes=boxed,thickness=2,x=0..3
0,view=[0..30,-2..2,-2..2]):
tval:=19:
u1:=(x,t)->(cos(omega*t)*ReW5(x,t)+sin(omega*t)*ImW5(x,t)):
u2:=(x,t)->(-sin(omega*t)*ReW5(x,t)+cos(omega*t)*ImW5(x,t)):
fns:=subs(t=tval,[x,u1(x,t)*(1-H(x-(t+10))),u2(x,t)*(1-H(x-(t+10))
```

```
)]):
plot39:=spacecurve(fns,numpoints=150,axes=boxed,thickness=2,x=0..3
0,view=[0..30,-2..2,-2..2]):
tval:=19.5:
u1:=(x,t)->(cos(omega*t)*ReW5(x,t)+sin(omega*t)*ImW5(x,t)):
u2:=(x,t)->(-sin(omega*t)*ReW5(x,t)+cos(omega*t)*ImW5(x,t)):
fns:=subs(t=tval,[x,u1(x,t)*(1-H(x-(t+10))),u2(x,t)*(1-H(x-(t+10))
)]):
plot40:=spacecurve(fns,numpoints=150,axes=boxed,thickness=2,x=0..3
0,view=[0..30,-2..2,-2..2]):
tval:=20:
u1:=(x,t)->(cos(omega*t)*ReW5(x,t)+sin(omega*t)*ImW5(x,t)):
u2:=(x,t)->(-sin(omega*t)*ReW5(x,t)+cos(omega*t)*ImW5(x,t)):
fns:=subs(t=tval,[x,u1(x,t)*(1-H(x-(t+10))),u2(x,t)*(1-H(x-(t+10))
)]):
plot41:=spacecurve(fns,numpoints=150,axes=boxed,thickness=2,x=0..3
0,view=[0..30,-2..2,-2..2]):
> display([plot1,plot2,plot3,plot4,plot5,plot6,plot7,plot8,plot9,plo
t10,plot11,plot12,plot13,plot14,plot15,plot16,plot17,plot18,plot19
,plot20,plot21,plot22,plot23,plot24,plot25,plot26,plot27,plot28,pl
ot29,plot30,plot31,plot32,plot33,plot34,plot35,plot36,plot37,plot3
8,plot39,plot40,plot41],insequence=true);
```